THE CHARACTERIZATION AND POTENTIAL FUNCTIONAL ROLE OF *WDR81*, A NOVEL ZEBRAFISH GENE, ASSOCIATED WITH CEREBELLAR ATAXIA, MENTAL RETARDATION AND DYSEQUILIBRIUM SYNDROME (CAMRQ) IN HUMANS

A DISSERTATION SUBMITTED TO

THE GRADUATE SCHOOL OF ENGINEERING AND SCIENCE

OF BILKENT UNIVERSITY

IN PARTIAL FULFILLMENT OF THE REQUIREMENTS FOR

THE DEGREE OF

DOCTOR OF PHILOSOPHY

IN

MOLECULAR BIOLOGY AND GENETICS

By

Füsun Doldur-Ballı

April 2016

THE CHARACTERIZATION AND POTENTIAL FUNCTIONAL ROLE OF *WDR81*, A NOVEL ZEBRAFISH GENE, ASSOCIATED WITH CEREBELLAR ATAXIA, MENTAL RETARDATION AND DYSEQUILIBRIUM SYNDROME (CAMRQ) IN HUMANS

By Füsun Doldur-Ballı
April, 2016

We certify that we have read this dissertation and that in our opinion it is fully adequate, in scope and in quality, as a thesis for the degree of Doctor of Philosophy.

_____	_____
Tayfun Özçelik	Michelle Adams
(Advisor)	(Co-Advisor)

_____
Ayşe Begüm Tekinay

_____
Hilal Özdağ

_____
Özlen Konu

_____
Stefan Fuss

Approved for the Graduate School of Engineering and Science

_____
Levent Onural
Director of the Graduate School

Abstract

THE CHARACTERIZATION AND POTENTIAL FUNCTIONAL ROLE OF *WDR81*, A NOVEL ZEBRAFISH GENE, ASSOCIATED WITH CEREBELLAR ATAXIA, MENTAL RETARDATION AND DYSEQUILIBRIUM SYNDROME (CAMRQ) IN HUMANS

Füsun Doldur-Ballı

PhD in Molecular Biology and Genetics

Advisor: Tayfun Özçelik

Co-Advisor: Michelle Adams

April, 2016

Cerebellar ataxia, mental retardation and dysequilibrium syndrome (CAMRQ) is a neurodevelopmental disorder. The gene encoding WD repeat containing protein 81 (*WDR81*) was reported to be associated with CAMRQ2 [MIM 610185]. Human and mouse studies indicated the potential importance of *WDR81* in neurodevelopment. The first aim in this study was to characterize the transcript and to reveal the expression profile of *wdr81* in zebrafish. The second aim was to perform the initial characterization of *wdr81* morphants. *In silico* analysis indicated that the conserved domains are shared in human, mouse and zebrafish orthologous proteins, implying a conserved function of WDR81 in three species. The characterization of the transcript revealed that *wdr81* possessed one ORF and one 5'UTR structure. The predicted sequence for 3'UTR was confirmed along with detection of some variants and an insertion site in samples from ten developmental timepoints and in several adult tissues. This region was not detected in kidney, intestine and gills, which might be pointing out an alternative polyadenylation event. *wdr81* appeared to be maternally supplied. 5 hpf and 18 hpf were detected as crucial timepoints regarding *wdr81* expression. Expression of *wdr81* was found to be increased in the eye and brain regions at 18 hpf and 48 hpf. *wdr81* was found to be ubiquitously expressed in the

adult zebrafish. The expression of *wdr81* in the adult brain and eye was detected in several regions including retinal layers, presumptive Purkinje cells and some proliferative zones. The splice blocking morpholino which targets the exon 2-intron 2 junction of *wdr81* worked at 3 tested doses; 2 ng, 4 ng and 8 ng. The effect of the *wdr81* morpholino was detected to add the intron, which is downstream of the target exon, to the transcript and introduce a stop codon. Preliminary results indicated a significant reduction in the head sizes at a ratio of 3.88% (p:0.027) in the *wdr81* morphant group compared to uninjected group and *gbx2* expression was observed to be higher in *wdr81* morphants compared to the control groups.

In short, findings of this study emphasize the significance of *wdr81* in neurodevelopment and suggest a potential role in neuronal proliferation. This study also serves as a basis for future functional studies.

Keywords: *wdr81*, zebrafish, RACE, gene expression, morpholino

Özet

İNSANLARDAKİ SEREBELLAR ATAKSİ, ZEKA GERİLİĞİ VE DENGESİZLİK SENDROMU İLE İLİŞKİLENDİRİLEN VE ZEBRABALIĞINDA YENİ BİR GEN OLAN *WDR81*'İN KARAKTERİZASYONU VE MUHTEMEL İŞLEVSEL ROLÜ

Füsun Doldur-Ballı

Moleküler Biyoloji ve Genetik, Doktora

Tez Danışmanı: Tayfun Özçelik

Eş Danışmanı: Michelle Adams

Nisan, 2016

Serebellar ataksi, zeka geriliği ve dengesizlik sendromu nörogelişimsel bir hastalıktır. WD tekrarı içeren protein 81'i kodlayan genin bu sendrom ile ilişkilendirildiği daha önce rapor edilmiştir. *WDR81* geninin sinir sisteminin gelişim sürecindeki potansiyel önemi insan ve fare çalışmalarıyla ortaya konmuştur. Bu çalışmada ilk amaç, *wdr81*'in zebrabalığında karakterize edilmesi ve ifade profilinin gösterilmesiydi. İkinci amaç *wdr81* morfantlarının öncül karakterizasyonunun yapılmasıydı. *In siliko* analizler insan, fare ve zebrabalığına ait ortolog proteinlerin korunmuş domeynleri paylaştığını gösterdi, bu durum da WDR81'ın işlevinin bu üç türde korunmuş olabileceğine işaret etmektedir. Transkriptin karakterizasyonu, *wdr81*'in bir açık okuma çerçevesine ve bir 5'UTR yapısına sahip olduğunu gösterdi. 3'UTR'nin öngörülen dizisi, bazı varyantların ve bir içine yerleştirme (insertion) bölgesinin varlığı tespit edilmekle birlikte, teyit edildi. Bu içine yerleştirme (insertion) bölgesi on gelişimsel evreye ait örnekte ve çeşitli yetişkin dokularında tespit edilmiş olup böbrek, bağırsak ve solungaçlarda bulunmadı. Bu durumun da alternatif poliadenilasyon işlemine işaret ettiği öngörülmektedir. *wdr81*'in yumurta hücresi tarafından sağlanan transkriptler arasında olduğu tespit edildi. *wdr81*'in ifadesi açısından döllenme sonrası 5. ve 18. saatler kritik evreler olarak saptandı. Döllenme sonrası 18. ve 48. saat evrelerinde *wdr81* ifadesinin göz ve beyin bölgelerinde

artmış olduğu gözlendi. *wdr81*'in test edilen yetişkin dokularının tümünde ifade edildiği, yetişkin göz ve beyin dokularında ise retina katmanları, muhtemel Purkinje hücreleri ve bazı proliferatif alanların da bulunduğu çeşitli bölgelerde ifade edildiği belirlendi. Uçbirleştirmeyi (splicing) etkileyen morfolino *wdr81* genine ait ekzon 2-intron 2 bölgesini hedefleyecek şekilde tasarlandı ve denenen üç dozun (2 ng, 4 ng ve 8 ng) da çalıştığı tespit edildi. *wdr81* morfolinonun etkisinin, hedef ekzonun aşağı yönündeki intronu transkripte dahil etmek olduğu ve bu dizinin de durdurma kodonu içerdiği tespit edildi. Öncül sonuçlar, *wdr81* morfant grubuna ait kafa bölgelerinin ölçümünde, enjeksiyon yapılmayan gruba kıyasla %3,88 oranında anlamlı (p: 0,027) bir düşüş olduğu sonucunu verdi. Ayrıca, *gbx2* ifadesi *wdr81* morfant grupta kontrol gruplarına kıyasla daha yüksek gözlendi.

Özetle, bu çalışmaya ait bulgular *wdr81*'in nörogelişimsel önemini anlamakta katkıda bulunmuştur ve bu gen için nöronların çoğalmasına (proliferasyonu) ilişkin olası bir rol önermektedir. Elde edilen veriler aynı zamanda ileride yapılacak fonksiyonel çalışmalar için de temel teşkil edecektir.

Keywords: *wdr81*, zebrabalığı, RACE, gen ifadesi, morfolino

To Mevlüt and Yaren Rüya…

Acknowledgements

Having a PhD degree was one of my life goals and I started the program in Department of Molecular Biology and Genetics at Bilkent University with the motivation that having a PhD degree was going to improve me in the progress of becoming the person I wanted to be. Prof. Dr. Tayfun Özçelik accepted to work with me, which was also my only plan when I registered to the program. Prof. Özçelik always guided me to try my best in science and encouraged me to develop critical thinking. I admire his way of synthesizing scientific information and concepts. Another thing I learned from him is to set the career goals at a level of quality and significance accepted by the scientific community in the world. My PhD thesis research continued under co-supervision of Prof. Dr. Tayfun Özçelik and Assoc. Prof. Dr. Michelle Adams. Dr. Adams was always caring, supportive, guiding and encouraging to me. I believe that all the feedback she gave during my thesis research will also help me in my future career. I always appreciated her attitude to the people who work with her. She provided an environment for us to feel comfortable, productive and to be creative. I am grateful to both of my supervisors because of providing me the opportunity to become an independent researcher and of trusting me in the project. I am very thankful to Assoc. Prof. Dr. Ayşe Begüm Tekinay for her patience with my questions, her feedback on the project, being a thesis progress committee and a jury member and most importantly for encouraging me and her belief in me. Her support is always invaluable. I would like to thank to Assoc. Prof. Dr. Özlen Konu for the feedback and perspective she provided during my research and for being a thesis progress committee and a jury member. I am thankful to Prof. Dr. Hilal Özdağ for evaluating my thesis and being a jury member. I thank to Assoc. Prof. Dr. Stefan Fuss for evaluating my thesis and hosting me in his lab in the beginning of my thesis to train me on morpholino microinjection. I also thank to Xalid Bayramlı from his lab for sparing time to teach me how to perform microinjection experiments.

I would like to express my gratitude to Assoc. Prof. Dr. Güneş Özhan for her contribution to the study by suggesting to characterize the morphants with marker genes and providing the plasmid constructs. She is always helpful and open to questions. I deeply appreciate her approach to science which is pure and sharing. I would like to express special thanks to Prof. Dr. Hamdullah Aydın who has been a mentor to me since my Master's degree studies. He broadened my perspective with outstanding ideas and comments.

I have always felt lucky by means of colleagues. One of the best things in my PhD education was to meet Dr. Gülşah Merve Kılınç. I am thankful to her for moral support, encouragement

and suggestions in my research. I also thank to Dr. Emre Onat and Dr. Süleyman Gülsüner as senior researchers of Özçelik Group for their contributions and help in various forms. I would like to record my sincere appreciation to Dr. Ayça Arslan-Ergül for her contributions and support during my research. Her perspective has been always inspiring to me. I would like to thank Dilan Çelebi-Birand for performing the head size and body measurements of injection groups and to Melek Umay Tüz for her help with the whole mount *in situ* hybridization experiment using *gbx2* probe. I also thank other members of Adams Group; Elif Karoğlu, Göksemin Şengül, Ayşegül Dede, Begün Erbaba, Özge Pelin Burhan and zebrafish laboratory technician Tülay Arayıcı for their contributions and help in various forms.

I am pleased to meet and to have known my friends from MBG, who are Dr. Verda Bitirim, Dr. Pelin Telkoparan, Dr. Nilüfer Sayar, Dr. Gurbet Karahan, Dr. Ender Avcı, Umur Keleş, Begüm Kocatürk, Andaç Kipalev Neşelioğlu, Buket Gültekin, Merve Mutlu, Begüm Han Horuluoğlu, Begüm Yıldız, Şahika Cıngır Köker, Ayşegül Örs, Gözde Güçlüler, Özlem Tufanlı, İnci Şimşek Onat, Zeynep Ayyıldız, Emre Yurdusev, Dr. Gökhan Yıldız, Defne Bayık, Merve Aydın and Dr. Çiğdem Özen. The peaceful work environment they created and their help was important, the conversation with them and their feedback was always supportive.

I dedicate this thesis to my spouse Mevlüt Ballı and our future daughter Yaren Rüya Ballı. I would like to express my heartfelt appreciation and eternal love to Mevlüt. He has always been understanding, supportive, encouraging and patient during my graduate studies. His help to my efforts for balancing my career goals with our family life is precious. I hope dedicating this thesis also to her will be a future surprise to our daughter, who will join us in a few months. I am deeply grateful to my parents Elif and Kemal Doldur and my brother Utku Doldur for their endless love, unhesitant support and encouragements during my whole education. My father has been the first and the most strongest inspiration for devising a career plan in science. I would like to also thank to Ayşe Mergenci, Ayşe Can, Hatice Yiğit and Canan Şişman Korkmaz for their support and belief in me.

I was supported by TÜBİTAK 1001 grants, 111S199 and 114S548, in part by a European Molecular Biology Organization Installation Grant to Michelle Adams and Department of Molecular Biology and Genetics during my PhD. Finally, I will share the quotation from Albert Einstein “Play is the highest form of research”, which also partially explains why I preferred a career in science over routine work. I am determined to put every effort to continue playing/practicing science in the future as well.

Table of Contents

List of Figures

List of Tables

Abbreviations

ANOVA, Analysis of variance	ISH, *In situ* hybridization
ATP8A2, ATPase, aminophospholipid transporter, class I, type 8A, member 2	MFS, Major facilitator superfamily
BA6, Brodmann area 6	MLF, Medial longitudinal fascicle
BEACH, Beige and Chediak-Higashi	ORF, Open reading frame
BrdU, 5-bromo-2'-deoxyuridine	P15, Post natal day 15
CA8, Carbonic anhydrase VIII	qRT-PCR, Quantitative real-time PCR
CAMRQ, Cerebellar Ataxia, Mental Retardation and Dysequilibrium Syndrome	RACE, Rapid amplification of cDNA ends
CNS, Central nervous system	RoP, Rostral primary motor neuron
DIG, Digoxigenin	SGZ, Subgranular zone
Dpf, Days post fertilization	SVZ, Subventricular zone
ENU, *N*-ethyl-*N*-nitrosourea	UTR, Untranslated region
GABA, Gamma-aminobutyric acid	VLDLR, Very low density lipoprotein receptor
gbx2, gastrulation brain homeobox 2	WD40, ~40 amino acid structural motifs, often ending with a Tryptophan-Aspartic acid (W-D) dipeptide
GFAP, glial fibrillary acidic protein	WDR81, WD repeat containing protein 81
Hpf, Hours post fertilization	ZFIN, The Zebrafish model organism database

Chapter 1. Introduction

1.1. Cerebellar Ataxia, Mental Retardation and Dysequilibrium Syndrome

Neurodevelopmental disorders are associated with mutations which might affect numerous cellular mechanisms leading to impairment of growth and development of the nervous system. These type of impairments during the neurodevelopmental processes give rise to neurological or psychiatric diseases[1]. Schizophrenia, autism spectrum disorder, fragile-X and Rett syndrome are a few examples of such neurodevelopmental disorders[2–5]. Cerebellar ataxia, mental retardation and dysequilibrium syndrome (CAMRQ) is also a neurodevelopmental disorder. The inheritance pattern is autosomal recessive and it is a rare condition, which is characterized by mental retardation, cerebellar ataxia and dysarthric speech with or without quadrupedal gait[6–14]. Quadrupedal gait, ie. walking on all fours, in humans is also referred to as Unertan Syndrome[6,15] and was first observed in 1914 in the Black Sea Region[16] (Figure 1). CAMRQ is associated with specific mutations and these mutations have been shown in consanguineous families with one exception[17]. Homozygosity mapping, linkage analysis and targeted next generation sequencing of homozygous regions revealed genetic heterogeneity in this syndrome.

Figure 1. Quadrupedal gait in a male in 1914 (left)[16] (by courtesy of Prof. Dr. Üner Tan) and in a female patient nowadays (right)[18] *(Reprinted with permission from Taylor and Francis Group, http://www.tandfonline.com).*

1.1.1. CAMRQ Associated Genes

VLDLR (very low-density lipoprotein receptor), *WDR81* (WD repeat containing protein 81), *CA8* (carbonic anhydrase VIII) and *ATP8A2* (ATPase, aminophospholipid transporter, class I, type 8A, member 2) have been reported to be associated with CAMRQ1 (MIM: 224050)[8–10,13,17,19–21], CAMRQ2 (MIM: 610185)[6–8,12], CAMRQ3 (MIM: 613227)[11,22,23] and CAMRQ4 (MIM: 615268)[14], respectively. The CAMRQ associated genes are mapped to chromosomes 8, 9, 13 and 17; *CA8* to chromosome 8q12, *VLDLR* to chromosome 9p24, *ATP8A2* to chromosome 13q12 and *WDR81* to chromosome 17p13.

1.1.1.1. Very Low Density Lipoprotein Receptor (VLDLR)

VLDLR is a gene made up of 19 exons[24] and encodes a receptor protein which is a member of the low-density lipoprotein receptor family[25]. It is an integrative element in the reelin pathway and functions in guiding neuroblast migration in the developing cerebral cortex and cerebellum[26,27]. ApoER2 (Apolipoprotein E Receptor 2) and VLDLR, which are reelin receptors, are both required for the coordination of alignment of Purkinje cell subsets in the developing cerebellum[28,29]. Reelin mediates cortical layer formation and dendrite development in hippocampus via VLDLR/ApoER2-Dab1 (Disabled 1) pathway[30]. Recent studies showed that *VLDLR* is actively involved in regulation of formation and development of dendritic spines[31,32]. In addition, *VLDLR* is expressed in synapses, both presynaptically and postsynaptically. Knockdown of *VLDLR is* reported to significantly decrease the synaptophysin puncta number and also to decrease glutamate receptor subunits such as GluN1 levels and levels of GluA1 at the cell surface[32]. Besides its role in the reelin signaling pathway, VLDLR fulfills critical functions in triglyceride metabolism. It has an effect on the uptake of VLDL triglycerides in peripheral tissues[33]. It is also shown that the expression of *VLDLR* is essential in promoting adipocyte differentiation[34]. The summary of the reported cases with VLDLR-associated CAMRQ (CAMRQ1) and the information about the *VLDLR* mutations are given in Table 1.

The common morphological abnormalities in the brains of the patients with CAMRQ1 are the hypoplasia of cerebellum[8,10,13,17,19–21] and moderate gyrial simplification of the cerebral cortex[8,10,13,17,20]. The pons was observed particulary small in some patients[8,13,17,21] while mild hypoplasia of the corpus callosum was observed by Turkmen *et al*. (2008)[19]. Moheb *et al.* (2008) was unable to obtain any MRI (magnetic resonance imaging) or CT (computerized tomography) scans of the brains from any patients, and for this reason the brain abnormalities of the patients in this study could not be evaluated[9].

1.1.1.2. WD Repeat Containing Protein 81 (WDR81)

The gene encoding WD repeat containing protein 81 (*WDR81*) was found to be mutated in some CAMRQ patients. It is a missense mutation and it lies in exon 1 of the *WDR81* isoform 1, WDR81 p.P856L. The most significant morphological changes in the CAMRQ patients carrying this mutation were significant decline in the volumes of cerebellum and corpus callosum. Additional analysis showed that morphological differences in the precentral gyrus and Brodmann areas BA6, BA44 and BA45 took place in the patients' brains[12] (Figure 2). When researchers investigated the neuro-ophthalmic aspect of CAMRQ, they observed that four patients who carry the missense mutation in *WDR81* gene had downbeat nystagmus and two male patients among four patients had also bilateral temporal disc pallor and ring-shaped macular atrophy[35]. A similar phenotype to CAMRQ was obtained with a mutant mouse line *nur5*. The *N*-ethyl-*N*-nitrosourea (ENU) induced mutation in this model was a missense mutation, L1349P, and it was also located in the predicted major facilitator superfamily domain of the Wdr81 protein as in patients. This homozygous missense mutation caused loss of Purkinje cells, which was detected at P28 (young adult) and loss of photoreceptor cells, which was detected on P15 (infant) the earliest tested timepoints in this mouse model[36].

The mitochondrial defects in the dendrites of Purkinje cells was detected in mutant mice at P21 (juvenile) and this finding led the conclusion that the mitochondrial abnormalities are followed up by death of Purkinje cells during development[36].

Table 1. Summary of the reported cases with CAMRQ1 (Adapted from Ali *et al*. 2012[20])

	Boycott *et al.* 2005	Moheb *et al* . 2008	Turkmen *et al* . 2008	Ozcelik *et al* . 2008	Ozcelik *et al* . 2008	Boycott *et al* . 2009	Kolb *et al* . 2010	Ali *et al* . 2012	Dixon-Salazar *et al* . 2012
Mutation	Homozygous deletion of the *VLDLR* gene	Homozygous c.1342 C>T (p.R448X)	Homozygous c.2339delT (p.I780TfsX3)	Homozygous c.769C.T (p.R257X)	Homozygous c.2339delT (p.I780TfsX3)	Compund heterozygous c.1561G>C + c.1711_1712dupT (p.D521H + p.Y571LfsX7)	Homozygous deletion, which begins in the 5'UTR and continues through a part of exon 1, includes exons 2,3,4 and a part of exon 5	Homozygous c.2117G>T (p.C706F)	Homozygous c.1247_53delGTTACAA (p.G1246fsX1305)
Ethnicity	Hutterite	Iranian	Turkish	Turkish	Turkish	Caucasian	Turkish	United Arab Emirates (Omani)	Turkish
Consanguinity	Present	Present	Present	Present	Present	Not present	Present	Present	Present
Ambulation	Delayed	No ability to walk independently	Delayed-Quadrupedal	Delayed-Quadrupedal	Delayed-Quadrupedal	Delayed	Delayed-Bipedal	Delayed-Bipedal	Delayed
Number of patients in the study	10	8	3	5	3	1	2	5	2

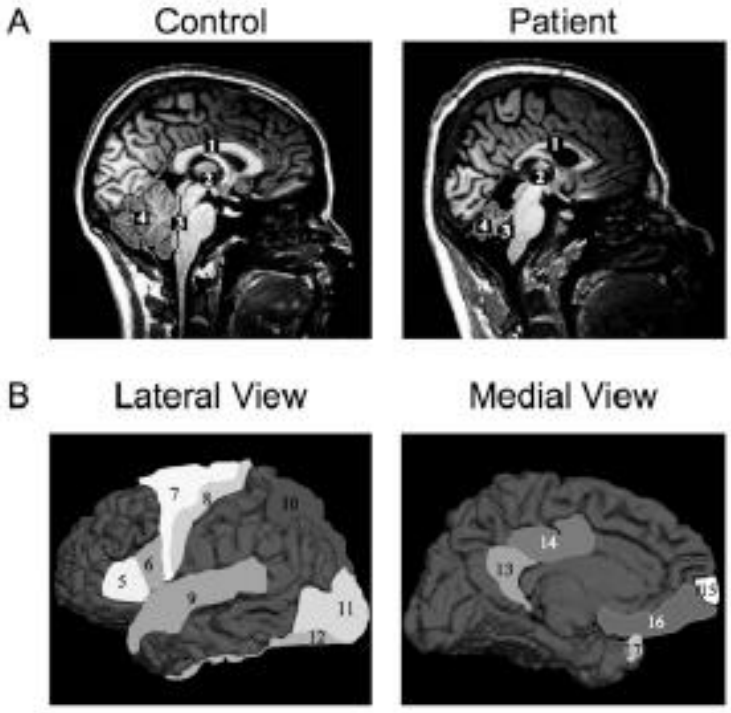

Figure 2. Brain morphology of a control individual and a patient were analyzed via magnetic resonance imaging (MRI). *The patient was reported to be affected from WDR81 associated CAMRQ (CAMRQ2, MIM: 610185). (A) A healthy control individual (left) and a patient (right) were scanned. The areas, which were assigned with numbers indicate regions where differences in volumes are distinguishable: corpus callosum (1), third ventricle (2), fourth ventricle (3), and cerebellum (4). (B) Lateral and medial views of a reference cortex on which the significantly affected morphometric parameters are numbered: BA45 (5), BA44 (6), BA6 (7), precentral (8), superior temporal (9), superior parietal (10), lateral occipital (11), fusiform (12), isthmus cingulated (13), posterior cingulated (14), frontal pole (15), medial orbitofrontal (16), and temporal pole (17)*[12]*. Reprinted with permission from Cold Spring Harbor Laboratory Press.*

WDR81 gene was shown to be mutated in cancer and it appears that it locates in a metabolically important loci. *WDR81* gene was reported to be mutated and expressed in >10% of the evaluated 23 colorectal cancer cell lines[37]. Transethnic meta-analysis of European ancestry and Japanese genome-wide association studies revealed that

SERPINF2-WDR81 loci as one of the six significant loci for serum albumin[38]. Serum albumin level is metabolically important because it is inversely associated with cardiovascular risk and mortality risk[39,40].

WDR81 was shown to be expressed in all of the tested human tissues and its level was the highest in cerebellum and corpus callosum among brain regions[12]. Expression of *Wdr81* was detected in Purkinje cell neurons, photoreceptor cells, deep cerebellar nuclei neurons and neurons of brainstem among the central nervous system neurons in wild-type adult mouse. Localization of Wdr81 was observed in the mitochondria of Purkinje cells using electron microscopy. *Wdr81* expression was also detected in all of the evaluated adult tissues[36]. Gulsuner *et al.* also revealed that *Wdr81* expression was higher in the Purkinje cell neurons and molecular layer of cerebellum in mouse embryonic brain[12].

The function of WDR81 is not currently known, however it can be predicted *in silico* with information about the domains of the protein. The presence of conserved domains in proteins may lead to the indication of their function as well. Moreover, conservation of the identical domains in homologous proteins from different species sheds light on the critical importance of the protein of interest at several evolutionary levels. WDR81 protein is conserved among vertebrates, the mutation also hits a conserved domain of the protein of interest[12] (Figure 3). The putative domains of human and mouse WDR81 proteins are Beige and Chediak-Higashi (BEACH) domain, a major facilitator superfamily (MFS) domain and six WD40 repeat domains. Both proteins are predicted to be transmembrane proteins[12,36]. A BEACH-domain containing proteins are proposed to perform as scaffold proteins. They are mostly large proteins and they take place in membrane-related events. These events include vesicle fusion and fission, so that they might function in vesicular transport, apoptosis, receptor signaling, formation of synapses, autophagy and membrane dynamics[41]. WD40 domain is given this name because of the length of the repeats of 40 aminoacids and the repeats often end with the conserved Tryptophan-Aspartic acid (WD) dipeptide.

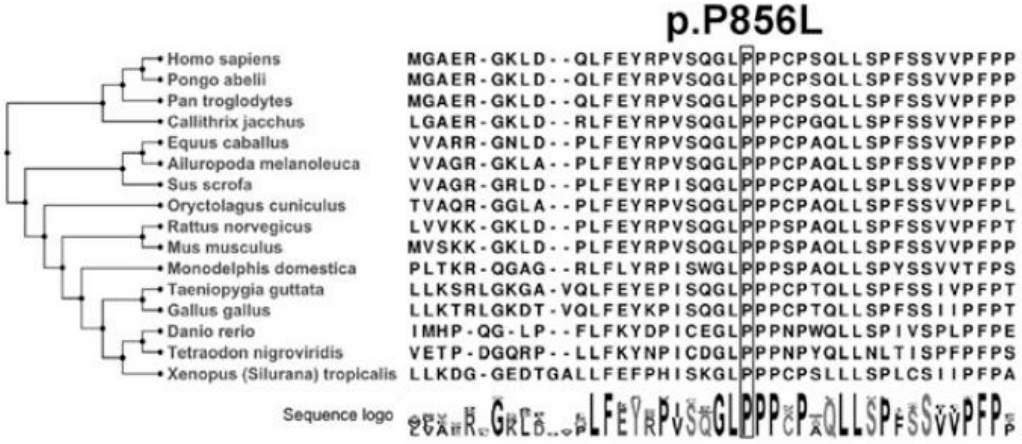

Figure 3. Phylogenetic tree of protein sequences of WDR81 in vertebrates. *The box implies the amino acid, mutated in CAMRQ patients[12]. Reprinted with permission from Cold Spring Harbor Laboratory Press.*

WD40 domain-containing proteins take place in numerous cellular functions such as cell cycle control, signal transduction, regulation of transcription, apoptosis, chromatin dynamics, vesicular trafficking and cytoskeletal assembly. The WD40 domains of BEACH domain-containing proteins serve as a scaffold for protein-protein or protein-DNA interactions[41,42]. The MFS transporters function in response to chemiosmotic ion gradients and they transport small molecules. They are single-polypeptide secondary carriers and act as uniporters, symporters or antiporters[43]. Taken together, the WDR81 protein might have an importance related to both the central nervous system and the metabolism. The findings from mouse and human studies indicate that *WDR81* might be a critical gene in neurodevelopment, but the exact function of the gene is still not fully understood.

The family of proteins named as WDR and followed by a number, is composed of almost 100 proteins in human genome. Some of them were reported to be associated with diseases. The association of *WDR10* with cranioectodermal dysplasia 1 [MIM 218330][44], *WDR11* with hypogonadotropic hypogonadism 14 with or without anosmia [MIM 614858][45], *WDR19* with Senior-Loken syndrome 8 [MIM 616307][46,47], *WDR34*

with short-rib thoracic dysplasia 11 with or without polydactyly [MIM 615633][48,49], *WDR35* with cranioectodermal dysplasia 2 [MIM 613610][50] and short-rib thoracic dysplasia 7 with or without polydactyly [MIM 614091][51], *WDR36* with primary open angle glaucoma [MIM 609887][52], *WDR56* with short-rib thoracic dysplasia 2 with or without polydactyly [MIM 611263][53,54], *WDR60* with short-rib thoracic dysplasia 8 with or without polydactyly [MIM 615503][55], *WDR62* with microcephaly 2, primary, autosomal recessive, with or without cortical malformations [MIM 604317][56–60] were reported. Dolichocephaly and high forehead were observed in cranioectodermal dysplasia as a result of abnormal development of the cranium and skeleton[44]. Anosmia was associated with the absence or underdevelopment of olfactory bulbs and their nerve fibers[61]. Hypogonadism was found to be related with the failure in migration of neurons which synthesize gonadotrophin releasing hormone during development[62]. Senior-Loken syndrome 8 is a progressive disorder characterized by retinal and renal failure[63]. Impairment in the organs such as brain, eye, heart, kidneys, liver, pancreas, intestines, and genitalia as wells as cleft lip/palate might accompany the short-rib thoracic dysplasia 11 with or without polydactyly condition[64]. Primary open angle glaucoma was characterized by the defect in the vision, optic nerve damage and increased intraocular pressure[65]. Primary microcephaly was characterized by mental retardation and brain size, which is smaller than normal[56]. The brain malformations found to be related with *WDR62* mutations were pachygria[56,57], underdevelopment of corpus callosum[57,59], polymicrogyria[58,59], schizencephaly, subcortical heterotropia[59], microlissencephaly, band heterotropias and dysplastic cortex[56]. Thus, mutations in several genes encoding WD40 domain containing proteins, similar to *WDR81*, were shown to be associated with brain and eye malformations during development.

1.1.1.3. Carbonic Anhydrase VIII (CA8)

Another CAMRQ associated gene *CA8* is comprised of 9 exons[24] and encodes a protein which has a critical function in motor control[66]. It has been classified as a member of the carbonic anhydrase gene family because of the sequence similarity, however the gene product of CA8 does not possess the enzymatic activity to catalyze the reaction of

hydration of carbon dioxide reversibly[67]. CA8 binds to IP_3R1 (inositol 1,4,5 triphospate receptor type 1) and binding of CA8 to IP_3R inhibits binding of IP3 to the receptor by decreasing its affinity. Expression of both CA8 and IP_3R1 is abundant in Purkinje cells and they co-localize in the cytoplasm, dendrites and axons. This might explain why the sensitivity of IP_3R1 to IP_3 for IP_3-induced Ca^{+2} release in this layer is low[68]. Expression of *CA8* in human fetal brain was detected in neuroprogenitor cells in the subventricular zone and in the neurons, which migrate to the cortex. In the adult human, *CA8* expression was found out in the neural cell bodies in most regions of the central nervous system, such as cerebrum, diencephalon, cerebellum, pons and medulla[69]. The "waddles" (*wdl*) mouse is an animal model of *Car8* null mutation[66]. Car8 is the homologous protein of CA8 in mouse which shows a 98% identity[70]. Ataxia and appendicular dystonia comprised the phenotype of the *wdl* mouse and the gait disorder continued througout life-time[66]. *CA8* overexpression in neuronal cell lines under staurosporine induced apoptotic stress reduced the cell death and overexpression of *CA8* in neuronal cell lines and mouse cerebellar granule neurons increased neuronal migration and invasion. *CA8* downregulation decreased cell migration and invasion ability and resulted in abnormal Ca^{+2} release in cerebellar granule neurons. Knockdown of *ca8* in zebrafish was achieved by using morpholino injection and *ca8* morphants at 3 days post fertilization exhibited a decrease in motility[71]. Knockdown of *ca8* via microinjection of morpholino oligonucleotides in another study resulted in neuronal death and malformations in cerebellum and muscle. Body axis was curved and motor functions and coordination were defective, showing a similar phenotype to human condition[72]. Also, *CA8* expression has been found to be increased in non-small lung cancer and colorectal cancer[73,74].

The summary of the reported cases with CA8-associated CAMRQ (CAMRQ3) and the information about the *CA8* mutations are given in Table 2. Among the three publications summarized in Table 2, only Kaya *et al.* (2011) provided results of brain imaging studies on patients. The MRI study showed variable volume loss in cerebellum and vermis in patients in this study[22].

Table 2. Summary of the reported cases with CAMRQ3

	Turkmen *et al.* 2009	Kaya *et al* . 2011	Najmabadi *et al* . 2011
Mutation	Homozygous c.298T>C (p.S100P)	Homozygous c.484G>A (p.G162R)	Homozygous chr8:61297790 C>T (p.R237Q)
Ethnicity	Iraqi	Saudi	N/A
Consanguinity	Present	Present	Present
Ambulation	Quadrupedal	Delayed-without quadrupedal gait	N/A
Number of patients in the study	4	7	4

N/A: not applicable, information not provided in the article.

1.1.1.4. ATPase, Aminophospholipid Transporter, Class I, Type 8A, Member 2 (ATP8A2)

ATP8A2 (ATPase, aminophospholipid transporter, class I, type 8A, member 2) is made up of 37 exons[24] and encodes a protein, which is a member of P4 ATPase protein family[75]. This protein family facilitates transport of phospholipids from exoplasmic leaflet to cytosolic leaflet and thereby are involved in formation of the asymmetry of the cell membrane. They are also called lipid flippases and they take roles directly or indirectly in dynamics of cytoskeleton, signaling and metabolism of lipids, cell division and membrane trafficking[76]. *ATP8A2* is expressed in brain, retina and testis among evaluated human tissues. Expression of *ATP8A2* in the brain was detected in both fetal and adult tissues[77]. In adult human brain, all the tested regions showed expression of the gene and the highest level of expression was found to be in cerebellum[14]. In mouse, *Atp8a2* expression was detected in brain, spinal cord, retina and testis[78,79]. The function of Atp8a2 was revealed as to transfer aminophospholipids (phosphatidylserine and phosphatidyethanolamine) from exoplasmic to cytosolic leaflet in an ATP-dependent manner[78]. Overexpression and downregulation studies on *Atp8a2*, in conjuction with the results from the overexpression and downregulation of *Cdc50a*, demonstrated that *Atp8a2* in synergy with *Cdc50a* functions in axon elongation of neurons which also

indicates a critical role in rat hippocampal neuronal differentiation[80]. A mutant mouse model, *wabbler lethal*, which has ataxia and neurodegeneration, was shown to carry loss of function mutations in *Atp8a2* gene. It was concluded *Atp8a2* is associated with axon degeneration and neurodegenerative disease[79]. Disruption of the *ATP8A2* gene was also reported to be associated with severe mental retardation and hypotonia in a patient[77].

ATP8A2-associated CAMRQ (CAMRQ4) was reported in a consangineous family from Turkey. Four CAMRQ patients were detected in the family, however DNA from one patient could not be included in the study. Patients showed delayed ambulation and have quadrupedal gait[8]. The index patient was unable to walk at the time of the study. A missense mutation in *ATP8A2* (c. 1128 C>G, p.I376M) was found out to be associated with the condition. Moderate hypoplasia of inferior cerebellum, corpus callosum and cerebral cortex were observed in the patients[14].

1.2. Zebrafish as a Model Organism

The model organism used in the current work is the zebrafish *(Danio rerio)* (Figure 4). George Streisinger and his colleagues established zebrafish as a genetic model system 35 years ago[81]. Zebrafish have become a promising model organism for scientists in developmental biology, neurophysiology, biomedical research and ethology fields[82]. Comparison of human reference genome and zebrafish reference genome revealed that one clear zebrafish orthologue gene exists for approximately 70% of human genes[83]. It is a vertebrate with an integrated nervous system and possesses common organs and tissues like brain and spinal cord[84]. Zebrafish produce large batches of externally fertilized and transparent embryos that enable observation of development with microscopy techniques. Moreover, embryos develop at a fast rate and key developmental events take place earlier and faster compared to mammalians. For example neurogenesis begins around 10 hours post-fertilization (hpf), synaptogenesis and the first behaviors of embryos begin around 18 hpf and hatching is observed around 52 hpf[82,84]. After approximately 2 days of development, zebrafish embryo has its internal organs, eyes, ears and a brain, which has been already divided into

compartments. Thus the embryo has formed all of the common main characteristics of a vertebrate body by this timepoint[85].

Figure 4. Lateral views of a female (F) and a male (M) adult zebrafish. *wt: wild type, L: left side of the bodies. Scale bar indicates 2 mm*[86]*. Reprinted with permission from Elsevier.*

Various molecular genetic techniques have been devised and used in zebrafish research and new techniques are continuing to emerge over time. For example, transgenic zebrafish lines, which express a fluorescent protein in specific types of neurons, are useful in studying the development of nervous system and neural circuits[87]. Bacterial artifical chromosome (BAC) mediated transgenesis is managed by using BAC which is engineered with homologous recombination to express fluorescent reporter in target cells[88]. Although the efficiency of BAC mediated transgenesis is low, this technique is advantageous in obtaining the reporter genes and regulatory sequences together in the construct instead of putting effort in laborious subcloning work[87,89]. The efficiency of integration of the DNA injected to the zebrafish embryos increases based on the activity of the transposases, such as sleeping beauty[90] and tol-2[91] transposases. Employing transgenes under control of heat-inducible promoters provides conditional control of gene expression[92,93]. Using the adapted form of the yeast galactose inducible[94] and Cre-loxP systems[95], which efficiently works in mouse models, also provide conditional control of gene expression and permanent labeling of cell lineages in zebrafish models.

Targeted mutation is managed by zinc finger nucleases (ZFNs)[96] and TAL effector nucleases (TALENs)[97,98] in zebrafish. A double strand break induced by these nucleases

is repaired by non-homologous end joining. This often results in insertion or deletions and ultimately a loss-of-function phenotype is obtained[96–98]. A recent method, Clustered regularly-interspaced short palindromic repeats (CRISPR)/Cas9 is reported to be more efficient than ZFN and TALEN methods in terms of germline transmission. This system is a genome editing tool, already used in various model organisms and has advantages over other mutagenesis methods by its simplicity in design, being practical to use and enabling to target more than one genes at the same time[99].

Morpholino antisense technology is used in loss-of-function experiments. Morpholino sequences knock down the gene of interest either by targeting the RNA splicing or the translation initiation. These sequences are stable and introduced to the embryos preferably at one-cell stage however their effect lasting for up to seven days and the concentration is diluted as cell division continues. Possible off-target effects needs to be evaluated as well. If apoptosis is triggered as an off-target effect of the morpholino, co-injection of p53 morpholino might be considered[89,100]. ENU mutagenesis is utilized to provide random mutagenesis also in zebrafish[101] and Targeted Induced Local Lesions in Genomes (TILLING) method can reveal the mutations caused by ENU[102].

Applying morpholino antisense technology was preferred in the present study since establishment of this technique would be faster compared to other genetic manipulation tools. The data obtained with the transient knockdown of the gene of interest might be investigated further by employing stable knockout systems. Besides, the effects of knockdown of *wdr81* gene in zebrafish is possible to be searched starting from early developmental stages up to seven days post fertilization, which encompasses the critical timepoints of neurodevelopment. This provides an important advantage when it is considered that CAMRQ is a neurodevelopmental disease.

Zebrafish was used as a model organism to investigate cerebellar disorders. Knockdown of ataxin-7 via morpholino microinjection was applied by producing mild and severe phenotypes in order to study spinocerebellar ataxia 7 (SCA7). SCA7 was characterized by loss of Purkinje cells and granule cells of cerebellum and rod-cone photoreceptors.

While severe phenotype ended up with increased lethality of embryos and developmental defects, moderate phenotype led the observations close to the human condition. The differentiation of photoreceptors, Purkinje cells and granule cells was prevented via partial depletion of ataxin-7. Moreover, the phenotypes could be rescued by using human transcript, which might be evaluated as an evidence of conserved function[103]. Another study in which involvement of a gene to a condition was searched by utilizing morpholino technique demonstrated cerebellar and cerebral atrophy. Knockdown of *clpb*, which encodes caseinolytic peptidase B protein homolog, led to this phenotype and proved involvement of the gene of interest to 3-methylglutaconic aciduria, progressive brain atrophy, intellectual disability, congenital neutropenia, cataracts and movement disorder. This phenotype was also rescued via injection of human transcript[104]. Microinjection of sorting nexin 14 (*snx14*) translation blocking morpholino to embryos of a zebrafish line, which expresses GFP in the hindbrain, showed decrease in the intensity of the signal from GFP. Microinjection of the morpholino to embryos of a wild type strain showed decreased number of Purkinje cells. Data from both experiments propose that *snx14* was necessary for hindbrain and formation and survival of Purkinje cells. Rescue was achieved by using the human transcript[105]. Epistatic interaction of two genes was investigated in association with ataxia, dementia and hypogonadotropism. *rnf216*, encoding a ubiquitin E3 ligase and *otud4*, encoding a deubiquitinase were silenced separately in zebrafish and impairments in the cerebellum, optic tectum and eye were obtained. Coinjection of morpholinos targeting both genes showed a more severe phenotype. All the phenotypes were rescued with human transcript[106]. Homozygous mutant zebrafish, carrying loss of function mutation in *qars*, which encodes glutaminyl tRNA synthetase, demonstrated a phenotype similar to human patients. The phenotype was composed of small brain, neurodegeneration and small eye size[107]. A transgenic zebrafish line was generated in order to examine whether excitability of motor neurons were affected by spinocerebellar ataxia type 13 (SCA13) associated mutations. Human dominant mutation in the Kv3.3 voltage-gated K^+ channel was expressed in zebrafish and this mutation was found to be associated with the loss in locomotion and decreased excitability[108]. Another research group utilized from several transgenic lines of zebrafish in order to screen mutations, which affect the development of cerebellum[109]. Hence, zebrafish became an attractive model organism for studying human diseases. Rescuing morphants with human

transcripts helps proving that the function of the gene of interest was conserved through evolution as well. Zebrafish community is also capable of generating stable models such as transgenic lines or mutants. These models might be used to examine the cellular changes underlying the diseases further.

1.2.1. Zebrafish Central Nervous System

Zebrafish central nervous system (CNS) will be discussed under two sections: the first "1.2.1.1. Central Nervous System in Zebrafish Embryos" and the second "1.2.1.2. Central Nervous System in Adult Zebrafish" in order to review information about both the development of the CNS and the developed CNS, respectively.

1.2.1.1 Central Nervous System in Zebrafish Embryos

The neuroectoderm needs to be specified on the dorsal part of the embryo via neural induction in order to form neural plate. The neural plate is transformed into a neural tube following a combination of signaling and morphogenetic movements. The anterior region of the neural tube forms the brain and the posterior region forms the spinal cord[110,111].

Emergence of some critical structures related with zebrafish CNS are earlier than that of mammalians. The brain rudiment appears at sphere stage (blastula, 4-4.33 hpf), primary motor neurons appear at 1-4 somites stage (segmentation, 10.33-11.66 hpf), neural tube appears at 10-13 somites stage (segmentation, 14-16 hpf), cerebellum appears at 26+ somites stage (segmentation, 22-24 hpf), spinal cord appears at prim-5 (pharyngula, 24-30 hpf) and immature eye appears at 5-9 somites stage (segmentation, 11.66-14 hpf)[112].

All of the main components of the brain have formed by 5 days post fertilization (dpf)[85]. The size of the larval brain at 5 dpf facilitates microscopic research *in vivo*. Its thickness is around 500 micrometers and the length is 1.5 milimeters (mm), makes all neurons possible to be studied with this technique[82] (Figure 5).

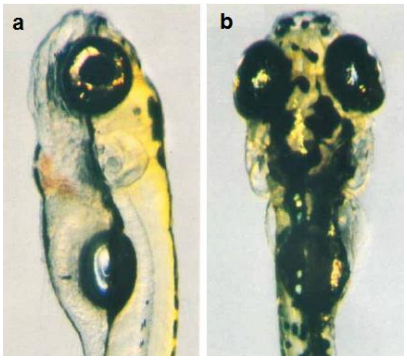

Figure 5. Five dpf wild type zebrafish embryo. *a) Lateral view b) dorsal view*[113]. *Reprinted with permission from John Wiley and Sons.*

1.2.1.2 Central Nervous System in Adult Zebrafish

The regions of the zebrafish adult brain are telencephalon (olfactory bulbs, *ventralis telencephali*, area *dorsalis telencephali*, telencephalic tracts and commissures), diencephalon (*area praeoptica*, epithalamus, dorsal thalamus, ventral thalamus, posterior tuberculum, hypothalamus, synencephalon, pretectum, diencephalic tracts and commissures), mesencephalon (*tectum opticum*, *torus semicircularis*, tegmentum), rhombencephalon (cerebellum, medulla oblongata), *medulla spinalis* and brain stem[114]. One of the most striking features of adult zebrafish brain is the dominance of the optic tectum in the dorsal midbrain, as also observed in other teleosts. One disadvantage of studying with zebrafish telencephalon is eversion of this region dorsally, which is not present in other vertebrates (Figure 6). This feature, partly causes difficulties in finding homologous regions between fish and mammalian forebrain regions[85].

The length of the adult zebrafish brain is around 4.5 mm and its thickness is between 0.4 -2 mm. The zebrafish brain size and number of neurons enable research with advanced microscopy techniques such as multiphoton microscopy and 3D electron microscopy (Figure 6). Since activity analysis and connectivity pattern studies possess size restrictions from a circuit neuroscience point of view[82].

1.3. Cell Proliferation in Zebrafish Nervous System

The differentiated cells of the central nervous system originate from multipotent neuroepithelial stem cells. These stem cells give rise to mature and functional neurons or glia after the processes called neurogenesis and gliogenesis, respectively[115]. Because of this phenomenon, cell proliferation in zebrafish central nervous system will be discussed under two titles of "1.3.1. Neurogenesis in Zebrafish" and "1.3.2. Gliogenesis in Zebrafish".

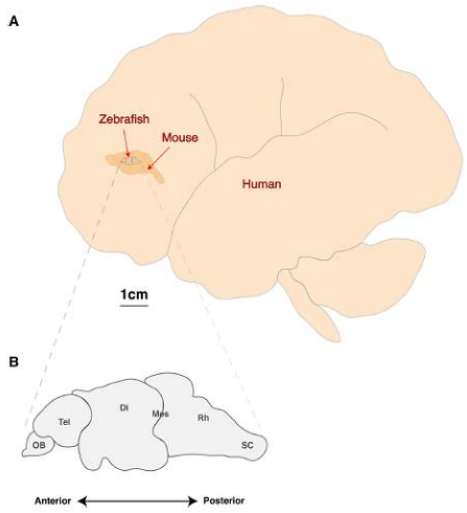

Figure 6. Illustration which compares the brain sizes of human, mouse and zebrafish. *(A) Comparison of the lateral views of the adult brains from three species to scale. (B) Major brain areas of zebrafish in a linear plane. OB, olfactory bulb; Tel, Telencephalon; Di, Diencephalon; Mes, Mesencephalon; Rh, Rhombencephalon; sc, Spinal cord*[116] *(By courtesy of Associate Professor Philippe Mourrain). The small size of the zebrafish brain enables observation of the whole brain under microscopy, especially in neuroscience research.*

1.3.1. Neurogenesis in Zebrafish

Neurogenesis is defined as the process which first starts with neural induction and ends up with differentiated functional neurons[117]. Neurogenesis in zebrafish will be discussed under two sections: the first "1.3.1.1. Neurogenesis in Zebrafish Embryos" and the second "1.3.1.2. Neurogenesis in Adult Zebrafish".

1.3.1.1. Neurogenesis in Zebrafish Embryos

Neural induction, which is defined as specification of the neuroectoderm, is required before neurogenesis. Neural induction is directed by extrinsic and intrinsic factors. Indeed, the interplay of extrinsic bone morphogenetic protein (BMP), wingless-integrated (Wnt) and fibroblast growth factor (Fgf) family members and intrinsic factors (SRY-box containing genes B1 (SoxB1) family members) decides the vertebrate neural induction. After the neuroectoderm is specified, it forms the neural plate[111]. The neural plate is converted into the neural tube as a result of the process called as neurulation. In contrast with most vertebrates, zebrafish generates the neural keel. The neural plate is firstly transformed into a solid structure in zebrafish instead of folding the lateral edges of the neural plate and forming a tube with a lumen by fusing the edges in the dorsal midline. However the typical neural tube is obtained after the cells in the center detach. Despite the differences, fish and mammals produce very similar neural tubes[111,118].

Neurogenesis take place in two stages in zebrafish: primary neurogenesis and secondary neurogenesis. Primary neurogenesis starts at late gastrulation and proceeds during embryogenesis. This process yields early-born, big neurons which possess long axons. The brain epiphyseal and post-optic clusters, Rohon-Beard sensory neurons, Mauthner cells, and the three types of primary spinal motoneurons (the rostral (RoP), middle (MiP) and and caudal (CaP) are produced as a result of primary neurogenesis. The primary neurons form the first functional neuronal scaffold at embryonic and early larval development. Axonogenesis starts to appear between 14-24 hpf[119]. Secondary

neurogenesis, which is also called postembryonic neurogenesis starts at around 2 dpf in zebrafish. This second stage of neurogenesis turns the primary system into a network which gets more fine-tuned and complex[120]. Neuronal migration, differentiation and survival are the critical steps of producing functional neurons after the cells leave mitosis and multipotent progenitors determine particular cell types[119].

1.3.1.2. Neurogenesis in Adult Zebrafish

Although adult mammals have a restricted neurogenic capacity, teleosts including zebrafish possess a larger potential for neurogenesis. Two neurogenic areas in adult mammalian brain are the subventricular zone (SVZ) of the lateral ventricle and the subgranular zone (SGZ) of the dentate gyrus in the hippocampus[121]. Neurogenic regions in the adult zebrafish brain are more widespread and there are regions homologous to mammalian SVZ and SGZ. The number of newly born cells in the adult zebrafish brain is approximately 6000 cells during every 30 minutes[111].

The zebrafish has become an attractive model for adult neurogenesis studies in recent years both because of the extensive capacity of neurogenesis and its advantages over mammalian models. In contrast to mammalian neural tissue, zebrafish brain does not exhibit scar formation after an injury. The zebrafish is a promising model organism to ultimately devise a theurapeutic approach for humans by providing the mechanisms of the plasticity and of regeneration by suppressing the scar formation[111].

1.3.2. Gliogenesis in Zebrafish

Gliogenesis, which is defined as the generation of mature glia cell types, in zebrafish will be discussed under two sections: the first is “1.3.2.1. Gliogenesis in Zebrafish Embryos” and the second is “1.3.2.2. Gliogenesis in Adult Zebrafish”.

1.3.2.1. Gliogenesis in Zebrafish Embryos

Glial cell types in central nervous system of mammals are macroglia (astrocytes, oligodendrocytes and ependymocytes) and microglia. Schwann cells, satellite glial cells, and enteric glia constitute the glial cell types in the peripheral nervous system of mammalian organisms. The glial cell types in zebrafish have not been described profoundly yet, however there is an accumulating data about the similarities between the glial cells of fish and mammals[89].

Glial cells appear at 26+ somites stage (segmentation, 22-24 hpf) in zebrafish[112]. Oligodendrocytes, in both mammals and zebrafish, appear to originate from the ventral regions of the neural tube. Oligodendrocyte precursor cells migrate to the appropriate regions and divide in the central nervous system. They, then leave the cell cycle and cover axons with myelin sheath[89,115]. Schwann cells of both mammalian organisms and zebrafish generate from neural crest tissues and the developmental process they pass through is similar. During the process, they migrate to and eventually cover peripheral axons with myelin sheath[89].

Radial glia cells and a subpopulation of astrocytes serve as neural stem cells in the adult mammalian brain. Neurons, ependymal cells, astrocytes, intermediate progenitor cells that give rise to neurons (nIPCs), and intermediate progenitor cells that give rise to oligodendrocytes (oIPCs) originate from the neuroepithelial-radial glia-astrocyte line[122].

1.3.2.2. Gliogenesis in Adult Zebrafish

As previously mentioned under "1.3.2.1. Zebrafish Embryo" section, zebrafish possesses mammalian counterparts of oligodendrocytes and Schwann cells. Expression analysis showed that satellite and enteric glia of zebrafish are also similar to their

mammalian counterparts[123,124]. Ependymal cells have not been detected in zebrafish and low number of cells are detected with the known star shaped morphology of astrocytes. Radial glia cells appear to carry the characteristics of ependymal cells and astrocytes and to fulfill their functions. A large number of radial glia cells in zebrafish express glial fibrillary acidic protein (GFAP), gluthamine synthase and aquaporin-4. GFAP and gluthamine synthase are markers often used to detect astrocytes in mammalian model organisms and aquaporin-4 is a water channel found on astrocytes[89]. Microglia are present in zebrafish. The origin of microglia cells is mesoderm[125] and they are mononuclear phagocytes, which function in the defense of the central nervous system[126,127].In both mammals and zebrafish this glial cell type takes place in the parenchyma of the central nervous system[126].

Gliogenesis continues in the adult zebrafish as neurogenesis does; radial glia cells and a subpopulation of astrocytes can re-enter the cell cycle and can give rise to macroglia cell types as well as to neurons[128]. The radial glia cell population reduces in the adult mammalian brain, but still in the neurogenic areas of the brain, which are the subventricular zone (SVZ) of the lateral ventricle in telencephalon and the subgranular zone (SGZ) of the dentate gyrus in the hippocampus, some radial glia cells serve as neural stem cells. In contrast to mammalian adult brain, zebrafish holds the large numbers of radial glia cells both in the late embryonic development and during adulthood[89].

1.4. Synaptogenesis in Zebrafish

Synaptogenesis is a multi-step process to form synapses. This process is critical in neurodevelopment and has a continuing significance in learning, memory, plasticity, cognition and adaptation throughout adulthood[129,130]. Synapses are the contact sites of neurons where one transfers signals to another. These signals might be either electrical or chemical. Chemical synapses are more common in the vertebrate nervous system. Electrical signals, in the form of action potential, start at the axon hillock and then move

through the axon of the neuron, arrive at the presynaptic terminal and this triggers a release of neurotransmitters into the synaptic cleft. This is where electrical signal is converted into a chemical one. The neurotransmitters bind to their receptors at the membrane of the postsynaptic neuron. The signal is converted back to electrical one within the postsynaptic dendrite. Excitatory chemical synapses are asymmetric structures, and inhibitory chemical synapses are symmetric structures and occur between neurons and other neurons, muscles or glands[130].

Synaptic vesicle fusion does not take place randomly, active zones are specialized sites for synaptic vesicles to dock and fuse with the plasma membrane in the presynaptic terminal. Another specialized region in the postsynaptic membrane which is occupied with the receptors, secondary messenger molecules and voltage-gated ion channels is called postsynaptic density. The size, organization and thickness of the active zone and postsynaptic density of the synapses in the central nervous system depend on three parameters: type of the synapse, function of the synapse and efficacy of the synapse. Type of the synapse is defined by the type of the released neurotransmitter. The synapse might be classified into three groups based on their functions: excitatory, inhibitory or modulatory. Efficacy of the synapses is determined by its reliable or unreliable, continous or sporadic activity[130].

Synaptogenesis in neurodevelopment starts in embryonic stages and continues through early postnatal stage. It is closely related with neuronal differentiation and formation of the neural circuits. The genes which encode synaptic proteins are activated a short time after the neurons differentiate and form their axons and dendrites. The axons and dendrites make some contacts and form synapses. These initial synapses are frequently transient. A set of molecules and proteins (such as receptors and cell surface adhesion molecules) and signaling process (specialization of active zone and postsynaptic density) are required for synapse formation. Eventually, the decision on keeping or eliminating a synapse is determined based on its activity both during neurodevelopment and processes going on in mature brain[130].

Synaptogenesis starts at around 18 hpf in zebrafish[84]. Zebrafish embryos are very suitable for *in vivo* time-lapse imaging since they are small in size and transparent and they develop externally and quickly. The central nervous system of the embryo is simpler than higher organisms. Research on synaptogenesis in order to answer fundamental questions using zebrafish embryos have been established by employing imaging techniques (confocal and multiphoton microscopy) and the genetic techniques which utilize flourosencent labeling of neuronal proteins[131]. Zebrafish mutants also serve to unravel the mechanisms underlying synaptogenesis. For example embryos of a motility mutant *sofa potato* revealed that the paralysis is because of the lack of nicotinic acetylcholine receptors. The synaptic transmission is defective and postsynaptic complex formation is not complete[132]. Neuromuscular junctions are also extensively used models of synaptogenesis studies in adult zebrafish. A zebrafish mutant line, which carries a homozygous null mutation in growth differentiation factor 6a (*gdf6a*) gene, was grown to adulthood. Nine months old *gdf6a*$^{-/-}$ adult zebrafish were found to develop impaired neuromuscular junction. Mean volume of the synapse was higher and the volume of presynaptic motoneuron was around 3 fold higher than the wild-type siblings in the mutants. These findings also serve as clues to the mechanisms of neuromuscular degenerative diseases[133].

1.5. Aim and Scope of This Study

Human and mouse studies indicate the potential importance of *WDR81* gene in neurodevelopment and metabolism. We conducted research on the orthologue of mammalian *WDR81* gene in zebrafish since this was a novel gene and this model organism is ideally suited to observe changes during development when the gene is knocked down. The observation of the changes during development when the protein product is depleted might indicate the causality and progression of CAMRQ. The hypothesis of this study is "*wdr81* is a critical gene in neurodevelopment as suggested for human and mouse orthologs and this can be proven by detecting the conserved domains and shared expression sites which will lead to reveal a conserved function among species". Our first aim in this study to test this hypothesis was to characterize the *wdr81* transcript and to reveal the temporal and spatial expression of the gene of

interest. Our second aim was to introduce the initial characterization of *wdr81* morphants. The findings from our work are expected to give rise to an understanding of the potential role of *wdr81* during development.

In order to fulfill our first aim in this study, we characterized the 5' untranslated region (UTR) and 3'UTR of *wdr81* transcript, amplified the open reading frame (ORF) of the transcript, and investigated the temporal and spatial expression of *wdr81* in zebrafish. We also aligned the sequences of human, mouse and zebrafish putative WDR81 proteins. This alignment showed that identical conserved domains are predicted in all three orthologous proteins, indicating that the function of the protein of interest might be conserved in these three species as well.

In order to address our second aim in this study, we performed morpholino microinjections to zebrafish embryos. Morpholino microinjections were performed to knockdown *wdr81* and to observe the development of the zebrafish embryos in the absence of a functional protein product of *wdr81*. We measured the head size of 4.25-4.5 dpf embryos by taking body length into consideration. This measurement would indicate a result related to the global changes in the development of the brain, such as a microcephaly phenotype. Another initial characterization study was carried out using whole mount *in situ* hybridization (WMISH) method with a cerebellum marker (*gbx2*) on *wdr81* morphants to see how the expression of a cerebellum related gene is affected by knockdown of *wdr81*. The findings from our work will provide a basis to fully discover the function of *wdr81* along with the future research.

Chapter 2. Materials and Methods

2.1. Methods

2.1.1. Zebrafish and Embryos

AB strain of zebrafish (*Danio rerio*) was used as a model organism in the experiments. Embryos from pairs were collected in petri dishes and raised in E3 medium[85]. The zebrafish and embryos were kept under 14 hours light and 10 hours dark cycle at 28°C in the zebrafish facility of the Department of Molecular Biology and Genetics, Bilkent University, Ankara, Turkey. The Bilkent University Local Animal Ethics Committee (HADYEK) approved the protocol for experiments in this study in which zebrafish samples are used. The approval date was 10 October 2010 and the protocol number was 2010/31.

2.1.2. Bioinformatics Analysis

The homologous protein sequences of WDR81 from human, mouse and zebrafish were aligned and compared in order to detect the presence and location of the conserved domains. The aminoacid sequences of human WDR81 (encoded by the transcript ENST00000409644), mouse Wdr81 (encoded by the transcript ENSMUST00000173320) and zebrafish wdr81 (encoded by the transcript ENSDART00000156621) were derived from Ensembl database[24] and aligned with Clustal Omega[134]. The file obtained as a result of the alignment was submitted to ESPript 3.0 software[135]. This software highlights the similar sequences at specific locations. The locations of BEACH and WD40 domains, which are predicted by SMART database[136] and MFS domain, which is predicted by CLC software (CLC Main Workbench software package, CLC Bio Inc) were detected on the ESPript 3 output file.

TMpred software was used to calculate the membrane spanning regions of the zebrafish wdr81[137]. The splice variants of *WDR81* of human (ENSG00000167716), mouse (ENSMUSG00000045374) and zebrafish (ENSDARG00000079702) genes were derived from Ensembl[24]. The WDR81 protein sequences of the species were aligned by using Clustal Omega[134]. The accession numbers for WDR81 orthologs were XP_002918082 (*Ailuropoda melanoleuca*), JAB47838 (*Callithrix jacchus*), XP_002664681 (*Danio rerio*), XP_001502383 (*Equus caballus*), XP_415806 (*Gallus gallus*), XP_007485816 (*Monodelphis domestica*), NP_620400 (*Mus musculus*), XP_002718930 (*Oryctolagus cuniculus*), XP_003952981 (*Pan troglodytes*), XP_002826860 (*Pongo abelii*), NP_001157281.1 (*Homo sapiens*), NP_001127832 (*Rattus norvegicus*), JAA74278 (*Sus scrofa*), XP_012424209 (*Taeniopygia guttata*), CAG08933 (*Tetraodon nigroviridis*), XP_002937192 (*Xenopus tropicalis*). A similar list of orthologous proteins were also used by Gulsuner *et al*. (2011) in order to prepare the phylogenetic tree of protein sequences of WDR81 in vertebrates[12] (Figure 3). Zebrafish wdr81 (encoded by the transcript ENSDART00000156621) amino acid sequence was submitted to the tblastn database of NCBI[138] in order to detect the rate of similarities between wdr81 and other genes encoding WD repeat containing proteins in zebrafish genome.

2.1.3. Characterization of the *wdr81* Transcript

The aim was the characterization of zebrafish *wdr81* transcript in order to reveal whether there are more than one transcripts as in human and mouse. In order to fulfill this aim, the open reading frame and cDNA ends of the transcript of interest were described. The transcript prediction released by Ensembl (ENSDART00000156621) was used as a model for designing primers in these experiments since *wdr81* was not characterized previously.

2.1.3.1. Amplification of the Open Reading Frame of *wdr81*

Thirty 24 hours post fertilization (hpf) zebrafish embryos and pooled brains of five 10 month old male zebrafish were collected. Total RNA of embryos and brains were isolated with a Trizol reagent (15596018, Ambion, USA) and genomic DNA was removed using DNase (AM1907, Turbo DNA free, Ambion, USA). Five hundred nanogram (ng) of total RNA was used to synthesize cDNA (04379012001, Transcriptor First Strand cDNA Synthesis Kit, Roche, USA). Ten primer pairs, which produce overplapping amplicons and cover the open reading frame (ORF) of *wdr81* were designed (Table 3).

Table 3. Primer pairs designed to characterize the open reading frame of *wdr81* *(Reprinted from Doldur-Balli et al., 2015*[139]*)*

		Primer Sequence	Annealing Temperature	Expected Amplicon Size (bp)
Pair 1	F	5'-GCAAACAGTGCAGAGCTTCTT-3'	60 °C	897
	R	5'-GCTGCTCATCAACTGCAATATC-3'		
Pair 2	F	5'-CCTATCCACCTGCTCAGCTC-3'	60 °C	874
	R	5'-AACATGGCTGCATAGCACAG-3'		
Pair 3	F	5'-CCAGATCTTGGTGGACCAGT-3'	60 °C	909
	R	5'-TCTGTGAAGCATGGCAGTTC-3'		
Pair 4	F	5'-TTGGTTTGGTTGTGTCTCCA-3'	60 °C	875
	R	5'-ATACCAGGCCGCATAAACAG-3'		
Pair 5	F	5'-CTCCATCATGCACTGGACAC-3'	60 °C	920
	R	5'-CCAACTGTTGTTGCTCCAGA-3'		
Pair 6	F	5'-GCCACATCTTCTGGCAAAGT-3'	55 °C	979
	R	5'-TGAGTACCACAGCACCCAAA -3'		
Pair 7	F	5'-GAGACCAGACTGCAAGACCAG-3'	55 °C	698
	R	5'-ACTTGCTCGTTCGTGGTAAGA-3'		
Pair 8	F	5'-GCAGAGTGCACATACCTGGA-3'	60 °C	704
	R	5'-TGGAAGTGGAAGTGGGAGTC-3'		
Pair 9	F	5'-AACAGGACCTTCCACGTAGC-3'	60 °C	896
	R	5'-TGTGCTGTCCAGAATGGAGT-3'		
Pair 10	F	5'-CACAAGCCACTCCACCAGTA-3'	60 °C	429
	R	5'-CGCGGAGGTTGTAAGTTCTC-3'		

Negative control templates, which do not include reverse transcriptase enzyme in the cDNA synthesis reaction (-RT), were added to the experiment in order to eliminate the possibility of genomic DNA contamination. The amplicons obtained as a result of amplification of ORF were loaded to a 1% agarose gel.

2.1.3.2. Rapid Amplification of cDNA Ends (RACE)

The rapid amplification of cDNA ends (RACE) method was utilized in order to characterize 5' UTR (untranslated region) and 3'UTR of zebrafish *wdr81*. The samples were DNase treated (RNase free DNase set, 79254, Qiagen, Germany) total RNA (RNeasy Mini Kit, 74104, Qiagen, Germany) from forty 24 hpf embryos and pooled brains of three 10 month old male zebrafish.

2.1.3.2.1. Characterization of the 5'RACE Product

The GeneRacer™ kit (L1500-01, RLM-RACE, Invitrogen, USA) was used to define the 5' end of *wdr81*. The experiments were performed by following the manual from the kit. Twenty-four hpf embryo and adult brain total RNA samples were treated with a few enzymatic steps before being converted into RACE-ready cDNAs. The enzymatic steps are composed of treatment with calf intestinal phosphatase (CIP) and tobacco acid pyrophosphatase (TAP) and ligation with an RNA oligonucleotide. Briefly, CIP enzyme clears away the RNA structures, which are not capped, by removing the 5' phosphates and then TAP renders full length mRNA with a 5' phosphate group by removing the 5'cap structure. Then, RNA oligonucleotide (GeneRacer™ RNA oligo), whose sequence is known, is ligated to the full-length mRNA with the 5' phosphate group. RNA oligonucleotide is ligated to serve as a binding site for the GeneRacer™ 5′ primer and GeneRacer™ 5′ nested primer. The mRNA samples, which have the GeneRacer™ RNA Oligo in the 5' upstream region, were converted to RACE-ready cDNAs with Cloned AMV reverse transcriptase and the GeneRacer™ oligo dT primer. A touch

down PCR was performed to amplify the RACE-ready cDNA with a primer pair composed of GeneRacer™ 5′ Primer (5'CGACTGGAGCACGAGGACACTGA-3') and a gene specific primer (wdr81_Racer-5E2, 5'-ACAGTTTCTGCAGGGCTTGACGAAC-3'). The reaction conditions of touch down PCR were: 30 sec. at 94 °C, 30 sec. at 94 °C, 40 sec. at 72 °C, 45 sec. at 68 °C for 5 cycles; 30 sec. at 94 °C, 40 sec. at 71 °C, 45 sec. at 68 °C for 5 cycles; 30 sec. at 94 °C, 40 sec. at 70 °C, 45 sec. at 68 °C for 25 cycles; and 5 min. at 68 °C. The embryo and brain amplicons obtained from the touch down PCR were diluted at a 1:10000 ratio and used as templates for a nested PCR. Nested PCR following touch down PCR was performed to produce a specific *wdr81* 5'RACE product (Figure 14). A nested PCR using a primer pair composed of GeneRacer™ 5′ nested primer (5'-GGACACTGACATGGACTGAAGGAGTA-3') and a gene specific nested primer (wdr81_Racer-5E2_Nested, 5'-CTGCATATGGCTGCACATGAGTC-3') was performed under the following reaction conditions: 30 sec. at 94 °C; 30 sec. at 94 °C, 40 sec. at 72 °C, 50 sec. at 68 °C for 30 cycles; and 5 min. at 68 °C. PCR products were loaded to a 1% agarose gel, run and seperated using electrophoresis. One specific 5'RACE product of *wdr81* from embryo and brain samples were excised from the gel and purified (K220001, Pure-Link Quick Gel Extraction and PCR Purification Combo Kit, Invitrogen, USA). The purified DNA fragments from embryo and brain samples were cloned (45-0071, Topo TA Cloning Kit for Sequencing, Invitrogen, USA) and single colonies, that grew under both ampicilin and kanamycin treated conditions, were picked up. Plasmids isolated from the selected colonies (K2100-11, Purelink Quick Plasmid Miniprep Kit, Invitrogen, Germany) were analyzed with restriction endonuclease digestion (EcoRI, ER0271, Fermentas) and the insert containing plasmids were sequenced. The Sanger sequencing results were examined with CLCBio Main Workbench software package (CLCBio Inc).

2.1.3.2.2. Characterization of the 3'RACE Product

The GeneRacer™ kit (L1500-01, RLM-RACE, Invitrogen, USA) was used to define the 3' end of *wdr81*. The experiments were performed according to the manual from the kit. The total RNA isolated from 24 hpf embryo and adult brain were converted to RACE-ready cDNA with cloned AMV reverse transcriptase and the GeneRacer™ Oligo dT primer. While synthesizing cDNA, the GeneRacer™ Oligo dT primer introduces a sequence to the 3' downstream of the full length mRNA, which serves a binding site for GeneRacer™ 3′ Primer. The RACE-ready cDNA samples from embryo and adult brain were amplified with 3 primer pairs, which were designed to obtain 3 overlapping amplicons to ultimately obtain 3' RACE product of *wdr81* (Table 4, Figure 18). Negative control reactions, without a template, were included to the experiments as well. The steps of the reaction 1 with the primer pair 1 (Table 4) were: 40 sec. at 98 °C; 10 sec. at 98 °C, 30 sec. at 68 °C, 35 sec. at 72 °C for 30 cycles; and 5 min. at 72 °C. The steps of the reaction 2 with primer pair 2 (Table 4) were: 40 sec. at 98 °C; 10 sec. at 98 °C, 30 sec. at 64 °C, 40 sec. at 72 °C for 30 cycles; and 5 min. at 72 °C. The steps of the reaction 3 with primer pair 3 (Table 4) were: 2 min. at 95 °C; 30 sec. at 95 °C, 30 sec. at 61 °C, 60 sec. at 72 °C for 30 cycles; and 7 min. at 72 °C. The PCR products of these three experiments were run on a 1% agarose gel and a single band per reaction was observed, then the PCR products were sent to Sanger sequencing. The sequencing results were examined with CLCBio Main Workbench software package (CLCBio Inc).

Although the reactions 1 and 3 gave PCR products as predicted, the PCR product of the reaction 2 was observed to be larger than the predicted size. This result indicated presence of an insertion site within the PCR product obtained with primer pair 2 (Table 4). A new primer pair was designed to characterize the insertion site by amplifying it within a narrower frame. RACE-ready cDNA from the same source as used in reactions 1-3 was used as a template in a PCR experiment with this new primer pair, which was composed of a forward (5'-CATTATTATCTCCAGACATTCCAA-3') and a reverse primer (5'-TGAGGGAATTAGCGAACCAT-3'). The reaction conditions of this amplification were: 40 sec. at 98 °C; 10 sec. at 98 °C, 30 sec. at 58 °C, 30 sec. at 72 °C

for 30 cycles; and 5 min. at 72 °C. This experiment was designed to observe a 250 base pair (bp) long PCR product if the insertion site is not present in the sample and if at the same time the predicted sequences flanking the insertion site are present.

Table 4. Primer sets designed to obtain three overlapping amplicons in order to characterize 3'UTR of *wdr81* *(Reprinted from Doldur-Balli et al., 2015*[139]*)*

	Primer	Primer Sequence	Expected amplicon size, bp
Pair 1	F (Pair1F_Drwdr81_3 RACE)	5'-CTGACAACGGTGCCATCAGG-3'	717
	R (Pair1R_Drwdr81_ 3RACE)	5'-TTCAGGACCATCCCATTGCATA-3'	
Pair 2	F (Pair2F_Drwdr81_3 RACE)	5'-CTGTATCCACGTCAATGGAGCGTAA-3'	757
	R (Pair2R_Drwdr81_ 3RACE)	5'-GAAGCATTGTTCAATGTACGTTCGGTA-3'	
Pair 3	F (Pair3F_Drwdr81_3 RACE)	5'-CATTTATGGTTCGCTAATTCCCTCAA-3'	634
	R (GeneRacer™ 3′ Primer)	5'-GCTGTCAACGATACGCTACGTAACG-3'	

Firstly, embryo and brain samples were amplified with this primer pair and the amplicons were cloned (A1360, pGEM-T Easy Vector System I, Promega, USA). Single white colonies generated based on blue/white screening were picked up. The plasmids from the selected colonies were isolated (K2100-11, Purelink Quick Plasmid Miniprep Kit, Invitrogen, Germany) and 3 plasmids per sample type (ie. 24 hpf embryo and adult brain) were sent to Sanger sequencing. The results of the sequencing were examined with CLCBio Main Workbench software package (CLCBio Inc). Then the

presence of the insertion site in samples from different developmental timepoints and different adult tissues was planned to test. In order to fulfill this purpose, cDNAs of 10 adult tissues and of samples from 10 developmental timepoints were amplified with the same primer pair. The cDNA samples from the same sources were amplified with a house keeping gene primer pair (a beta-actin gene primer pair-forward, 5'-ATTGCTGACAGGATGCAGAAG-3' and reverse, 5'-GATGGTCCAGACTCATCGTACTC-3')[140] to observe whether the samples were present and intact. The PCR products of this experiment were run on a 1% agarose gel. The band intensities of the amplicons were measured by using Image J program[141].

2.1.4. Analysis of the Expression of *wdr81* in Wild Type Zebrafish

The expression of *wdr81* in wild type adult zebrafish and during developmental stages were studied with quantitative real-time pcr (qRT-PCR) and *in situ* hybridization methods.

2.1.4.1. Quantitative Real-Time PCR (qRT-PCR)

The temporal expression of *wdr81* was studied with the samples from 10 developmental timepoints. Thirty embryos from 1 hpf, 5 hpf, 10 hpf, 18 hpf, 24 hpf, 48 hpf, 72 hpf and 5 dpf, eight larvae from 15 dpf and eight juvenile fish from 35 dpf stages were collected. Spatial expression of *wdr81* was studied with 10 adult tissues; brain, testis, heart, kidney, liver, intestine, eye, gills, tail and muscle. Each tissue was pooled from five 10 month old male zebrafish. A Trizol reagent (15596018, Ambion, USA) and a homogenizer (Bullet Blender, Next Advence, Storm 24) were utilized to isolate total RNA from all samples. The isolated total RNA samples were treated with DNase (AM1907, Turbo DNA free, Ambion, USA) and 500 nanogram (ng) of RNA, after removal of genomic DNA, were used in cDNA synthesis reaction (05081955001,

Transcriptor High Fidelity cDNA Synthesis Kit, Roche, Germany). The Roche Light-Cycler 480 System was employed to perform the qRT-PCR experiments.

The cDNA samples were used at 1:4 dilution ratio and 5 microliters (µl) of diluted cDNA was used as a template in each reaction. The primers and probes designed to detect *wdr81* expression were selected from Universal Probe Library Assay Design Center, which provides zebrafish specific assays (Table 5, Figure 7). A primer pair and a probe to detect ß-actin expression were added as well (Table 5). The experiments were planned to include 400 nanomolar (nM) of forward and reverse primers and 200 nM of probes in a 20 µl reaction volume. The experiments were carried out in duplicates on each plate and were repeated 3 times and included negative control samples, -RT and without a template. The reaction steps were composed of 10 min. at 95 °C; 10 sec. at 95 °C, 30 sec. at 60 °C, 1 sec. at 72 °C for 45 cycles; and 30 sec. at 40 °C. The Ct values were derived from LCS480 software (Roche, Germany) and the $2^{-\Delta\Delta Ct}$ method was applied to calculate the fold changes for comparison. The ΔCt value of each reaction was obtained by substracting the Ct value of ß-actin reaction from the Ct value of *wdr81* reaction. Fold changes in expression were calculated according to the ΔCt value of 15 dpf larva in order to obtain relative temporal expression profile and of brain in order to obtain relative spatial expression profile. $2^{-\Delta\Delta Ct}$ formula was applied on Excel program (Microsoft Office Excel 2007) and standard error of the mean (SE) was calculated using Graphpad[142]. The graphics of the relative temporal and spatial expression including +standard error were prepared with GraphPad[142].

Table 5. Primer pairs and probes to be used in qRT-PCR *(Reprinted from Doldur-Balli et al., 2015[139]).*

Gene	Primers	Sequence	Probes
wdr81	F	5'-TCTCATGCAGGGAGTATCACA-3'	Probe 46 (cat. no.04688066001, Roche)
	R	5'-AGGTGTCTGCTCAACGGAAT-3'	
ß-Actin	F	5'-GCCTGACGGACAGGTCAT-3'	Probe 104 (cat. no.04692225001, Roche)
	R	5'-ACCGCAAGATTCCATACCC-3'	

2.1.4.2. *In situ* Hybridization Experiments

The expression of *wdr81* both on whole mount embryos from several developmental stages and on adult tissues, brain and eye, was examined using a gene specific probe.

2.1.4.2.1. Whole Mount *In Situ* Hybridization (WMISH) on Embryos

The spatio-temporal expression of *wdr81* on whole mount embryos from 6 hpf, 10 hpf, 18 hpf, 24 hpf, 48 hpf and 72 hpf timepoints was investigated with an RNA probe. The probe was prepared by amplifying the region of *wdr81* transcript between primer pair 5 (5F) and primer pair 6 (6R) from Table 3. This region is corresponding to the site of mutation in patients. The template for probe preparation was 24 hpf embryo cDNA and the reaction steps for amplification were: 2 min. at 95 °C, 30 sec. at 95 °C, 30 sec. at 62 °C, 2 min. at 72 °C for 35 cycles; and 7 min. at 72 °C. The amplicon was observed in a 0.8% agarose gel, the single band was excised from the gel and the DNA fragment was purified (D4007, Zymoclean Gel DNA Recovery Kit, USA). The fragment was cloned into a pGEM-T Easy vector (A1360, pGEM-T Easy Vector System I, Promega, USA) and single white colonies which grew based on blue/white screening were picked up. The plasmids were analyzed with restriction endonuclease digestion (NspI, ER1472, Fermentas) to observe the presence and orientation of the insert. The selected plasmid was linearized with NdeI (ER0582, Fermentas) and SalI (ER0645, Thermo Sceintific) double digestion in order to use it as a template in antisense probe synthesis. The linearized plasmid was excised from a 0.8% agarose gel and was purified (D4007, Zymoclean Gel DNA Recovery Kit, USA) and the probe synthesis reaction was set up with T7 enzyme mix (AM1320, MaxiScript SP6/T7 *In Vitro* Transcription Kit, Ambion, USA) and DIG labeling mix (11277073910, DIG RNA Labelling Mix, Roche, Germany).

The embryos from the timepoints mentioned above were collected, fixed in 4% paraformaldehyde (FB001, Invitrogen IC Fixation Buffer, Invitrogen, USA) and saved in 100% methanol after dehydration steps with increasing percentages of methanol. Embryos can stay in 100% methanol at -20°C until they are used in the experiment. The rehydration, bleaching, proteinase K digestion, post fixation, hybridization, probe wash, antibody incubation (anti-digoxigenin-AP, Fab fragments, 11093274910, Roche, Germany) and staining steps (BM purple, 11442074001, Roche, US) were performed by following the previously described protocol[143] with some modifications. The images of embryos from 6 hpf, 10 hpf, 18 hpf, 24 hpf, 48 hpf and 72 hpf stages were obtained with Zeiss Stereomicroscope Discovery V220 (Carls Zeiss, Germany) at 72x, 130x, 105x, 61x, 50x and 46x magnifications, respectively. The images of head regions of embryos from 18 hpf, 48 hpf and 72 hpf stages were obtained at 150x, 118x and 100x magnifications, respectively. Transverse sections at 20 micrometer (µm) thickness were collected from the head regions of 18 hpf, 48 hpf and 72 hpf embryos, which were WMISH specimens, with a cryostat (CM 1850, Leica) and the images of the sections were obtained with a brightfield upright microscope (Fluorescent and DIC equipped upright microscope, Zeiss, Germany).

2.1.4.2.2. *In Situ* Hybridization (ISH) on Brain and Eye Tissues

The expression of *wdr81* was investigated on coronal sections at 10 µm thickness from brain and eye tissues. A cryostat (CM 1850, Leica, Germany) was used to obtain sections from the tissues of a wild type 10 month old adult male. The antisense probe was synthesized as explained in the "2.4.2.1. Whole Mount *In Situ* Hybridization (WMISH) on Embryos" section and the same plasmid construct was used in preparation of sense probe. The plasmid was linearized with NcoI (FD0573, Thermo Fisher Scientific) and ApaI (ER1411, Thermo Fisher Scientific) double digestion in order to use it as a template in sense probe synthesis. The linearized plasmid was excised from a 0.8% agarose gel and was purified (D4007, Zymoclean Gel DNA Recovery Kit, USA). The probe synthesis reaction was set up with SP6 enzyme mix (AM1320, MaxiScript

SP6/T7 *In Vitro* Transcription Kit, Ambion, USA) and DIG labeling mix (11277073910, DIG RNA Labelling Mix, Roche, Germany).

The experiment was performed as previously described[12]. The sections were fixed in 4% paraformaldehyde (FB001, Invitrogen IC Fixation Buffer, Invitrogen, USA), acetylated, and incubated with the probes at 60 °C overnight. Following these steps, the probe was washed, the tissue sections were incubated with antibody (anti-digoxigenin-AP, Fab fragments, 11093274910, Roche, Germany) and stained with the solution including 4-Nitro blue tetrazolium chloride solution (NBT) (11383213001, Roche, Germany), 5-bromo-4-chloro-3-indolyl-phosphate 4-toluidine salt (BCIP) (11383221001, Roche, Germany) and levamisole (SP-5000-18, Vector Lab). The images of the sections were taken with a brightfield upright microscope (Fluorescent and DIC equipped upright microscope, Zeiss, Germany).

2.1.5. Morpholino Microinjections to Knockdown *wdr81*

Morpholino antisense oligos contain morpholine rings instead of deoxy ribose or ribose rings in DNA and RNA, respectively and contain adenine, cytosine, guanine and thymine bases. They contain uncharged phosphorodiamidate intersubunit bonds instead of negatively charged phosphodiester bonds, which take place in the nucleic acids. The length of a morpholino sequence is generally 25 oligos. The morpholino oligos are used to knockdown a gene of interest and they are introduced to the yolk region of zebrafish embryos via microinjection. They might be designed to target the translation initiation site, pre-mRNA splicing or maturation of microRNAs[144]. Since targeting translation initiation site of a maternally supplied transcript might end up with a more severe phenotype and because of lack of an efficient antibody to detect the effect of a translation initiation site targeting morpholino on protein level, a splice blocking morpholino was ordered to knock down *wdr81* in zebrafish. Its sequence was 5'-CACTTGTTCAAACTTACCTAATAGT-3' which targets the exon intron junction between exon 2 and intron 2 (Figure 28). Whether *wdr81* is maternally supplied or not

was detected by amplifying cDNA samples from 1 hpf, 2 hpf, 3 hpf, 6 hpf, 12 hpf, 24 hpf and 48 hpf timepoints and their –RT negative control samples with a primer pair. This primer pair was composed of a forward primer with 5'-ACAAGCAGCAAACAGTGCAG-3' sequences (wdr81_5UTR_B) and a reverse primer with 5'-TGTCTGCTCAACGGAATCTG-3' sequences (wdr81_5UTR_C). The reaction steps of amplification were: 30 sec. at 94 °C; 30 sec. at 94 °C, 40 sec. at 58 °C, 35 sec. at 68 °C for 35 cycles; and 5 min. at 68 °C. The amplicons were run on a 1% agarose gel.

2.1.5.1. *wdr81* Morpholino Dose Curve

Three doses of the morpholino antisense oligonucleotide sequence, which was designed to target splicing of *wdr81* transcript, were tested. Two nanograms (ng), 4 ng and 8 ng doses of *wdr81* morpholino were evaluated. Microinjection of the same doses of standard negative control morpholino were also performed in order to observe the specific effect of *wdr81* morpholino on splicing. The 24 hpf morpholino injected and uninjected control group embryos were collected after recording their survival rates. Microinjection of *wdr81* morpholino and negative control morpholino to zebrafish embryos, which were collected from the same clutch, was applied when they were at 1-4 cell stage. Total RNAs from the three experiment groups of each dosage were isolated with a Trizol reagent (AM9738, Ambion, USA) and cDNAs were synthesized (04 379 012 001, Transcriptor First Strand cDNA Synthesis Kit, Roche, Germany) using 500 ng of DNase treated (AM1907, Turbo DNA free, Ambion, USA) total RNA. The cDNA samples of embryos from three experiment groups of three doses were amplified with the a primer pair whose sequences were 5'-CAGAACCAAAGCACAGCAAA-3' for forward primer (Mo_wdr81_E2F) and 5'-CCAAGTTTTGCAGACAACCA-3' for reverse primers (Mo_wdr81_E3R) (Figure 29). The reaction conditions were: 2 min. at 95 °C, 30 sec. at 95 °C, 30 sec. at 61 °C, 50 sec. at 72 °C for 35 cycles; and 5 min. at 72 °C. The amplicons were run on a 1% agarose gel and on a 4% agarose gel.

2.1.5.2. Initial Characterization Studies

We set up two experiments in order to detect the effect of *wdr81* morpholino microinjection on zebrafish embryos. We searched for a possible microcephaly phenotype and tested the morphants with gastrulation brain homeobox 2 (*gbx2*) probe hybridization using WMISH method.

2.1.5.2.1. Head Size Measurement

Since *wdr81* is suggested to be a neurodevelopmentally important gene and the gene knockdown is expected to affect the central nervous system, in a parallel study while establishing a morpholino dose curve, head size measurements were carried out on morphant embryos[145]. Golzio *et al*., (2012) performed a measurement of the distance between the convex edges of the cornea of two eyes and of somitic length on the experiment groups in order to find out changes in head size, which are not caused by developmental delay. In our study, 8 ng. *wdr81* morpholino and 8 ng. standard negative control morpholino were injected to embryos and an uninjected control group was seperated. The experiment groups were composed of equal number of embryos from the same fish pair. The injections were applied to the yolk regions of embryos between 1-4 cell stages. The embryos, which comprise experiment groups were anesthetized at the timepoint between 4.25-4.5 dpf. The images of the embryos were taken with the same parameters every time by using a Leica MZ10F microscope. The distance between the convex edges of the cornea of two eyes and the body length of the experiment groups were measured with software (Leica Application Suite 4.3, LASv 4.3) by a researcher who was blind to the experimental groups. The body lengths of the embryos were measured from the tip of the mouth to the tail, where pigments end (Figure 31). Significant differences in the measurements between groups was tested by applying one-way ANOVA and Tukey's posthoc test. One-way ANOVA and the following Tukey's posthoc test were performed by using SPSS program (IBM, Turkey). Standard

error of the mean was also calculated by the same program. The survival rates of the embryos in the experiment were recorded.

2.1.5.2.2. Phenotype Characterization With WMISH Method

Another phenotypic characterization study following morpholino antisense knockdown was to compare the expression of *gbx2* in the three experimental groups. Expression of *gbx2* is established in the literature as being crucial for development of both midbrain and anterior hindbrain[146]. Two ng. morpholino microinjection was performed in the one-cell stage embryos. An uninjected control group among the siblings was separated as well. Two dpf *wdr81* morpholino injected embryos, 2 ng. standard negative control morpholino injected embryos and uninjected control group embryos were fixed in 4% paraformaldehyde (FB001, Invitrogen IC Fixation Buffer, Invitrogen, USA) and saved in 100% methanol after dehydration steps. The experiment was performed as explained in the "2.4.2.1. Whole Mount *In Situ* Hybridization (WMISH) on Embryos" section. The plasmid construct carrying the *gbx2* insert was a kind gift from Assoc. Prof. Gunes Ozhan. The plasmid was linearized with BamHI (FD0055, ThermoFisher Scientific) digestion in order to use it as a template in antisense probe synthesis. The linearized plasmid was excised from a 0.8 % agarose gel and purified (D4007, Zymoclean Gel DNA Recovery Kit, USA). The probe synthesis reaction was set up with T7 enzyme mix (AM1320, MaxiScript SP6/T7 *In Vitro* Transcription Kit, Ambion, USA) and DIG labeling mix (11277073910, DIG RNA Labelling Mix, Roche, Germany).

2.2. Materials

2.2.1. General Chemicals, Reagents and Enzymes

Chemicals in general use were agar (214010, Bacto Agar), agarose biomax (144503PR, Prona), agarose reducta (085501PR, Prona), ampicillin sodium salt (A0839, Biochemica), beta mercaptoethanol (M3148, Sigma-Adrich), bovine serum albumin fraction V (10 735 094 001, Roche), 5 bromo 4 chloro 3 indolyl beta-D galactoside (X-gal, A4978, Applichem), calcium chloride dihydrate ($CaCl_2.2H_2O$, 327 607, Carlo Erba), calcium nitrate tetrahydrate ($Ca(NO_3)_2.4H_2O$, A361521 215, Merck), Chaps (C9426, Sigma-Aldrich), citric acid anhydrous (C0759, Sigma-Aldrich), diethyl pyrocarbonate (DEPC, D5758, Sigma), D-sucrose (A1125, Applichem), ethanol (32221, Sigma-Aldrich), ethidium bromide (E-7637, Sigma, MO), ethyl 3-aminobenzoate methanesulfonate (E10521, Sigma-Aldrich), ethylenediaminetetraacetic acid (EDTA, A3562, Applichem), ficoll type 400 (F4375, Sigma-Aldrich), formamide (F7503, Sigma-Aldrich), glacial acetic acid (272225, Sigma-Aldrich), glycerol (GL00262500, Scharlau), heparin sodium salt from porcine intestinal mucosa (H3393, Sigma-Aldrich), Hepes free acid (0511, Amresco), hydrochloric acid (HCl, 07102, Riedel de Haen), hydrogen peroxide (H_2O_2, 18312, Sigma-Aldrich), isopropanol (34137, Sigma-Aldrich), isopropyl-beta-D-thiogalactopyranoside (IPTG, A4773, Applichem), kanamycin sulfate (A1493, Applichem), magnesium chloride dihydrate ($MgCl_2$. $2H_2O$, A146417 052, Applichem), magnesium chloride hexahydrate ($MgCl_2.6H_2O$, 105833.1000 Merck), magnesium sulfate heptahydrate ($MgSO_4.7H_2O$, M2773, Sigma), manganese (II) chloride dihydrate ($MnCl_2.2H_2O$, 105917.1000, Merck), methanol (32213, Sigma-Aldrich), methylene blue (M9140, Sigma-Aldrich), mineral oil (M8410, Sigma-Aldrich), nuclease free water (AM9937, Ambion), OCT (4583, Tissue-Tek), phenol red (P0290, Sigma), pipes (A1079.0100, Applichem), polyvinylpyrrolidone (PVP, P5288, Sigma-Aldrich), potassium chloride (KCl, 12636, Sigma-Aldrich), potassium hydroxide (KOH, 105012.1000, Merck), potassium phosphate monobasic (KH_2PO_4, 04243, Sigma-Aldrich), pronase E (protease from *Streptomyces griseus* type XIV, P5147, Sigma), proteinase K (P2308, Sigma-Aldrich), sodium chloride (NaCl, 13423, Sigma-Aldrich), sodium citrate tribasic ($Na_3C_6H_5O_7.5,5H_2O$, 6858-44-2, Carlo Erba), sodium

hydroxide (NaOH, 06203, Riedel de Haen), sodium phosphate dibasic dihydrate ($Na_2HPO_4.2H_20$, 04272, Sigma-Aldrich), triethanolamine HCl (TEA-HCl, T1502, Sigma), tris HCl (T3253, Sigma), trizma base (T1503, Sigma Aldrich), tryptone (1612.00, Conda Pronadisa), tween-20 (0777, Amnesco) and yeast extract (1702.00, Conda Pronadisa).

Reagents used in the experiments were bakers yeast RNA (R6750, Sigma), BAN phase separation reagent (BN191, Molecular Research Center), blocking reagent (11 096 176 001, Roche), DNA loading dye (R0611, ThermoFisher Scientific), deoxynucleotide (dNTP) mix (R1121, Fermentas), fetal bovine serum (10270, Gibco), light cycler 480 probes master (04707494001, Roche), lithium chloride solution (L7026, Sigma), magnesium chloride for PCR (25 mM $MgCl_2$, 00051040, Fermentas), mounting solution (Clear mount, 008010, Life Tech), salmon sperm DNA (AM9680, Thermo Scientific) and torula RNA (R6625, Sigma).

Enzymes routinely used in the experiments were Fast Start High Fidelity kit (03553400001, Roche), One Taq Hot Start (M0484S, New England Biolabs), Phusion HS Flex (M0536, New England Biolabs) and Taq polymerase (M0267S, New England Biolabs).

2.2.2. General Materials and Equipments

Materials used in the experiments were capillaries to prepare microinjection needles (BF100-50-10, Sutter Instrument Company), microloader (5242956003, Eppendorf), mold for microinjection (TU-1, Adaptive Science Tools), stage micrometer (35037, Olympus) and superfrost plus slides (631-0108, VWR).

Equipments routinely used in the experiments were centrifuges (Biofuge Pico, Heraeus Instrument and GS15R Beckman), gel documentation equipment (Vilber Lourmat), gel

running tank (Midicell EC350), heat block (SHT1, Stuart Scientific Test Tube Heater), hybridization incubator (combi-H12, FinePCR), incubator (WTB binder), microinjection system (Femtojet, Eppendorf), NanoDrop 1000, PCR Thermal cycler (TC 512, Techne and 2720 Thermal Cycler, Applied Biosystems), pipette puller (P30, Sutter Instrument Company), power supply (Pac 200 Biorad), vortex (Genie Scientific Industries) and water bath (Nüve bath).

2.2.3. Buffers and Solutions

Ingredients of the buffers and solutions used in this study are mentioned in Appendix A.

2.2.4. Molecular Size Markers and Plasmid Vectors

Molecular size markers (pUC mix 8, SM0303, Fermentas and MassRuler DNA Ladder, SM0403, Thermo Scientific) used in this study are given in Appendix B. The maps of the plasmid vectors (pCR4-Topo, Invitrogen and pGEM-T Easy, Promega) are given in Appendix C.

Chapter 3. Results

3.1. Zebrafish Orthologue of WDR81

WD repeat containing protein 81 was shown to be highly conserved among vertebrates (Figure 3 and Appendix D)[12]. Based on the report of Ensembl database, the highest identity of zebrafish putative wdr81 was detected with its orthologues from orangutan (*Pongo abelii*) among primates (61%), Guinea pig (*Cavia porcellus)* and kangaroo rat (*Dipodomys ordii*) among rodents (58%), megabat (*Pteropus vampyrus*) among Laurasiatheria (59%), Chinese softshell turtle (*Pelodiscus sinensis*) among Sauropsida (71%) and cod (*Gadus morhua*) and stickleback (*Gasterosteus aculeatus*) among fish (79%)[24]. Clustal Omega alignment was utilized to detect the degree of identity of WDR81 sequences among three species. The results of alignment showed that human WDR81 and mouse Wdr81 carry 56.94% and 56.68% identity with the putative wdr81 protein in zebrafish, respectively[134]. The mutation site in human patients, proline at residue 856, was also shown to be conserved among various species of vertebrates (Appendix D). *wdr81*, which is one copy and not duplicated, is mapped to chromosome 15 in zebrafish genome. The transcript of zebrafish *wdr81* gene (wdr81-001, ENSDART00000156621) is made up of 12 exons containing open reading frame (ORF) and putative UTRs (Figure 7). The length of this novel transcript is predicted as 8249 base pairs (bp) and it encodes a predicted protein composed of 2065 amino acid residues[24].

The conserved domains of the zebrafish putative wdr81 protein were predicted as BEACH, MFS and WD40 repeat domains by the SMART database[136] and CLC Main Workbench software. The BEACH domain was detected to reside between the 337th–598th residues, the MFS domain was predicted locate between the 951st-1513th residues and seven WD40 repeats were concluded to take place between 1758th–1797th, 1807th–1844th, 1850th–1889th, 1892nd–1936th, 1939th-1977th, 1980th–2017th and 2027th–2065th residues of zebrafish wdr81. The number of transmembrane regions of the protein were

predicted to be six[137]. These regions were predicted to reside between 665th–686th, 1031st–1055th, 1413th–1435th, 1463rd–1483rd, 1690th–1712th and 1920th–1943rd (Figure 8 and 9). The same domains and the presence of membrane spanning regions were also predicted in human WDR81 and mouse Wdr81 proteins[12,36].

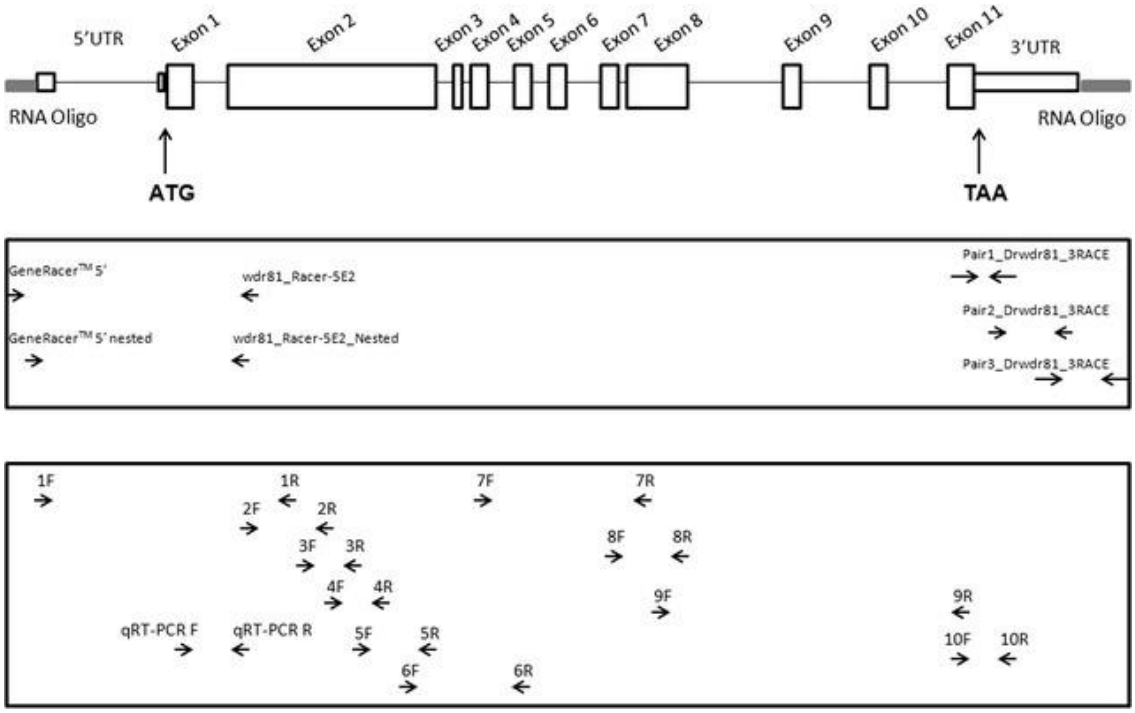

Figure 7. Zebrafish *wdr81* gene, illustration of its genomic structure and binding regions of primers. *Sequences of wdr81-001 (ENSDART00000156621), which was the prediction from Ensembl database, was utilized as a model. Boxes indicate the exons, lines indicate the introns and gray boxes stand for the RNA oligonucleotides (RNA oligo), which were ligated to the mRNA by the use of RACE kit. The approximate locations of the primers for RACE experiment were indicated with arrows in the upper box. The binding regions of the primer pairs designed to characterize the open reading frame and the primer pair to be used in the qRT-PCR were depicted as arrows in the below box*[139] *(Reprinted from Doldur-Balli et al., 2015*[139]*).*

The alignment file of human, mouse and zebrafish WDR81 orthologous proteins obtained from Clustal Omega was submitted to ESPript 3 software. The location of the domains were highlighted on the generated file. This study indicated that the most

conserved domain was the BEACH domain among human, mouse and zebrafish. A difference in the number of WD40 repeat domains were detected; seven WD40 repeat domains were predicted in zebrafish wdr81 whereas the number of predicted WD40 repeat domains were six in human and mouse (Figure 9).

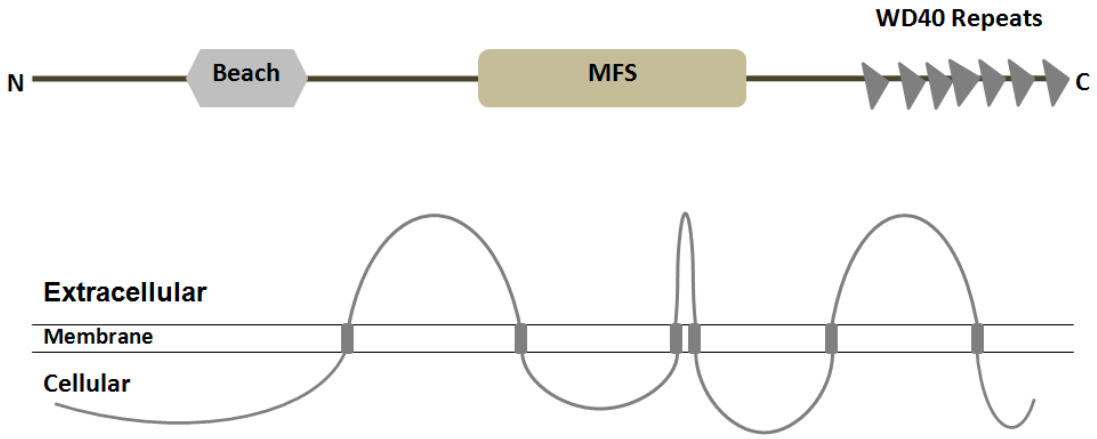

Figure 8. The conserved domains and the structural organization of zebrafish wdr81, predicted *in silico*. *The predictions of BEACH, MFS and WD40 repeat domains and being a transmembrane protein were also shared for the human and mouse WDR81 proteins*[139] *(Reprinted from Doldur-Balli et al., 2015*[139]*).*

3.2. Zebrafish *wdr81* Transcript Possesses One ORF

A search on the splice variants of human *WDR81* exhibited nine protein coding transcripts which are *WDR81*-001 (ENST00000409644), *WDR81*-002 **(**ENST00000309182), *WDR81*-004 (ENST00000446363), *WDR81*-005 (ENST00000419248), *WDR81*-007 (ENST00000455636), *WDR81*-009 (ENST00000468539), *WDR81*-010 (ENST00000418841), *WDR81*-014 (ENST00000575206) and *WDR81*-201 (ENST00000437219) (Figure 10). Mouse had three protein coding transcripts of *Wdr81*, which are *Wdr*81-001 (ENSMUST00000117392), *Wdr*81-003 (ENSMUST00000132442) and *Wdr*81-201 (ENSMUST00000173320) (Figure 11)[24]. *wdr81*-001 (ENSDART00000156621) was

predicted to be one transcript of zebrafish *wdr81* (Figure 12)[24] and I investigated the presence or absence of splice variants experimentally, since more than one transcript were predicted for orthologous genes from human and mouse[12,24,36].

In order to characterize the transcript of zebrafish *wdr81*, I firstly focused on the ORF and obtained 10 overlapping amplicons using the primer pairs mentioned in Table 3 and cDNAs from 24 hpf embryo and adult brain as templates. The location of the primers designed to amplify ORF were given in Figure 7. They cover the ORF and the experiment was designed so that absence of an exon, because of alternative splicing process, would be observed since common regions would exist between consecutive amplicons. Observing one PCR product per reaction with both 24 hpf embryo template and adult brain template pointed out that zebrafish *wdr81* transcript possesses one ORF (Figure 13).

3.3. Characterization of 5' End of *wdr81* Verified the Prediction and an Insertion Site Was Detected in the 3' End of Some Tissues

The 5' end and 3' end of the zebrafish *wdr81* transcript were characterized in order to observe possible transcript variants regarding these regions. The RACE method was utilized in order to characterize the UTRs of *wdr81*. The gene specific primers and the primers included in the kit (GeneRacer™ primers) were employed (Figure 7, top box). RACE-ready cDNAs from 24 hpf embryo and adult brain were amplified with a touch down PCR and then the amplicons were used as a template in a nested PCR (Figure 14). A single DNA band was obtained from each reaction revealing that *wdr81* transcript possesses one 5'UTR (Figure 15). The experiment was designed so that the PCR products would include the 5'UTR, exon 1 and initial sequences of exon 2 of *wdr81* (Figure 16). The amplicons were sequenced after cloning. Sanger sequencing results of 5'RACE product of *wdr81* verified the predictions. The 5'UTR of *wdr81* was found to be 264 bp long and the prediction was 6 bp longer than it, at the 5'end (Figure 17).

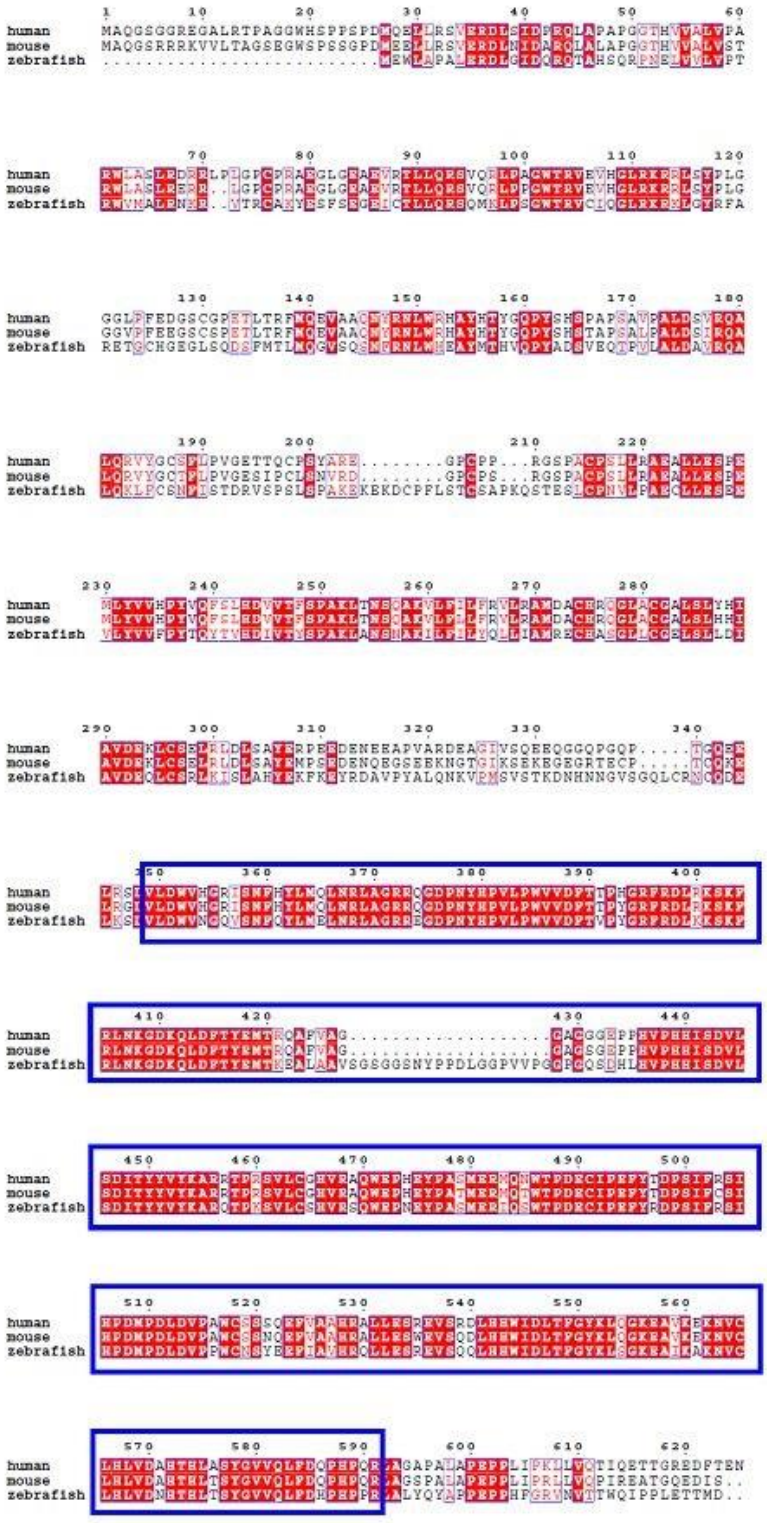

Figure 9. Alignment of the protein sequences of human, mouse and zebrafish WDR81. *The conserved amino acid residues in three species were coloured with red background. The blue boxes emphasize the location of the predicted BEACH domain*[139] *(Reprinted from Doldur-Balli et al., 2015*[139]*).*

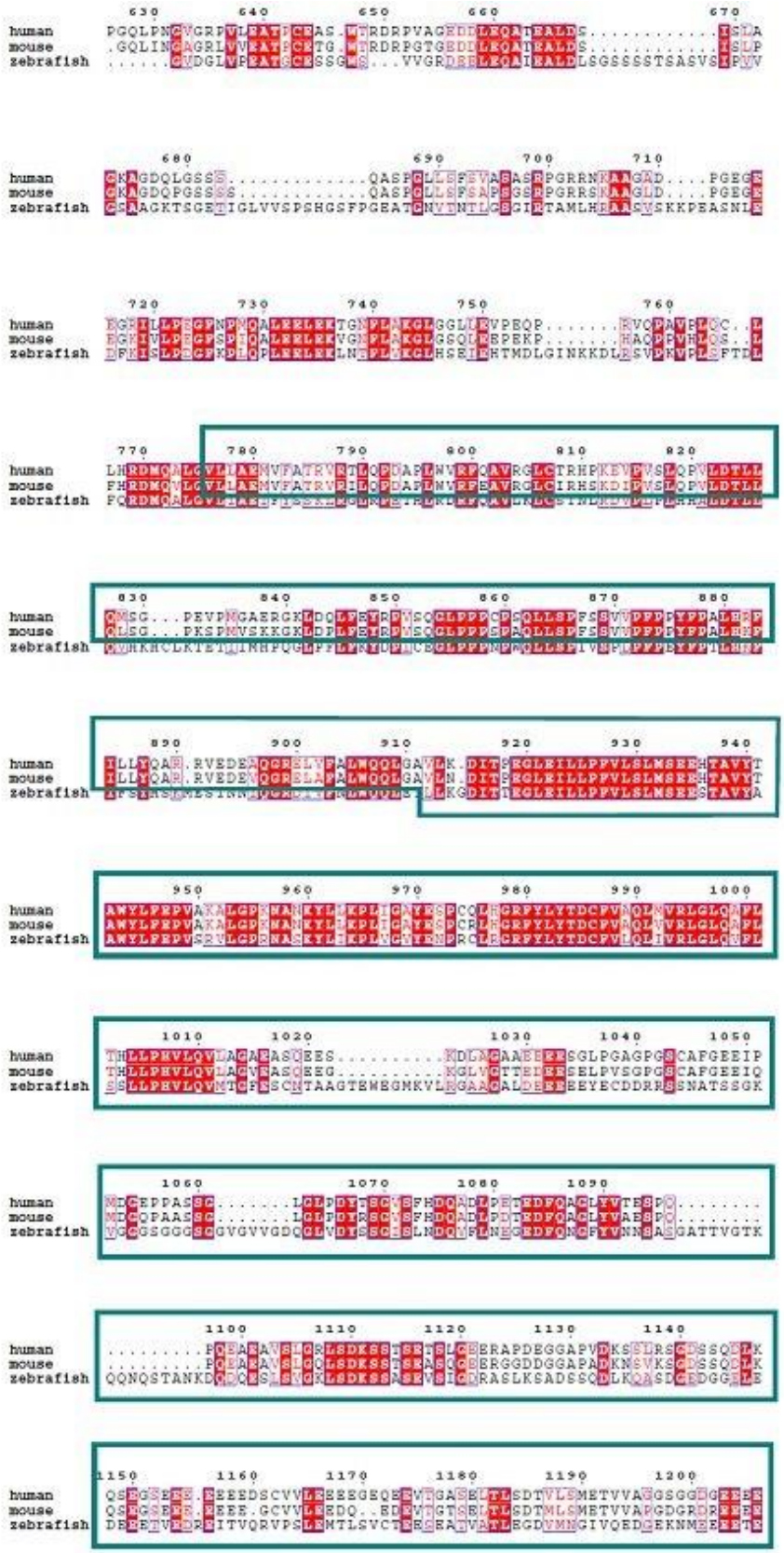

Figure 9. (continued) *The green boxes emphasize the location of the predicted MFS domain*[139].

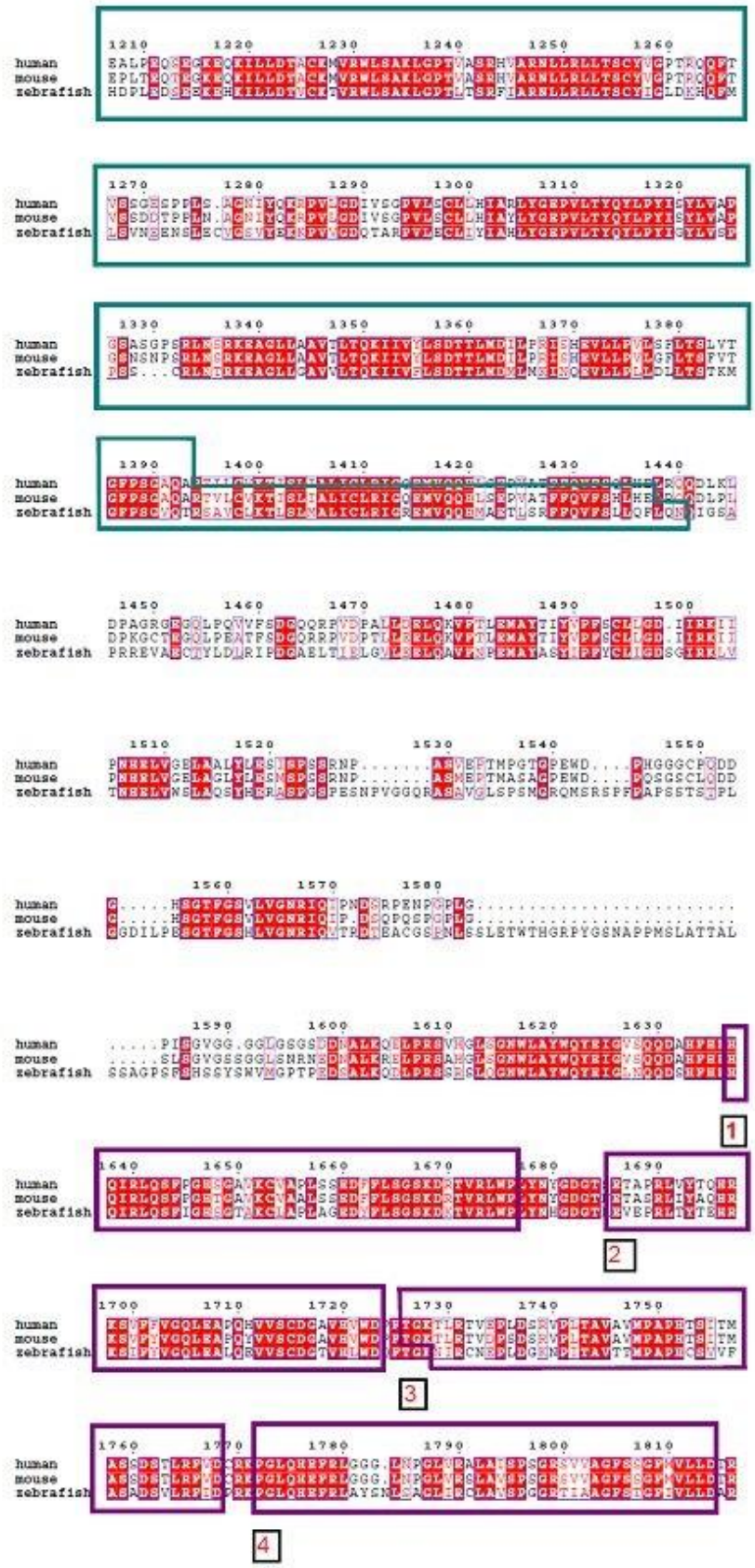

Figure 9. (continued) *The purple boxes emphasize the location of the predicted WD40 repeat domains. WD40 repeat domains were numbered*[139].

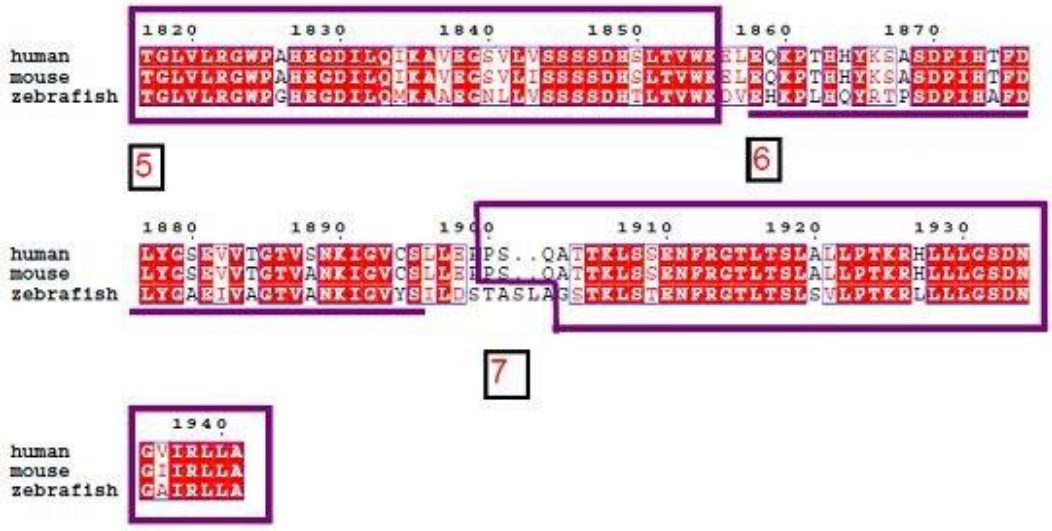

Figure 9. *Number 6 was predicted to be present only in zebrafish wdr81*[139].

The strategy in this study to obtain 3'RACE product of *wdr81* was to amplify the RACE-ready cDNAs from 24 hpf embryo and adult brain as 3 overlapping PCR products. The experiment was designed so that the PCR products would include the 3'UTR and exon 11 of *wdr81* (Figure 18). A single DNA band was obtained from each reaction at expected sizes as a result of the reactions with primer pairs 1 and 3 from Table 4, revealing that *wdr81* transcript has one 3'UTR**.** The reaction with primer pair 2 from Table 4 also gave a single DNA band from each reaction however it was longer than expected, which pointed out presence of an insertion site. Obtaining a single DNA band from each reaction with primer 2 also showed that there is one *wdr81* transcript regarding the 3'UTR structure (Figure 19). The PCR products of the reactions were sent to Sanger sequencing, the results of the reactions with primer pairs 1, 2 and 3 (Table 4) confirmed the predictions along with several nucleotide variants and indels (Table 6). In addition an insertion site in amplicon 2 was detected (Figure 19b). The location of the insertion site was detected between the 7564th and 7565th nucleotides of cDNA of *wdr81*. This site was amplified with a new primer, which was designed to characterize the insertion site by amplifying it within a narrower frame. The templates were again from 24 hpf embryo and adult brain. The PCR products were sent to Sanger sequencing after cloning.

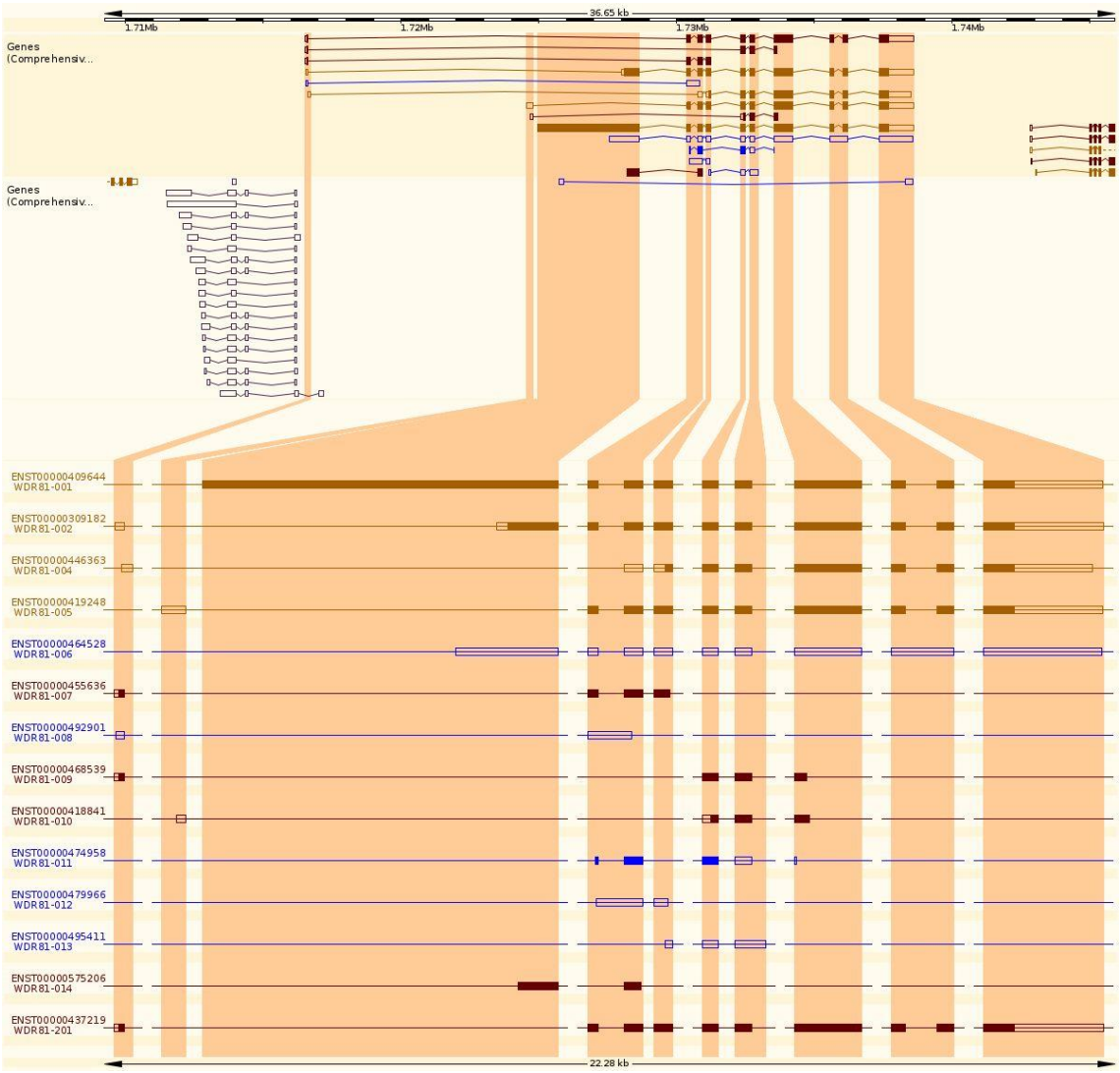

Figure 10. Diagram showing the splice variants of human *WDR81*, derived from Ensembl [24]. *Human WDR81 encodes 9 protein coding splice variants.*

Three plasmids per sample (embryo and adult brain), obtained from single colonies were aligned in order to obtain the sequence of the insertion site. Plasmids 1-1, 1-5 and 1-8 were from 24 hpf sample origin, plasmids 2-3, 2-4 and 2-6 were from adult brain origin. A 266 bp. long insertion site was revealed as a result of sequencing and alignment (Figure 20). Detection of the 266 bp long insertion site in both embryo and brain samples brought up a question about the presence of the same insertion site in other adult tissues and samples from other developmental stages.

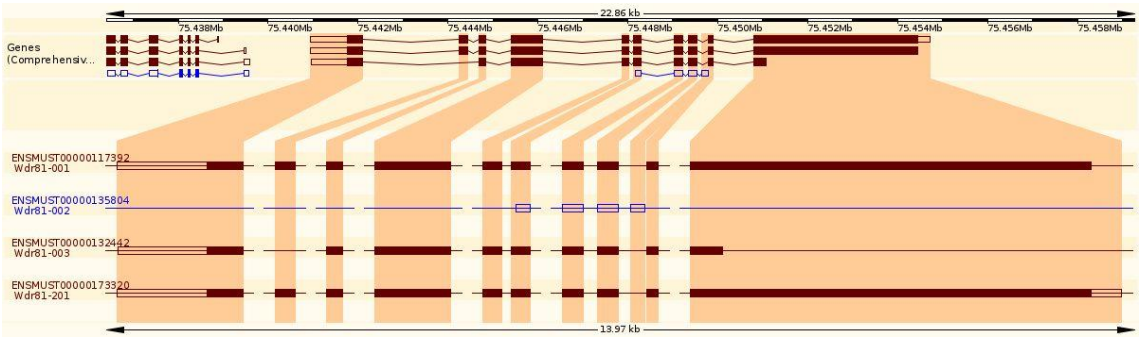

Figure 11. Diagram showing the splice variants of mouse *Wdr81*, derived from Ensembl[24]**.** *Mouse Wdr81 encodes 3 protein coding splice variants.*

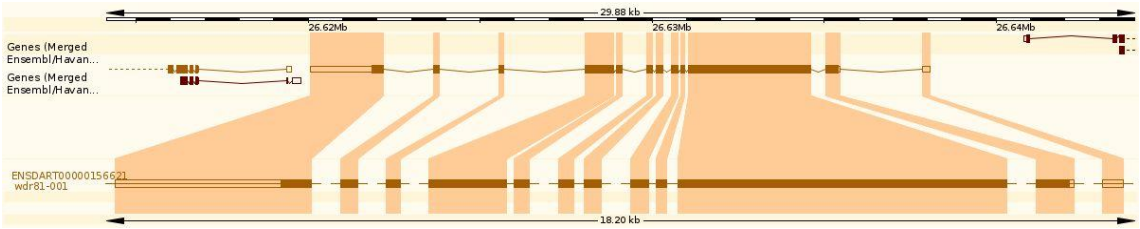

Figure 12. Diagram showing the zebrafish *wdr81* transcript, derived from Ensembl[24]**.** *Zebrafish wdr81 is predicted to encode one protein coding transcript.*

Reactions with all of the evaluated samples from ten different development timepoints, including 24 hpf embryo sample, demonstrated the presence of the insertion. Reactions with the adult tissues; brain, testis, heart, liver, eye, tail and muscle also demonstrated the presence of the insertion however reactions with kidney, intestine and gills did not give any PCR products (Figure 21). The band intensities of the amplicons in Figure 21 were measured (Table 7). The intensity of the band amplified from the 35 dpf juvenile zebrafish had the lowest intensity among the other developmental timepoint samples (Table 7a). The comparison of the band intensities of the amplicons obtained from adult tissues resulted in observing the highest and nearly equal values from the brain and the testis, followed by the values from the eye. The band intensities obtained from the amplification of the insertion region in heart and muscle samples were nearly equal, and were followed by that of tail and liver, respectively (Table 7b).

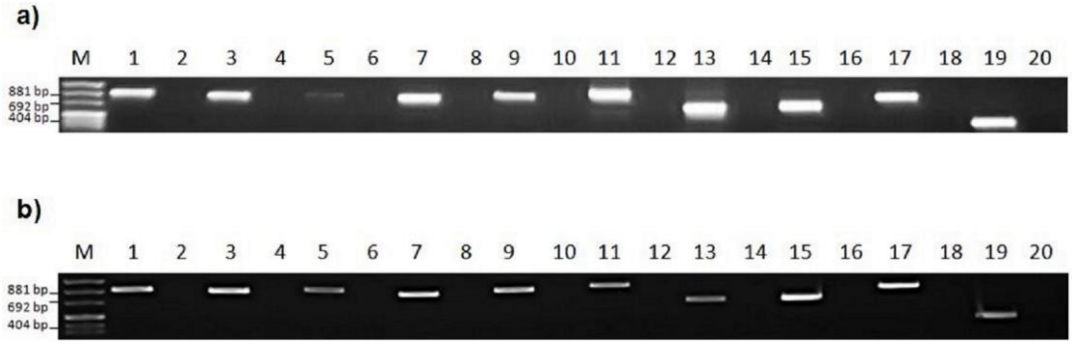

Figure 13. Agarose gel electrophoresis image of the PCR products of the reactions, which zebrafish *wdr81* open reading frame was characterized. *a) 24 hpf embryo cDNA template was amplified. b) Adult brain cDNA template was amplified. Amplicons obtained with primer pairs 1-10 were loaded to the lanes 1, 3, 5, 7, 9, 11, 13, 15, 17 and 19, respectively. The reaction with –RT controls, which were the same primer pairs were loaded to the lanes 2, 4, 6, 8, 10, 12, 14, 16, 18 and 20. Lanes marked as M include pUC mix DNA Marker (SM0301, Thermo Scientific) (Reprinted from Doldur-Balli et al., 2015*[139]*).*

As a conclusion, characterization of the 5'end of *wdr81* indicated that there is one 5'UTR structure of the transcript and there are not any other transcript variants regarding 5'UTR. In addition, detection of the insertion site in 3'UTR in most of the evaluated tissues might be a result of an alternative polyadenylation process among tissues and so that various lengths of 3'UTR might be observed.

3.4. Expression of *wdr81* is Increased at 5 Hpf and 18 Hpf During Development and is Enriched in the Eye and Brain of Embryos

Expression of *wdr81* during various developmental stages was investigated by employing both qRT-PCR and WMISH methods. The primer pairs, qRT-PCR F and R, whose locations were depicted in Figure 7 were utilized in quantification of expression values at ten developmental timepoints.

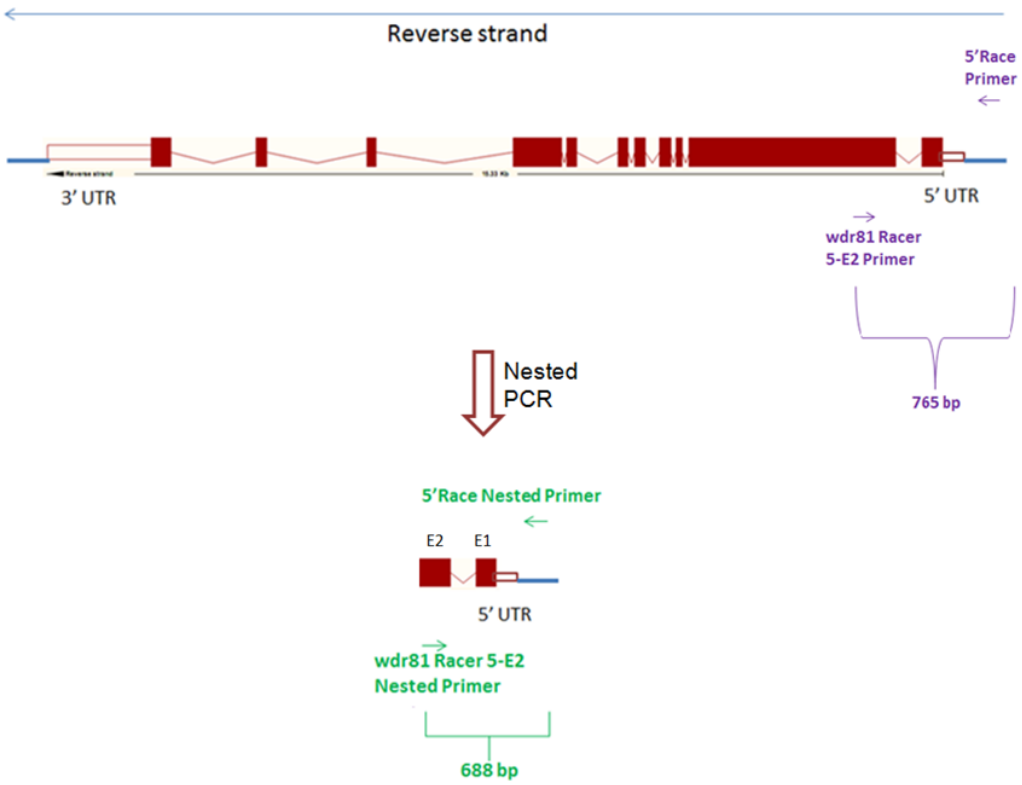

Figure 14. The illustration of the strategy in this study to obtain 5'RACE product of *wdr81* by performing a nested PCR following a touch down PCR. *The experiment was designed so that the 5'RACE product of wdr81 would include 5'UTR, exon 1 and initial sequences of exon 2.*

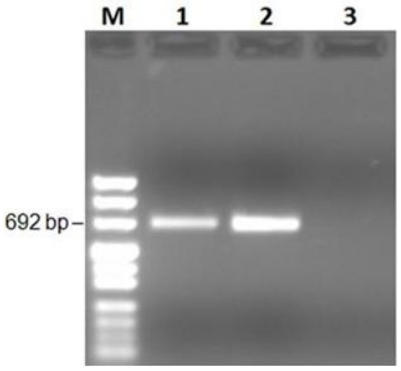

Figure 15. Agarose gel electrophoresis image of the 5'RACE product of *wdr81* transcript. *A single DNA band was obtained from each reaction revealing that wdr81 transcript possesses one 5'UTR.* ***Lane 1:*** *wdr81 5'RACE product from 24 hpf embryo template; lane 2: wdr81 5'RACE product from adult brain template; lane 3: control reaction which did not include any templates. Lane marked as M included pUC mix marker 8 (SM0301, Thermo Scientific) (Reproduced from Doldur-Balli et al., 2015*[139]*)*

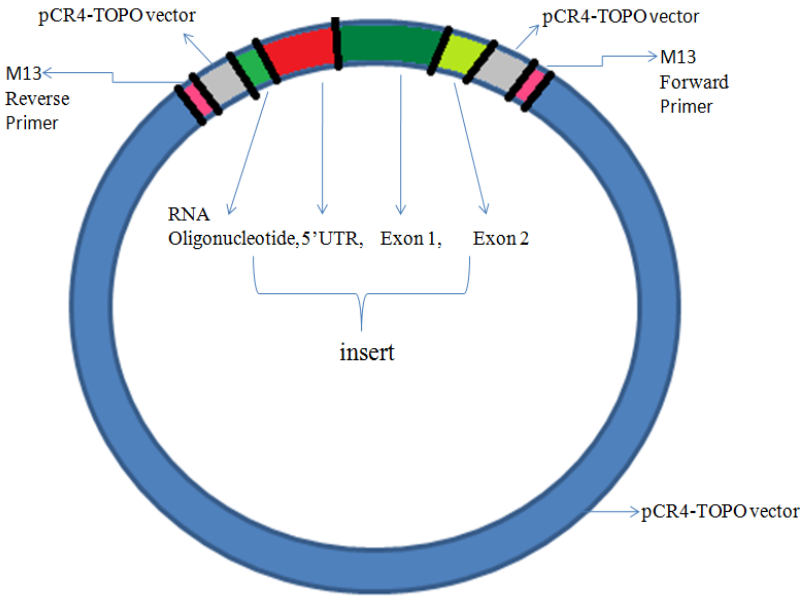

Figure 16. The schematic illustration of the order of sequences in plasmids whose inserts are 5'RACE product of *wdr81*.

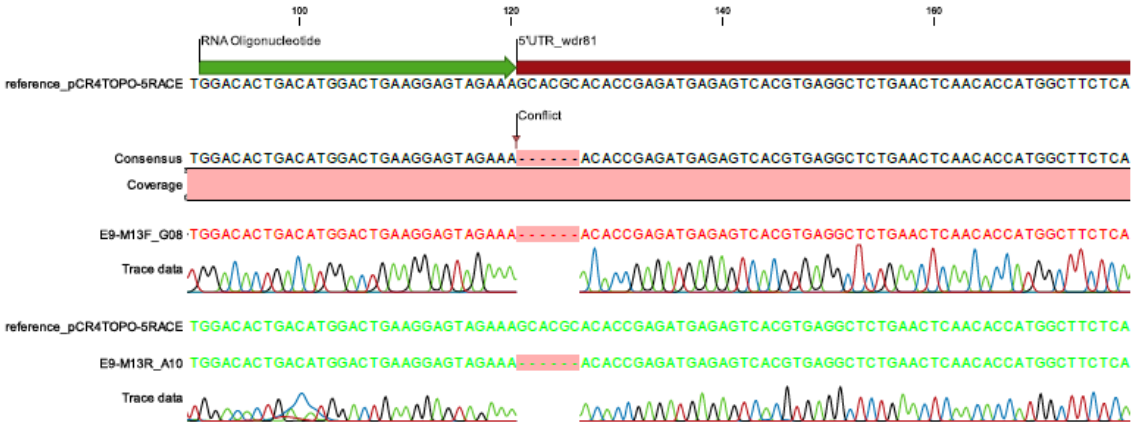

Figure 17. A CLCBio Main Workbench software analysis diagram showing a representative Sanger sequencing result of 5'RACE product with a 6 bp shorter 5'UTR than the prediction.

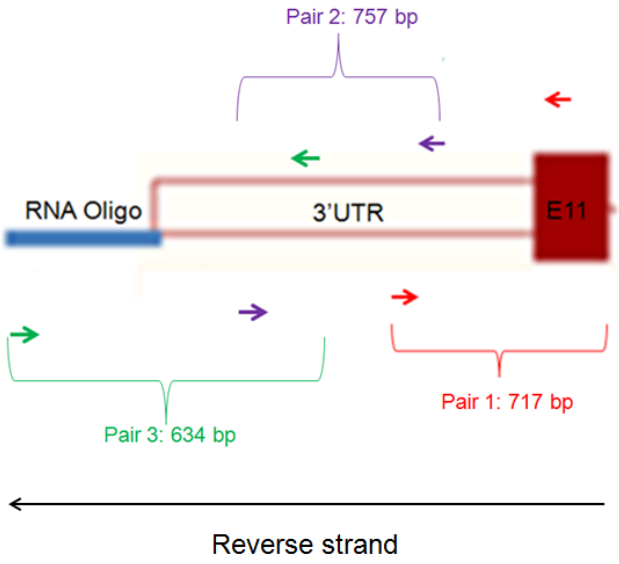

Figure 18. The illustration of the strategy in this study to obtain 3'RACE product of *wdr81* by amplifying RACE-ready cDNAs as three overlapping PCR products. *The experiment was designed so that the 3'RACE product of wdr81 would include 3'UTR and last nucleotides of exon 11.*

Relative temporal expression analysis exhibited that there was expression at all timepoints, which were 1 hpf, 5 hpf, 10 hpf, 18 hpf, 24 hpf, 48 hpf, 72 hpf, 5 dpf, 15 dpf and 35 dpf and the level of expression was higher at 1 hpf, 5 hpf and 18 hpf stages (Figure 22). Zygotic expression in zebrafish was reported to start at 3 hpf[147,148]. Observation on the relative temporal expression of *wdr81* led to a conclusion that the expression level was high at 1 hpf and 5 hpf timepoints which are before and after the beginning of zygotic expression, respectively. Observing the high level of expression at 1 hpf also emphasized that *wdr81* was maternally supplied. A dramatic decline was detected at the level of expression at 10 hpf timepoint and a clear raise was observed at 18 hpf development stage. The level of expression again dropped down at 24 hpf and similar low levels of expression continued during the rest of the timepoints (Figure 22). 5 hpf and 18 hpf appeared to be crucial timepoints related with *wdr81* expression during development of zebrafish in regard to the stages after transition to zygotic expression. Results of WMISH experiment were generally in parallel with the qRT-PCR results.

An RNA probe, which was designed to detect the region corresponding to the mutation site in patients, was synthesized. The length of the probe was 1.7 kb.

The probe was synthesized by amplifying the region between the forward primer of the primer pair 5 and the reverse primer of the primer pair 6, which were previously designed to amplify the open reading frame of *wdr81* (Table 3, Figure 7 lower box). Differential expression of *wdr81* at six developmental stages (6 hpf, 10 hpf, 18 hpf, 24 hpf, 48 hpf, 72 hpf) was studied with this probe. The signal was strong in the early development timepoints (6 hpf-18 hpf), and it decreased at 24 hpf timepoint. The signal was decreased in the trunk of the embryos at 48 hpf and was not significant in the whole embryo at 72 hpf. The expression was ubiquitous at the embryonic stages of 6 hpf, 10 hpf, 18 hpf and 24 hpf. The signal of the RNA probe was focused in the eye and brain regions of embryos at 18 hpf and 48 hpf stages. At 18 hpf, *wdr81* expression was enriched in the optic vesicle and midbrain. At 48 hpf, *wdr81* expression was concentrated in the lens, diencephalon, midbrain and medial longitudinal fascicle (Figure 23).

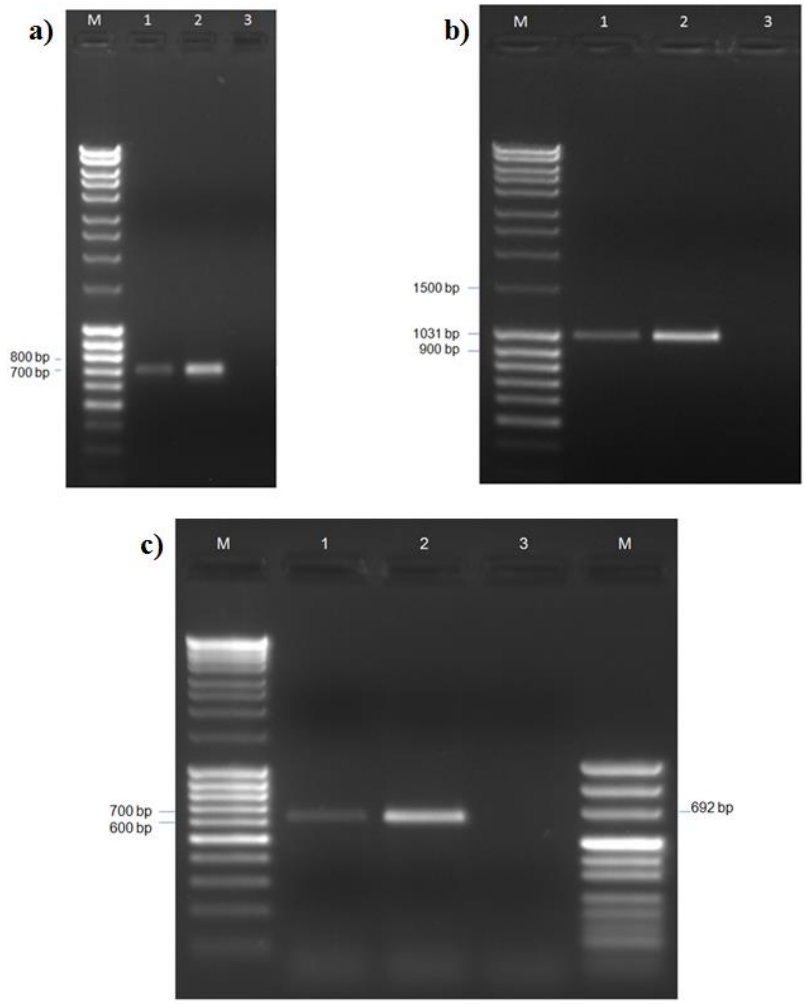

Figure 19. Agarose gel electrophoresis images of the overlapping amplicons obtained from the experiment in which 3'end of the zebrafish *wdr81* was characterized. *A single DNA band was obtained from each reaction at expected sizes as a result of the PCRs with primer pairs 1 (a) and 3 (c) (Table 4), revealing that wdr81 transcript possesses one 3'UTR***.** *The reaction with primer pair 2 also gave a single DNA band from each reaction however it was longer than the prediction (b), which pointed out presence of an insertion. Obtaining a single DNA band from the reaction with primer pair 2 (Table 4) also showed that there is one wdr81 transcript regarding the 3'UTR structure. In all of the gels, templates in lane 1: RACE-ready cDNA from 24 hpf embryo, lane 2: RACE-ready cDNA from adult brain. Lane 3: control reaction which did not include any templates. Lane marked as M: MassRuler Mix DNA Marker (SM0403, Thermo Scientific). Second DNA marker in (c) was pUC mix marker 8 (SM0301, Thermo Scientific) (Reproduced from Doldur-Balli et al., 2015*[139]*).*

Table 6. Variants detected in the 3'RACE products of 24 hpf embryo and adult brain *wdr81* except the insertion site which was found to be 266 bp long *(Reprinted from Doldur-Balli et al., 2015*[139]*)*

c.6506 T>C
c.6707 A>T
c.6733 C>G
c.7007_7008insG
c.7015delT
c.7019_7023delACTCT
c.7103 T>C
c.7296 T>A
c.7331_7334delATAT
c.7512 A>G
c.7546 A>G
c.7770 G>T
c.7985 C>T
c.8050 A>G
c.8136 T>C
c.8252 A>G

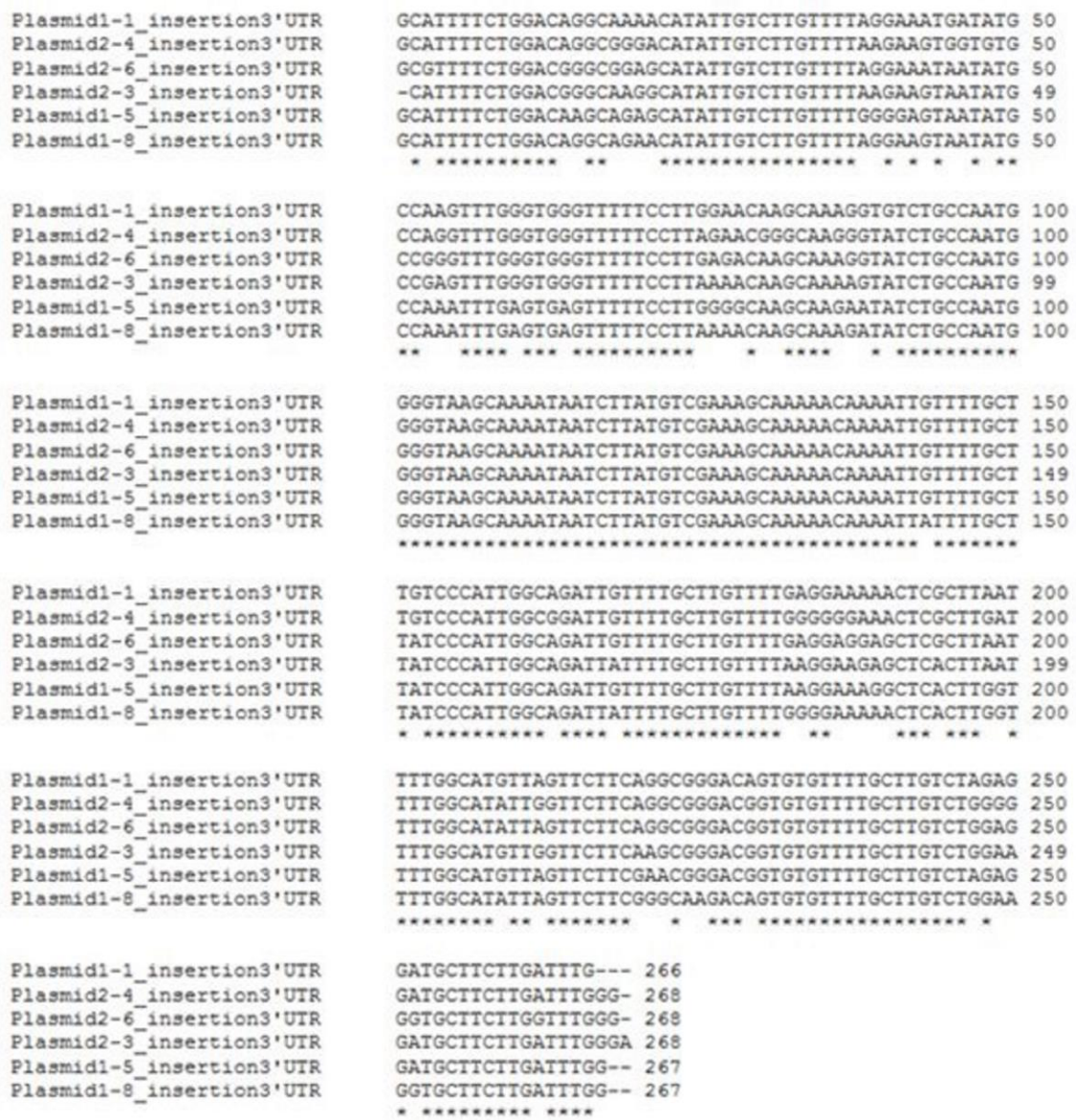

Figure 20. Alignment of the clones of the insertion site detected in 3'UTR of zebrafish *wdr81* transcript revealed its length as 266 bp. *Three plasmids per sample (24 hpf embryo and adult brain), which included the insertion site as their inserts were sequenced. Plasmids 1-1, 1-5 and 1-8 carried the insert cloned from 24 hpf embryo sample, plasmids 2-3, 2-4 and 2-6 carried the insert cloned from adult brain sample (Reprinted from Doldur-Balli et al., 2015*[139]*).*

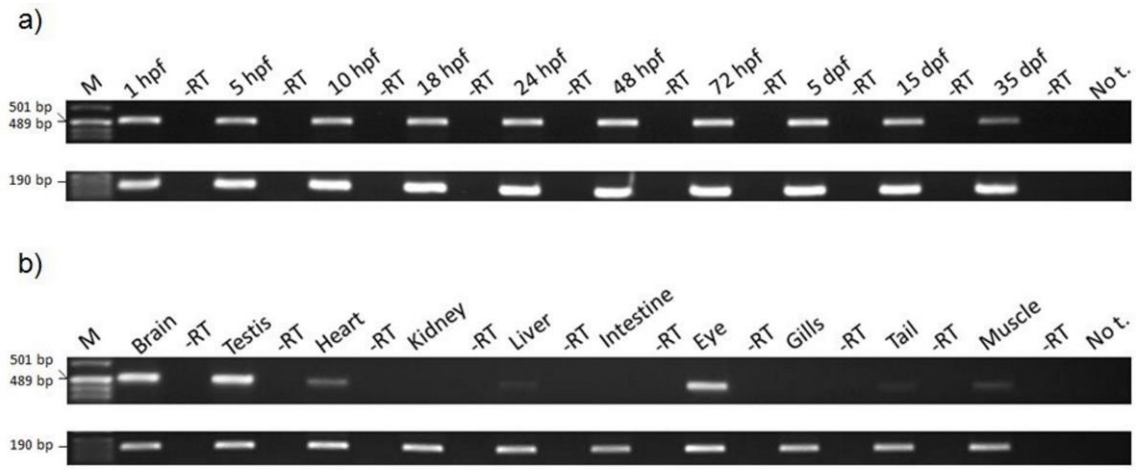

Figure 21. Agarose gel electrophoresis image of the amplicons obtained from the reactions in which presence of the insertion site was tested in samples from developmental stages and in adult tissues. *a) Samples from ten developmental stages were amplified (upper gel image) and amplification of the same samples with a house keeping gene primer pair (beta-actin) confirmed the integrity of the cDNA templates (below gel image). B) Ten adult tissue samples were amplified (upper gel image) and integrity of the cDNA templates was confirmed with amplification using beta-actin primers (below gel image). The lanes in all of the gels were loaded with the amplicons from cDNA templates that they are labelled with. Lane marked as M included pUC mix DNA Marker (SM0301, Thermo Scientific). "No t." stands for the control reaction which did not include any templates (Reprinted from Doldur-Balli et al., 2015*[139]*).*

3.5. Spatial Expression of *wdr81* and its Detection in Proliferation Zones

The head regions of WMISH specimens from 18 hpf, 48 hpf and 72 hpf stages were sectioned in order to detect the sites of expression in more detail. The intensity of the signal produced by the probe was the highest in the section from 18 hpf specimen. The signal was homogenous in the brain and the optic vesicle (Figure 24d). This might be implying that *wdr81* expression was taking place in all types of cells in these tissues.

Table 7. Intensities of the bands of PCR products from Figure 21 (*Reprinted from Doldur-Balli et al., 2015*[139]*).*

a) Intensities of the bands of PCR products from Figure 21a.

Developmental stage	Intensities of the amplicons obtained from the insertion site	Intensities of the amplicons obtained with ß-actin primers
1 hpf	8938.29	9821.86
5 hpf	7941.21	11415.03
10 hpf	8265.58	13168.54
18 hpf	8280.21	13521.12
24 hpf	8379.09	13497.54
48 hpf	9394.56	12853.64
72 hpf	9327.96	13705.19
5 dpf	9390.74	13497.32
15 dpf	7502.30	13005.18
35 dpf	4343.33	12577.55

b) Intensities of the bands of PCR products from Figure 21b.

Adult tissue	Intensities of the amplicons obtained from the insertion site	Intensities of the amplicons obtained with ß-actin primers
Brain	9475.08	7483.83
Testis	10441.17	8470.90
Heart	2206.91	9003.5
Kidney	N/A	8421.62
Liver	407.82	8001.1
Intestine	N/A	6438.65
Eye	7023.97	9123.22
Gills	N/A	7566.79
Tail	415.84	7496.79
Muscle	1044.75	7563.46

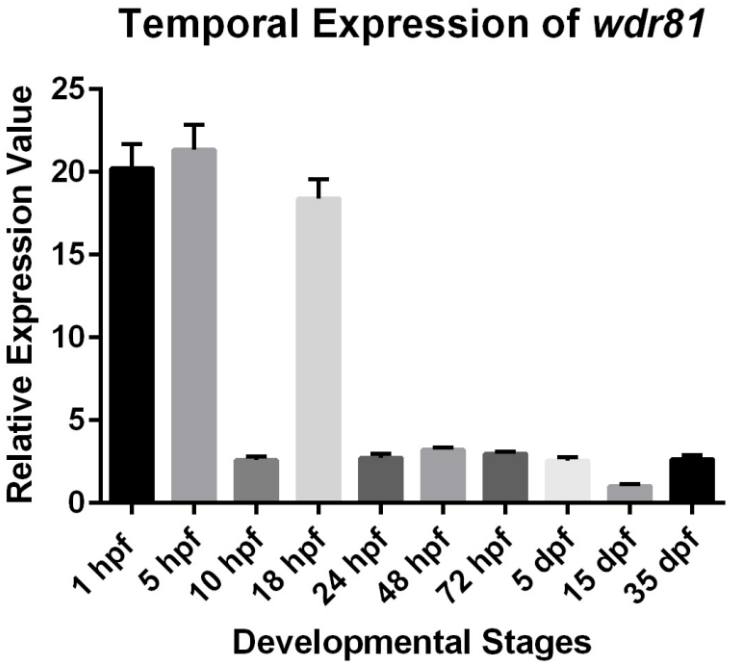

Figure 22. Relative expression of *wdr81* at ten developmental stages. *The peaks in relative expression levels were detected at 1 hpf, 5 hpf and 18 hpf timepoints. Templates were cDNAs from 1 hpf embryo, 5 hpf embryo, 10 hpf embryo, 18 hpf embryo, 24 hpf embryo, 48 hpf embryo, 72 hpf larva, 5 dpf larva, 15 dpf larva, 35 dpf juvenile zebrafish. Error bars stand for +SE (Reprinted from Doldur-Balli et al., 2015*[139]*).*

The sections from 48 hpf specimen revealed expression of *wdr81* throughout the diencephalon (Di), preoptic area (Po), midbrain tegmentum (T), optic nerve, lens, nucleus of the medial longitudinal fascicle, and the retina. Observation of more condensed and distinct expression sites, along with the stained axonal fibers most probably were associated with cells, neuronal in origin (Figure 24 a-c). The intensity of the signal produced by the probe was the lowest in the sections obtained from 72 hpf specimen. The signal was observed in the midbrain tegmentum (T) and the retina (Figure 24 e-f). Relative spatial expression of *wdr81* in adult tissues was investigated using qRT-PCR. The same primer pairs used in the temporal expression study, qRT-PCR F and R (Table 5, Figure 7), were employed in quantification of expression values of ten adult tissues.

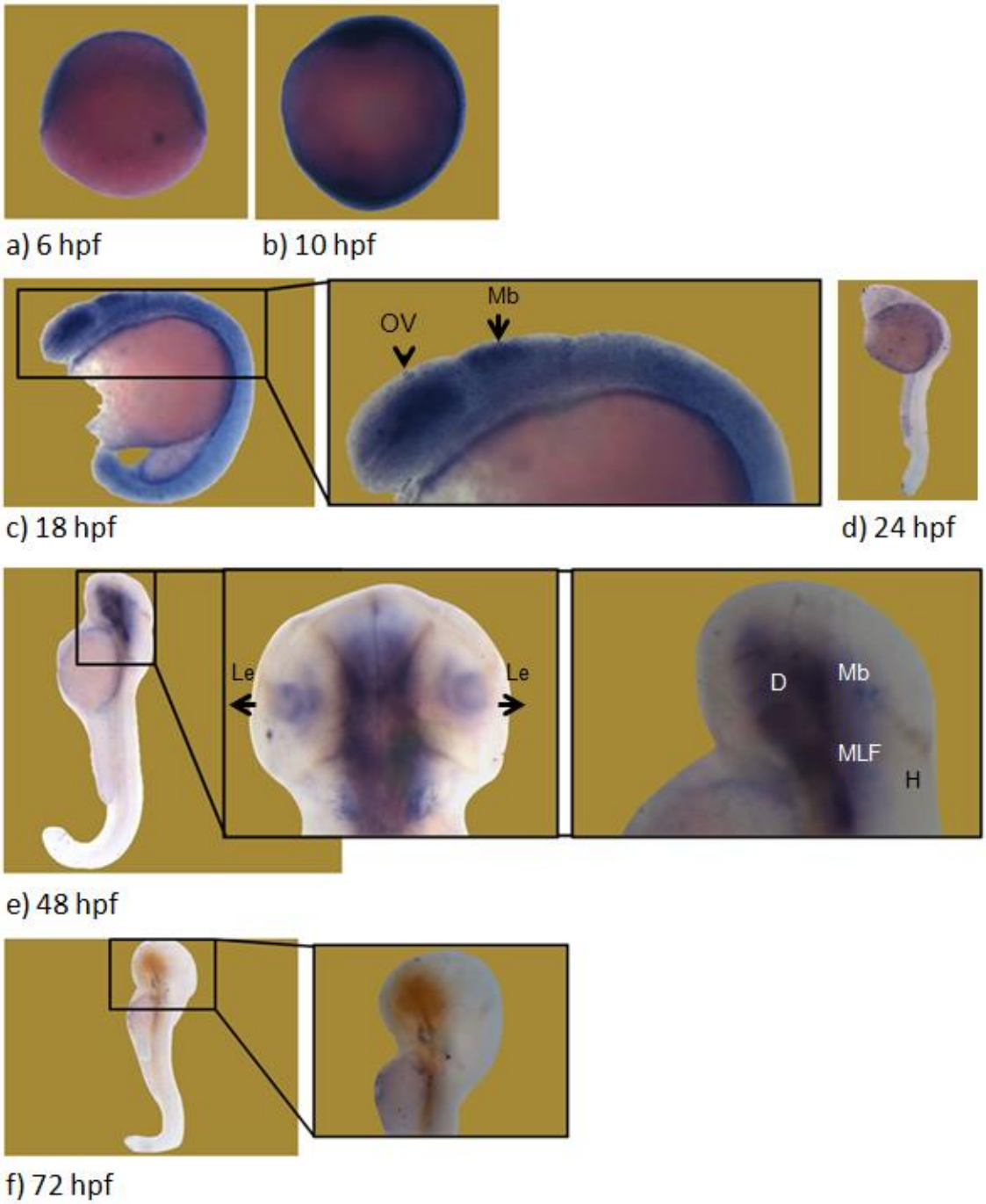

Figure 23. Spatio-temporal expression of *wdr81* during early development revealed via WMISH. *The signal of the riboprobe was strong in the first 18 hours of development (a-c), then the intensity of the signal declined and continued during the other evaluated timepoints (d-f). The signal was enriched in the eye and brain at 18 hpf and 48 hpf timepoints (c,e). OV: Optic vesicle, Mb: midbrain, Le: lens, H: hindbrain, D: diencephalon, MLF: medial longitudinal fascicle (Reprinted from Doldur-Balli et al., 2015*[139]*).*

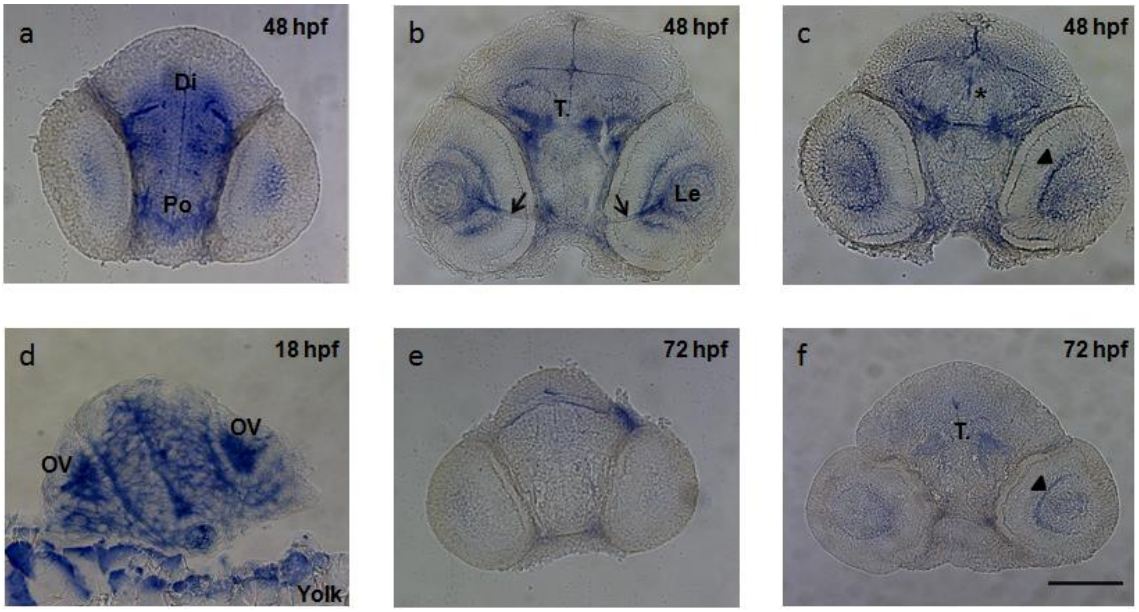

Figure 24. Transverse sections obtained from the head regions of WMISH specimens from 3 developmental stages. *The signal of the riboprobe which implies wdr81 expression was condensed in specific regions by 48 hpf (a-c), though the signal was homogenous at 18 hpf (d), and dropped down by 72 hpf (e and f). Optic nerve was indicated by arrows, the region of the nucleus of the medial longitudinal fascicle was indicated by an asterix, and the retina was indicated by an arrowhead. Po: preoptic area; Di: diencephalon; T.: midbrain tegmentum; Le: lens; OV: optic vesicle; Yolk: yolk sac. Scale bar equals 100 micrometers (Reprinted from Doldur-Balli et al., 2015*[139]*).*

Expression of *wdr81* was detected in all of the evaluated tissues, which were brain, testis, heart, kidney, liver, intestine, eye, gills, tail and muscle. This data suggested that *wdr81* was ubiquitously expressed and still variation among the relative expression values of tissues was existing (Figure 25). Another aspect of spatial expression study in adult tissues was accomplished by applying ISH to the brain and eye. Expression of *wdr81* in these tissues was demonstrated with qRT-PCR method (Figure 25) and this data indicated the expression in whole tissues. We showed the distribution of the expression of *wdr81* on sections from two tissues by hybridizing the same riboprobe used in WMISH method (Figure 26).

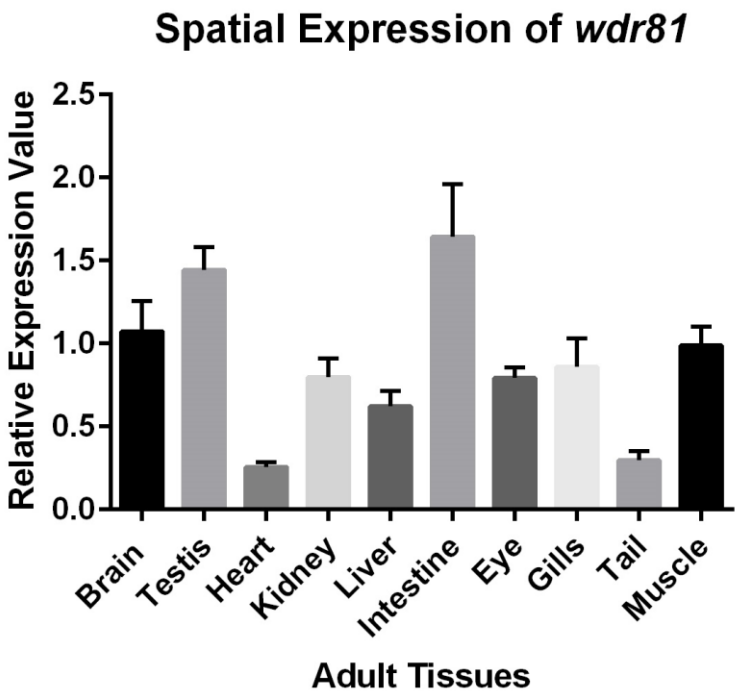

Figure 25. Relative expression of *wdr81* in ten adult tissues. *Expression of wdr81 was detected to be ubiquitous. Templates were cDNAs from brain, testis, heart, kidney, liver, intestine, eye, gills, tail and muscle. Error bars stand for +SE (Reprinted from Doldur-Balli et al., 2015*[139]*).*

Expression of *wdr81* was detected in the retinal layers, presumptive Purkinje cells of cerebellum, tectal ventricle, brain stem and optic tectum (Figure 26). The expression of *wdr81* was observed in the cells which possess a morphology like neurons in the brain areas, *lobus vagus* and optic tectum (Figure 26 f,g). Intriguingly, the areas, tectal ventricle (midline ventricle), *lobus vagus* and periventricular gray zone of optic tectum, which gave strong signals were known proliferation zones in zebrafish brain (Figure 26 c, f,g). Thereby, the data obtained from ISH experiment provided an association between *wdr81*-positive areas, which appeared to have a neuronal phenotype, and neurogenesis.

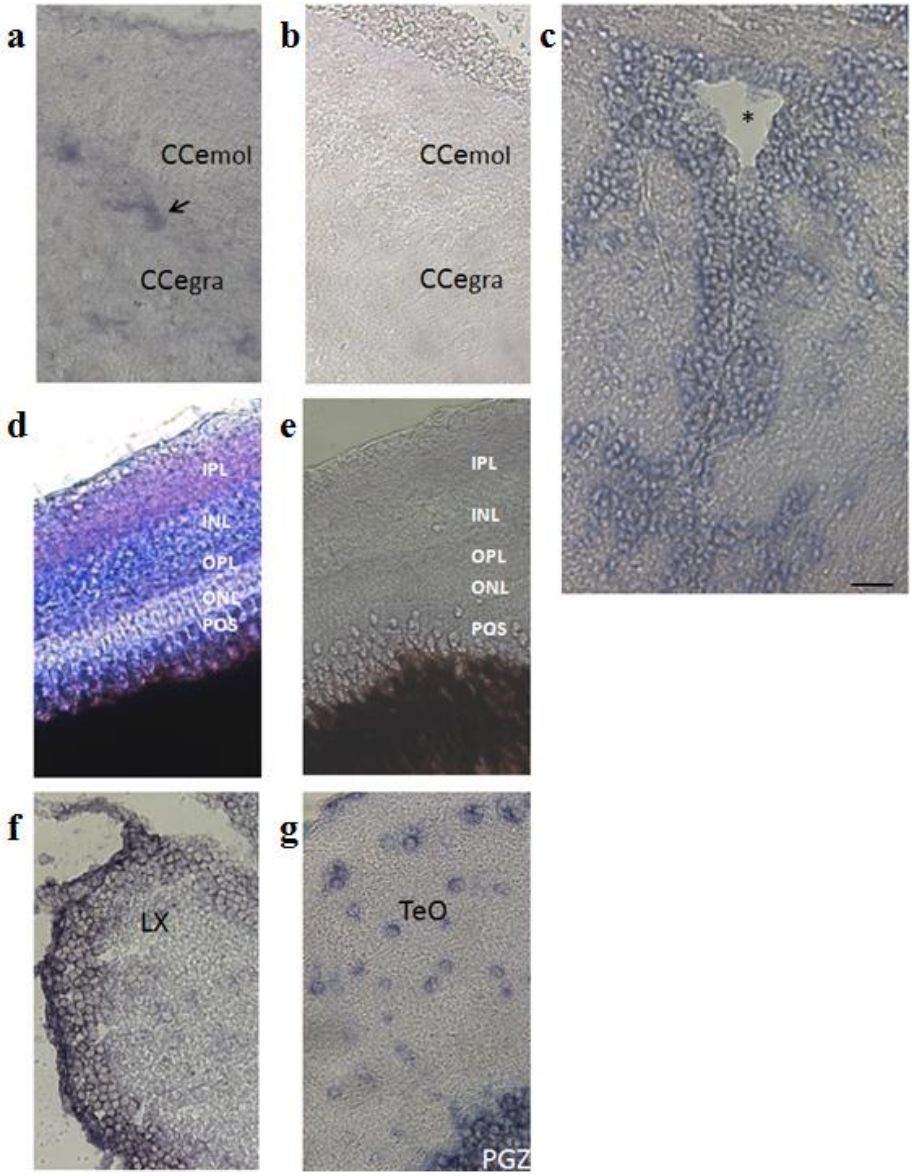

Figure 26. Distribution of the signal of riboprobe revealed the expression of *wdr81* in the adult brain areas and eye tissue. *Cerebellum (a), tectal ventricle (c), retina (d), brain stem (f), and optic tectum (g) were positive for wdr81 expression. A sense probe was used in cerebellum (b) and retina (e) sections in order to confirm that the signals from the antisense riboprobe were specific. CCe_{mol}: Cerebellar molecular layer; CCe_{gra}: Cerebellar granular layer; POS: photoreceptor outer segments; ONL: outer nuclear layer; OPL: outer plexiform layer; INL: inner nuclear layer; IPL: inner plexiform layer; LX: lobus vagus; TeO: optic tectum; PGZ: periventricular gray zone of the optic tectum. Purkinje cell layer was indicated by an arrow and the tectal ventricle was indicated by an asterix. Scale bar implies a length of 200 micrometers (Reprinted from Doldur-Balli et al., 2015*[139]*).*

3.6. Initial Characterization of Morphants

3.6.1. Dose Curve of *wdr81* Morpholino

Detecting whether *wdr81* was maternally supplied or not was needed before ordering the morpholino sequence since microinjection of a translation blocking morpholino may produce more severe phenotypes than that of a splice blocking morpholino[149]. In order to fulfill this aim, cDNA samples from 1 hpf, 2 hpf, 3 hpf, 6 hpf, 12 hpf, 24 hpf and 48 hpf timepoints were amplified with a gene specific primer pair which produces an amplicon in 495 bp length. Zygotic expression in zebrafish was reported to start at 3 hpf[147,148]. I previously showed the expression at 1 hpf timepoint (Figure 22), then cDNA samples from 2 hpf and 3 hpf timepoints were added to this experiment. The expected amplicon was obtained from all of the templates (Figure 27). This data indicated that *wdr81* was maternally supplied since there was amplification at 1 hpf, 2 hpf and 3 hpf stages. A splice blocking morpholino to knockdown *wdr81* was ordered because of two reasons: 1) *wdr81* is maternally supplied and using a translation blocking morpholino might result with a more severe phenotype, 2) lack of an efficient antibody, reacting with zebrafish samples, to detect the effect of a translation blocking morpholino on protein level. The location of the *wdr81* morpholino sequence and its target is depicted (Figure 28). When the *wdr81* splice blocking morpholino sequence was searched for any off target sequences by using NCBI Blast database[150], the obtained list was examined carefully and none of the hits were targeting any translation initiation sites or exon-intron junctions. WD repeat containing genes which were hit by the *wdr81* morpholino sequence, other than *wdr81*, were the genes encoding WD repeat-containing protein on Y chromosome-like isoform X1 and WD repeat-containing protein 49-like isoform X2. These hits were corresponding to intronic sequences, for this reason the risk of producing an off-target effect was evaluated to be unlikely. Tblastn database of NCBI[138] was also utilized to reveal the genes which encode proteins similar to *wdr81*. The list of genes obtained as a result of this search (Appendix E) included some genes which encode WD repeat-containing proteins. They were the genes encoding WD repeat and FYVE domain-containing protein 3 isoform X3, WD repeat and FYVE domain-containing protein 3 isoform X7, WD repeat and FYVE domain-containing protein 4

isoform X1 and WD repeat and FYVE domain-containing protein 4 isoform X2. The number of matching aminoacids was 70 with WD repeat and FYVE domain-containing protein 4 and 72 with WD repeat and FYVE domain-containing protein 3. The hits were obtained at the BEACH domain. The rest of the hits were also obtained at the BEACH domain with an exception of the gene encoding transcription initiation factor TFIID subunit 5, hitting WD40 repeats. The number of matching aminoacids in the rest of the list, except the genes encoding WD repeat-containing proteins, were maximum 90 over 2065 aminoacids. None of the results showed an overlap with neither the corresponding mutation site (residue 894) nor the morpholino target site (residues 1296-1298) in zebrafish *wdr81*. Effect of three doses of the morpholino antisense oligonucleotide sequence, which were 2 nanograms (ng), 4 ng and 8 ng, on splicing were evaluated. Similar doses of standard negative control morpholino, which did not have a target in zebrafish[144], were included. Uninjected control group from the same clutch were also collected. The survival rates of each experiment group were recorded (Table 8) and cDNAs from the samples were amplified in order to understand the effect of each dose of morpholino on splicing. The primer pair, which was used to understand the effect of the *wdr81* morpholino on splicing, was designed so that the amplicon would be 572 bp long if intron 2 was introduced between exon 2 and exon 3 and it would be 449 bp long if the template was a wild-type mRNA (Figure 29).

The PCR products were run on a 1% agarose gel firstly, then the rest of the reaction volumes of each sample were run on a 4% agarose gel in order to observe a better resolution. Results of the experiment showed that all of the evaluated doses efficiently worked and there was a band shift from 449 bp length to 572 bp length in the lanes where the reactions belonging to 2 ng, 4 ng and 8 ng *wdr81* morpholino injected embryos were loaded. Five hundred and seventy two bp long band had a stronger signal than the 449 bp long band in these lanes, indicating an introduction of intron 2 between exon 2 and exon 3 in the morpholino effected *wdr81* transcripts (Figure 30).

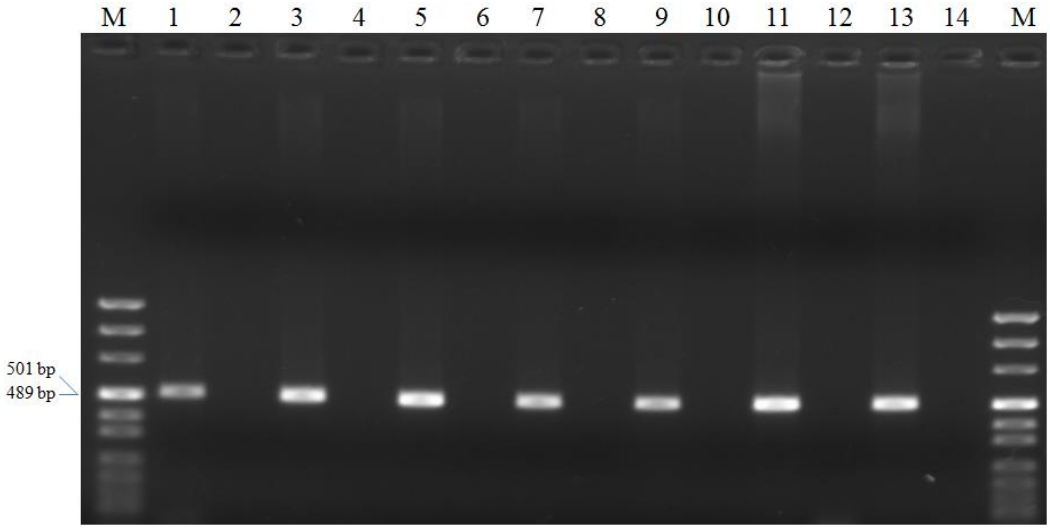

Figure 27. Agarose gel electrophoresis of the PCR products from a reaction showing *wdr81* expression between 1-48 hpf timepoints. *Detecting its expression earlier than 3 hpf indicated that wdr81 was maternally supplied. Templates in lane 1: cDNA of 1 hpf embryo, lane 2: -RT control for 1 hpf embryo, lane 3: cDNA of 2 hpf embryo, lane 4: -RT control for 2 hpf embryo, lane 5: cDNA of 3 hpf embryo, lane 6: -RT control for 3 hpf embryo, lane 7: cDNA of 6 hpf embryo, lane 8: -RT control for 6 hpf embryo, lane 9: cDNA of 12 hpf embryo, lane 10: -RT control for 12 hpf embryo, lane 11: cDNA of 24 hpf embryo, lane 12: -RT control for 24 hpf embryo, lane 13: cDNA of 48 hpf embryo, lane 14: -RT control for 48 hpf embryo. Lane indicated as M was loaded with pUC mix DNA Marker (SM0301, Thermo Scientific).*

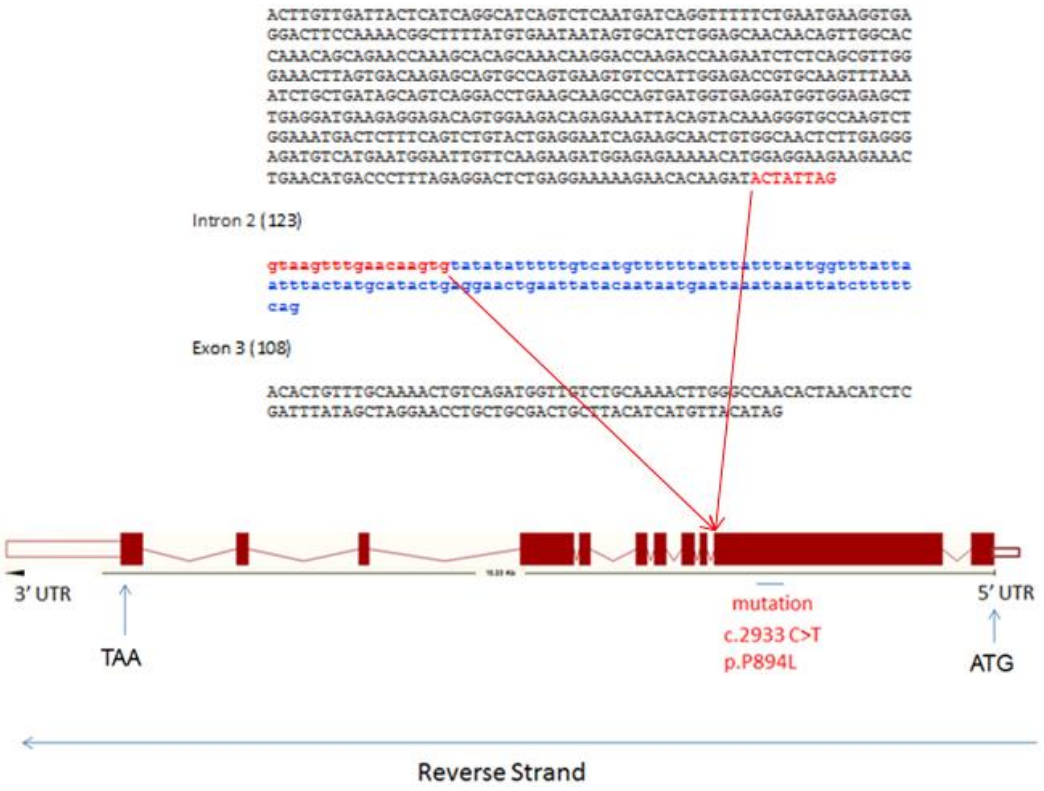

Figure 28. Illustration of the location of the target of the morpholino sequence (shown in red) which was designed to knock down *wdr81*. *The splice blocking morpholino was designed to bind to the last 6 nucleotides of exon 2 and initial 17 nucleotides of intron 2.*

Table 8. Survival rates of the embryos from experiment groups in the *wdr81* morpholino dose curve study.

Experiment Groups	Number of Surviving Embryos	Number of Dead Embryos	Survival Rate	Dose
wdr81 morpholino injected group	11	40	21.57%	2 ng (data from 3 experiments were collected)
Standard negative control morpholino injected group	10	46	17.86%	
Uninjected control group	23	36	38.98%	

Experiment Groups	Number of Surviving Embryos	Number of Dead Embryos	Survival Rate	Dose
wdr81 morpholino injected group	19	43	30.65%	4 ng (data from 3 experiments were collected)
Standard negative control morpholino injected group	31	22	58.50%	
Uninjected control group	31	29	51.66%	

Experiment Groups	Number of Surviving Embryos	Number of Dead Embryos	Survival Rate	Dose
wdr81 morpholino injected group	13	35	27.08%	8 ng (data from 3 experiments were collected)
Standard negative control morpholino injected group	6	26	18.75%	
Uninjected control group	21	24	46.66%	

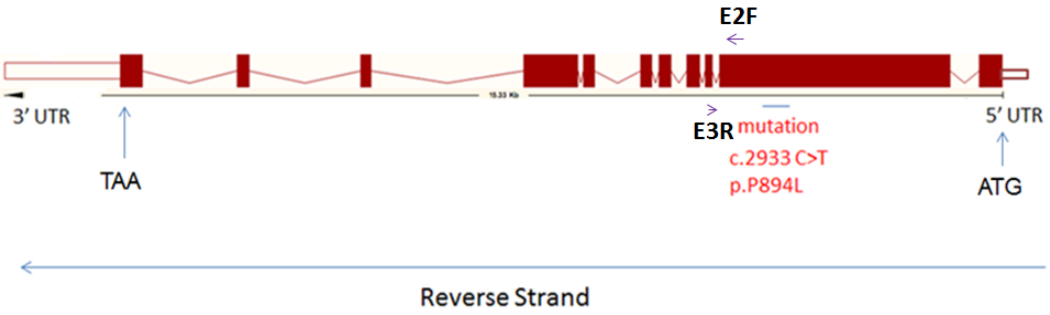

Figure 29. Illustration showing the location of the primer pair, which was designed to reveal the effect of *wdr81* morpholino on splicing. *The forward primer was designed to bind exon 2 and the reverse primer was designed to bind exon 3 so that a shift in the band size would be detected as a possible outcome of the morpholino microinjection. The length of the intron 2 is 123 bp. long. The size of the band amplified from the morphant samples was expected to be 123 bp higher than that of the wild type samples.*

3.6.2. Initial Results from Phenotype Characterization of *wdr81* Morphants

Since *WDR81* was suggested to be a neurodevelopmentally important gene in the literature[12,36] and by our data, knockdown of this gene was expected to affect the central nervous system. Head size measurements were carried out in the morphant embryos firstly, in order to search for a possible widespread effect of the *wdr81* morpholino. One of the possibilities was hypothesized to be a microcephaly phenotype since significant decline in the volumes of cerebellum and corpus callosum in patients were detected[12]. Head size measurements were performed by following the report of Golzio *et al.*, (2012) in parallel with the dose curve study.

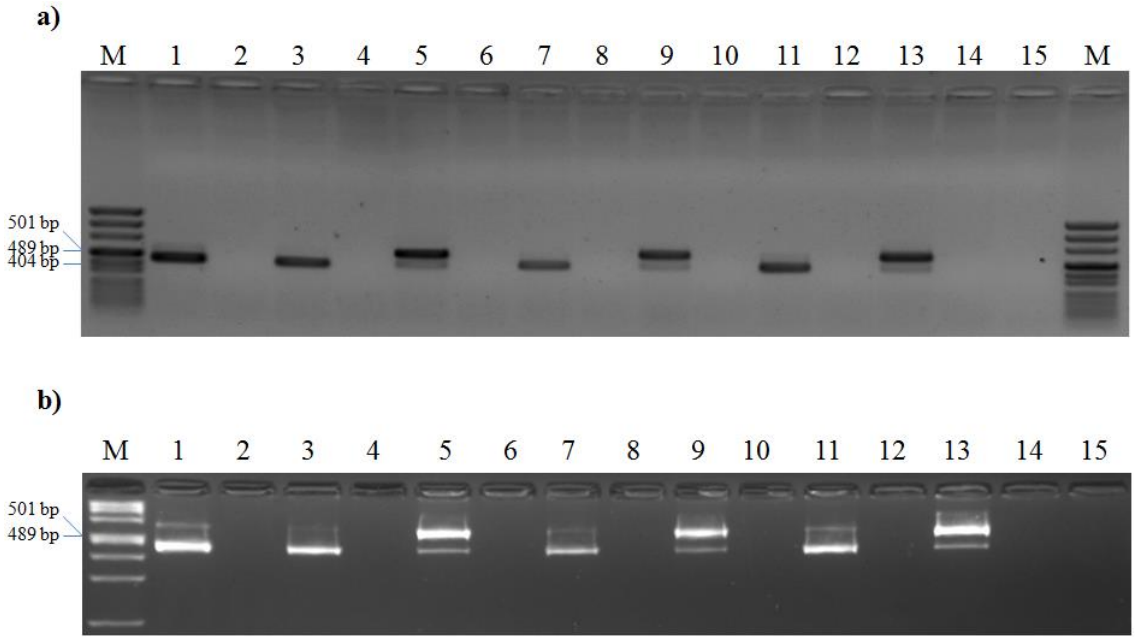

Figure 30. Agarose gel electrophoresis of the PCR products from a reaction showing the effect of three doses of *wdr81* morpholino on splicing. *a) The PCR product were run on a 1% agarose gel, b) The same PCR products were run on a 4% agarose gel. Both (a) and (b) gels, templates in lane 1: cDNA of uninjected embryo, lane 2: -RT control for uninjected embryo, lane 3: cDNA of 2 ng standard negative control morpholino injected embryo, lane 4: -RT control for 2 ng standard negative control morpholino injected embryo, lane 5: cDNA of 2 ng wdr81 morpholino injected embryo, lane 6: -RT control for 2 ng wdr81 morpholino injected embryo, lane 7: cDNA of 4 ng standard negative control morpholino injected embryo, lane 8: -RT control for 4 ng standard negative control morpholino injected embryo, lane 9: cDNA of 4 ng wdr81 morpholino injected embryo embryo, lane 10: -RT control for 4 ng wdr81 morpholino injected embryo, lane 11: cDNA of 8 ng standard negative control morpholino injected embryo, lane 12: -RT control for 8 ng standard negative control morpholino injected embryo, lane 13: cDNA of 8 ng wdr81 morpholino injected embryo, lane 14: -RT control for 8 ng wdr81 morpholino injected embryo, lane 15: no template negative control. Lane indicated as M was loaded with pUC mix DNA Marker (SM0301, Thermo Scientific).*

Changes in the head size of embryos from experiment groups were detected with the measurement of the distance between the convex edges of the cornea of two eyes between the timepoints 4.25 and 4.5 dpf. Body lengths of the embryos were also measured to compare their development (Figure 31).

Figure 31. A representative picture (taken with a Leica MZ10F microscope) of an embryo, whose head size and body length were measured via Leica Application Suite 4.3 (LASv 4.3) software. *The body length measurements among experiment groups were not hypothesized to change significantly since a developmental delay was not expected, instead a significant change in the head size measurements among experiment groups were hypothesized based on the assumption that knockdown of wdr81 would cause impairments in development of the nervous system.*

8 ng *wdr81* morpholino and 8 ng standard negative control morpholino were injected to embryos and an uninjected control group was seperated. The survival rates of the experiment groups were recorded (Table 9). A researcher from our research group, who was blind to the experiment groups, performed the measurements, then the data was sorted according to the experiment groups. One way Anova analysis was performed in order to evaluate whether the differences between groups were statistically significant or not. As a result, 3.88% reduction in the head size of *wdr81* morpholino injected group compared to uninjected group was found to be significant with a p value of 0.027 and 2.53% reduction in the body length of negative control morpholino injected group compared to uninjected group was found to be significant with a p value of 0.043. The mean of head size measurements were 0.545 mm ± 0.042 in *wdr81* morpholino injected group; 0.560 mm ± 0.034 in negative control morpholino injected group and 0.567 mm ± 0.032 in uninjected group. The mean of body size measurements were 3.45 mm ± 0.22 in *wdr81* morpholino injected group; 3,46 mm ± 0,24 in negative control morpholino injected group and 3,55 mm ± ,098 in uninjected group.

Table 9. Survival rates of the embryos from experiment groups in the head size measurement study

Experiment Groups	Number of Surviving Embryos	Number of Dead Embryos	Survival Rate	Dose
wdr81 morpholino injected group	28	77	26.66%	8 ng (data from 4 experiments were collected)
Standard negative control morpholino injected group	55	50	52.38%	
Uninjected control group	75	30	71.43%	

After testing differences in head sizes of experiment groups and after the dose curve was established, we set up another experiment design in order to evaluate changes in expression of a marker gene in the *wdr81* morphants. *gbx2* expression was compared in the three experiment groups, which were 2 ng *wdr81* morpholino injected group, 2 ng standard negative control morpholino injected group and uninjected control group. *gbx2* expression is known to be crucial for development of both midbrain and anterior hindbrain[146]. In morpholino microinjection experiments, after the effect of the morpholino on the protein level or on splicing is shown, general approach is to check how the expression of relevant genes are affected from the knockdown of the gene of interest. Whole mount *in situ* hybridization method is generally utilized for this purpose because of the lack of a variety of antibodies in zebrafish research. This approach might be applied in order to reveal the downstream or upstream targets in the same pathway[151], to observe how specific cell types are affected from the knockdown of the gene of interest by labelling them with probes[152] or to check how expression of patterning markers such as *gbx2* are affected[153]. *gbx2* was preferred in this study as a marker gene because of being a crucial gene for development of both midbrain and anterior hindbrain, where cerebellum takes place. *WDR81* was reported to be associated with CAMRQ and cerebellar hypoplasia was observed in patients[12]. Knockdown of *wdr81* needed to be evaluated by taking this information into account. In addition, expression of *wdr81* was detected in the midbrain in zebrafish embryos. Testing how expression of *gbx2* was affected from the knockdown of *wdr81* was an appropriate approach because of combining both of the significant expression sites, ie. midbrain and cerebellum. Microinjection of 2 ng dose was preferred in this experiment set up because the dose curve was already established and all the tested doses were shown to be efficient. When all the doses are efficient, the common approach is to use the lowest dose of morpholino in order to avoid toxicity and higher mortality rates. The WMISH experiment was carried out under the same conditions for all three groups and their images were also taken using the same parameters. The *wdr81* morphant group appeared to be stained stronger than the control groups (Figure 32).

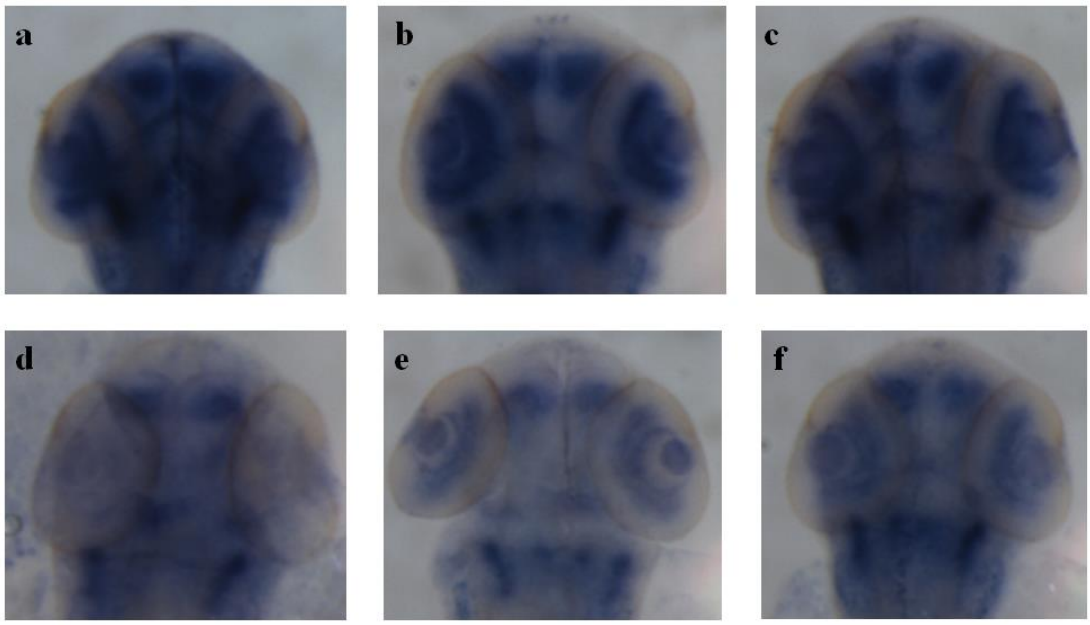

Figure 32. Comparison of *gbx2* expression among 3 experiment groups, which were 2 ng *wdr81* morpholino injected (a-c), 2 ng standard negative control morpholino injected (d,e) and uninjected (f) embryos. *The intensity of the gbx2 probe was found to be stronger in the wdr81 morphant group (a-c) compared to the control groups. The only variable was the microinjection of wdr81 splice blocking morpholino in the embryo group, whose repsentative pictures were shown in the a-c panel and the rest of the experimental conditions were identical in control groups. This result might be indicating a compensation mechanism since gbx2 functions in the development of midbrain and anterior hindbrain and WDR81 is associated with cerebellar hypoplasia. Also, the expression of wdr81 in 2 dpf wild type embryo was detected the highest in the midbrain, eye region, diencephalon and MLF.*

Chapter 4. Discussion

WDR81, the gene which encodes WD repeat containing protein 81 was reported to be associated with CAMRQ. Quadrupedal gait as a movement disorder was observed in the patients. The most significant abnormalities detected in the brains of the patients were cerebellar hypoplasia and volume loss in corpus callosum[12]. While research on zebrafish model organism were ongoing, a study on the *Wdr81* was published, which reported a phenotype similar to CAMRQ in *nur5* mutant mouse model[36]. In the present study, the transcript of the zebrafish *wdr81* was characterized and its expression profile during several developmental stages and in tissues of adult wild type zebrafish was investigated. In addition, morpholino studies were started in order to reveal the function of the *wdr81* and initial investigation was performed in search of a possible phenotype in *wdr81* morphants. WDR81 was reported to be conserved among vertebrates[12]. *In silico* analysis indicated that conserved domains in human and mouse WDR81 proteins are also predicted to be present in the zebrafish orthologous protein (Figure 8, 9). This might also imply a conserved function of the protein of interest in three species. The characterization of the transcript structure and expression profile of *wdr81* was aimed in the first place since it was an uncharacterized gene in zebrafish. The information about *wdr81* in wild type zebrafish should provide a basis for future research such as genetic manipulations including morpholino experiments. Regarding morpholino studies, comprehensive information about the transcript structure and expression of *wdr81* in wild type zebrafish were necessary to design the morpholino sequence, to evaluate the effect of morpholino on splicing and to determine the critical timepoints and relevant tissues for characterization of morphants.

This study is the first to report the transcript structure and expression profile of *wdr81* in zebrafish along with attempts to characterize the *wdr81* morphants. The results of this study showed that zebrafish *wdr81* possessed one ORF and one 5'UTR structure (Figure 13, 15). The predicted sequence for 3'UTR was confirmed along with some variants (Figure 19, Table 6) and a detected insertion site in samples from ten evaluated

developmental timepoints and in several adult tissues such as brain, testis, heart, liver, eye, tail and muscle. The length of this region was determined as 266 bp and this region was not detected in rest of the adult tissues such as kidney, intestine and gills (Figure 20, 21). Detecting the insertion site in some adult tissues but not in the rest of the evaluated tissues might imply an alternative polyadenylation event. *wdr81* appeared to be maternally supplied based on the qRT-PCR study. Crucial timepoints during early development and after zygotic expression started were 5 hpf and 18 hpf because the temporal expression study revealed the peaks in *wdr81* expression at these timepoints (Figure 22). *wdr81* was also shown to be expressed in all of the evaluated adult tissues (Figure 25). In embryos, the signal of the riboprobe which showed the site of expression was stronger in the eye and brain regions at 18 hpf and 48 hpf timepoints (Figure 23). In particular, the intensity of the signal was the highest in the midbrain and optic vesicle at 18 hpf and the signal was mainly detected in lens, preoptic area, optic nerve, retina, diencephalon, midbrain, midbrain tegmentum, medial longitudinal fascicle (MLF) and nucleus of the MLF at 48 hpf. The signal, which was weaker compared to the previous developmental stages, was detected in the midbrain tegmentum and retina at 72 hpf (Figure 23, 24). The expression profile of *wdr81* in the adult brain and eye indicated that *wdr81*-positive cells had neuronal morphology and some *wdr81*-positive regions were proliferative zones (Figure 26). After establishing the expression in the wild type organism, the number and structure of the transcript, splice blocking morpholino experiments were carried out in order to search for a phenotype. These attempts were mainly including two approaches: 1) searching for a microcephaly phenotype 2) initial characterization of morphants by comparing *gbx2* expression in experiment groups. Reduction in head size was 3.88% in *wdr81* morphant group compared to uninjected control group, which was significant (p:0.027). The signal of the riboprobe, which was synthesized to detect *gbx2* expression, was stronger in *wdr81* morphant group compared to negative control and uninjected groups (Figure 32).

Existence of nine protein coding splice variants in human (Figure 10) and three protein coding splice variants in mouse (Figure 11) motivated the study to detect the number of *wdr81* transcripts in zebrafish. This set of experiments were also performed to provide an experimental validation of the transcript prediction made by Ensembl (*wdr81*-001,

ENSDART00000156621) (Figure 12), which was taken as a model for designing gene specific primers. UTR structures were characterized also because these significant regions mediate gene expression at the post-transcriptional level[154]. RACE method was applied in order to characterize the UTR regions. Tissue specific transcription start sites[155,156], and 3'UTR structures in different lenghts[156] are possible to be detected by employing this method. One ORF and one 5'UTR structure were detected as predicted (Figure 13, 15). One 3'UTR structure along with a detected insertion site appeared to exist in the tested samples which were brain and 24 hpf embryo (Figure 19). Detecting the insertion region in most of the evaluated tissues and not in kidney, intestine and gills (Figure 21b) might be explained by the fact that alternative cleavage and polyadenylation processes were identified in tissue specific regulation of protein levels encoded by most of the ubiquitously transcribed genes. This mechanism was suggested to change the proportion of 3'UTR variants and so that result in switching the targets for microRNAs and regulatory elements[157]. When the signals of the bands from the reaction, in which the insertion site was amplified, were measured, the strongest signals were detected from brain, testis and eye (Table 7). Gene expression profiles across brain, cerebellum and testis were previously reported to be the most similar in human and mouse compared to the similarity among other tissues[158]. The eyes, in particular the retina or neural part of it, are components of the central nervous system[159]. A similar mechanism in 3'UTR mediated post-transcriptional regulation might take place in brain and eyes. The potential mechanisms mentioned above might have roles in producing different levels of proteins and in changing the activity of *wdr81*.

As the temporal expression study revealed that the crucial timepoints of development regarding *wdr81* expression were 5 hpf and 18 hpf (Figure 22), relevant critical anatomical developments at these timepoints were searched. At 5 hpf, presumptive brain is expected to have formed since it is known to appear between 4-4.33 hpf at sphere stage. At 18 hpf, the brain structure and optic vesicle is expected to have formed since they are known to appear between 14-16 hpf and 11.66-14 hpf at the segmentation stage, respectively[112]. The lower levels of expression during rest of the timepoints after 18 hpf also implied that this maintained level of *wdr81* was required for development (Figure 22). WMISH results were in parallel with the qRT-PCR results in general. The

signal intensity of the riboprobe, which was designed to detect the site of *wdr81* expression, was high between 6 hpf and 18 hpf, and reduced after 18 hpf. The signal was homogenously distributed at 6 hpf, 10 hpf, 18 hpf and 24 hpf, it was condensed in the brain and eye at 48 hpf. The signal was clearly diminished at 72 hpf (Figure 23). Increased expression of *wdr81* in the brain and eye regions at 18 hpf and 48 hpf were in parallel with the previous reports from human and mouse studies[12,35,36]. Observing the *wdr81* RNA probe signal highest in the brain and eye regions at 18 hpf and 48 hpf timepoints (Figure 23) and detecting the peaks regarding *wdr81* relative temporal expression at the early developmental stages such as 1 hpf, 5 hpf and 18 hpf (Figure 22) imply the potential significance of *wdr81* in neurodevelopment. Microarray data from the literature verified that *wdr81* was expressed in the retina of zebrafish embryo[160] and in brain tissues of young and old adults[161]. The potential significance of *WDR81* in neurodevelopment of human and mouse was suggested in the previous reports as well[12,36]. Determining the critical stages of development regarding *wdr81* expression also served to designate the timepoints for characterization of *wdr81* morphants.

The spatial expression study revealed that *wdr81* was expressed in all of the evaluated adult tissues, which is also called as ubiquitous expression (Figure 25). Human and mouse *WDR81* were also detected to be expressed in all of the evaluated adult tissues[12,36]. The levels of the expression were changing across tissues of adult zebrafish (Figure 25). The signal of the *wdr81* RNA probe was homogenously distributed at 6 hpf, 10 hpf, 18 hpf and 24 hpf timepoints, too (Figure 23). Cerebellum was not detected to be one of the brain regions with strong signal in zebrafish embryos from six developmental timepoints, which might be evaluated to be in contrast with the mouse data obtained from embryonic brain because expression of *Wdr81* was found to be increased in cerebellum[12]. The expression data from juvenile mouse (P21) also showed expression in the cerebellum and retina[36]. Nevertheless the regions detected with higher signals in embryos had connection with either cerebellum or the eye. The MLF is a group of axons, which starts from the nucleus of the MLF continues ventral to the rhombencephalic ventricle through the caudal end of the medulla oblongata, functions in coordinating conjugate eye movements[112,162]. The diencephalon is made up of thalamus and hypothalamus. The retina originates from the diencephalon, it forms a

vesicle out from diencephalon to form the retina and is called as optic vesicle and invagination of the optic vesicle end up with the optic cups. The retina develops from the inner wall of the optic cup and the pigment epithelium develops from the outer wall of the optic cup[162]. The midbrain (mesencephalon) also participate in motor function and sensory functions[163]. The expression of *wdr81* of the adult brain and eye tissues was observed on the sections from the cerebellum, retina, tectal ventricle, brain stem and optic tectum (Figure 26). Although strong signals were not detected from the cerebellum of the embryos, the expression of *wdr81* was detected in the retinal layers and presumptive Purkinje cells of cerebellum in adult study (Figure 26) which was consistent with the data from human and mouse studies[12,36]. In the human study, retinal expression of *WDR81* was not mentioned[12] however neuro-ophthalmic examination of four patients from the same reported family revealed downbeat nystagmus diagnosis[35]. This eye disorder might be indicating the expression of *WDR81* in the eye since it is an accompanying case in the patients affected from the mutation in the *WDR81* isoform 1. *Wdr81* expression was also detected in brain stem of wild type adult mouse[36]. The common expression sites in three species are also providing a supporting evidence for conserved function of *WDR81*.

Detecting *wdr81* RNA probe in the presumptive Purkinje cells, retina, optic tectum, optic nerve and other nerve fibers (Figure 24, 26) suggested that the expression product of this gene in both embryos and adult zebrafish was located in several neuronal phenotypes. Confirmation of the neuronal phenotypes in future studies is needed to be performed using both *wdr81* RNA probe and immunostaining with neuronal markers. Some of the neuronal markers used in zebrafish research are *gad1* or *gad2* to detect GABAergic neurons[164], which fulfill inhibitory action, and antibodies against glutamate receptor 1, glutamate receptor 2, glutamate receptor 2/3 or glutamate receptor 4 to detect glutamatergic neurons[165], which fulfill excitatory action. Purkinje cells can be detected with zebrin 2[166] or M1[167] antibodies. Proliferation status of cells in zebrafish studies is possible to detect with antibodies against phosphohistone 3[168], proliferating cell nuclear antigen (PCNA)[169], histone H1[170] or 5-bromo-2'-deoxyuridine (BrdU)[171]. Also counterstaining with an early neuronal marker or a late neuronal marker is expected to exhibit the association of the expression of *wdr81* with the stage of the

neuronal proliferation. Hu as an early neuronal marker[171–173] and neuronal nuclei (NeuN) as a late neuronal marker[174,175] might be used in this type of study. Since glial cells appear at 26+ somites stage (segmentation, 22-24 hpf) in zebrafish[112] and *wdr81* expression was determined at the highest levels in the first 18 hpf (Figure 22, 23), this gene was not suggested to be associated with glial cells. Besides, the morphology of the cells, which were *wdr81*-positive in the adult brain sections (Figure 26a,c,f,g), were implying a neuronal morphology in nature. Neurogenesis starts at late gastrulation, around 10 hpf and proceeds during embryogenesis[119] and synaptogenesis starts around 18 hpf in zebrafish[84]. Observing the peak in expression of *wdr81* at 18 hpf (Figure 22) might also be indicating a potential role of this gene in neurogenesis, neuronal migration and survival of neurons in embryos. Furthermore, the brain regions where *wdr81* expression was detected, such as the tectal ventricle, vagal lobe, optic tectum and periventricular gray zone of the optic tectum (Figure 26) were reported as proliferative zones[176]. Retinal neurogenesis is a persistent process during whole life of teleost fish including zebrafish[177]. A microarray study, which demonstrated the differential expression of genes after a lesion occured in the retina, revealed that the expression of *wdr81* increased between 5 days and 7 days post-lesion[178]. This finding also contributes to the suggestion that *wdr81* might have a potential function relevant with neurogenesis, which might be retinal neurogenesis in this report. Detecting the expression of *wdr81* in retinal layers and other proliferative zones in the brain (Figure 26) also points out the potential role of this gene in neuronal proliferation, neuronal migration and survival of neurons in the adult zebrafish. Neurogenesis related function of *wdr81* was also predicted *in silico*[112,179]. The pattern of the strong signals in Figure 26 c and f might indicate the relevance of the function of wdr81 with neuronal proliferation since the signals strongly come from the proliferative zones and that in Figure 26 g might indicate the relevance of the function of wdr81 with neuronal migration since the signals in the optic tectum appear to come from the cells spread in this layer. This set of data obtained from the expression studies provide evidence about the potential role of *wdr81*.

Gulsuner *et al.* (2011) suggested that *WDR81* might be a critical gene in neurodevelopment and motor behavior[12]. Research on the *nur5* mutant mouse model,

which demonstrated a phenotype similar to CAMRQ, concluded that localization of *Wdr81* was the mitochondria of Purkinje cells and photoreceptor cells. The homozygous missense mutation, affecting the predicted MFS domain, caused loss of Purkinje cells and photoreceptor cells. Loss of Purkinje cells was suggested to take place after mitochondrial abnormalities occured during development[36]. *WDR81* gene was reported to be mutated in several colorectal cancer cell lines[37] and it was located in a metabolically important loci, which was found to be associated with serum albumin level[38]. Serum albumin level is metabolically important because of its inverse correlation with cardiovascular and mortality risk[39,40]. The potential function of wdr81 might be projected based on the conserved domains. Since BEACH-domain containing proteins have roles in membrane-related events, such as vesicular transport, receptor signaling and formation of synapses[41], WD40 domain-containing proteins function in cell cycle control, signal transduction, regulation of transcription, chromatin dynamics and vesicular trafficking[42] and the MFS transporters function in transport of small molecules[43], these functions together might be relevant to a potential function of wdr81 in synaptic plasticity and neuronal proliferation. A microarray study showed that the expression of *wdr81* in zebrafish was also affected by the presence of a mutation in p100 gene, which encodes a recycling factor in spliceosome cycle. The expression of *wdr81* showed a declining trend at 3 dpf and a rising trend at 5 dpf in *egy* mutants, the strain which carries the mutation in p100 gene, compared to the wild type siblings. The rising trend was interpreted as an indication of a compensation mechanism in the spliceosome cycle by the authors[180]. This finding might also be emphasizing that the expression of *wdr81*, as a critical gene in neurodevelopment, is tightly bound up with the changes in cellular functions. The functions of other CAMRQ associated genes in central nervous system were defined. *VLDLR*, in interaction with reelin, acts in guiding migration of neuroblasts in the cerebral cortex and cerebellum during development[26,27]. It also functions in coordination of Purkinje cell alignment in the cerebellum during development[28,29] and it is expressed in synapses[32]. *CA8* expression in human fetal brain was detected in neuroprogenitor cells in the subventricular zone and in the neurons migrating to the cortex[69]. Overexpression of *CA8* resulted in reduced cell death in neuronal cell lines and downregulation of the same gene decreased cell migration and invasion[71]. *Atp8a2* in coordination with *Cdc50a* functions in axon elongation of neurons and hippocampal neuronal differentiation in rats[80]. Thus, CAMRQ associated genes

have roles in neuronal migration, survival and differentiation, which overlap with the roles suggested for *wdr81* in this study. Although the data accumulated so far from the literature serves some clues about the function of *WDR81* and its significance in both neurodevelopment and metabolism, exact function of this gene is not fully understood.

The morpholino experiments, which were carried out in order to develop an understanding of the function of *wdr81*, were performed with 2 ng and 8 ng *wdr81* morpholino doses. The survival and mortality rates of embryos were recorded during experiments. Based on my observations during morpholino microinjection experiments, the differences in mortality rates of zebrafish embryos were based on the wild type strain used, regular and frequent feeding with artemia along with the dry food, and the age of the fish. We had AB strain zebrafish from two sources in our zebrafish facility, University of Madison and Karlsruhe Institute of Technology. The first wild type strain to be brought to the zebrafish facility was AB strain from University of Madison and using only this strain in breeding set-up gave low rates of survival, which might be related with inbreeding. Using zebrafish pairs in combination of two sources, ie. the strain from University of Madison and the strain from Karlsruhe Institute of Technology, for breeding gave better survival rates. Especially this observation is suggested to be the explanation to the discrepancy in survival rates reported in Table 8 and 9. The microcephaly phenotype search with 8 ng morpholino resulted in 3.88% reduction in head size in the *wdr81* morphant group compared to uninjected control group (p:0.027), however the microcephaly phenotype in the literature was reported to exhibit a higher ratio in the reduction, being around 20% reduction[145]. The reduction ratio in the head size should be obtained in the morphant group compared to the standard negative control morpholino injected group, not compared to the uninjected control group. Searching for a widespread change in the head size might be replaced with a strategy to search for regional changes or for changes at the molecular level because the detected abnormalities in the patients were morphological differences in the precentral gyrus and Brodmann areas BA6, BA44 and BA45, along with significant decline in the volumes of cerebellum and corpus callosum[12] instead of global changes such as microcephaly.

When *gbx2* expression among the experiment groups was compared, the signal of the *gbx2* RNA probe was observed to be stronger in *wdr81* morphant group compared to negative control and uninjected groups (Figure 32). Since *gbx2* is known to be a critical gene for development of both midbrain and anterior hindbrain[146], the stronger signal of the *gbx2* RNA probe in the *wdr81* morphant group could be interpreted as a possible compensation mechanism. Similar WMISH studies with other marker genes might be used to confirm this result. The changes in the structures of brain and eye might be investigated. Furthermore, the changes in the synapses, such as changes in the number, size and composition of synapses might be searched at the electron microscopy level in the morphant group compared to the control groups.

Chapter 5. Future Perspectives

The findings about the transcript structure and the expression profile of zebrafish *wdr81* serve both fundamental information about characterization of *wdr81* as a novel gene in wild type zebrafish and a basis for functional studies. In this study, morpholino studies and characterization of morphants were initiated. The search for a microcephaly phenotype in *wdr81* morphants did not give results comparable to the literature because the significant change in morphant group was not obtained compared to the negative control group and the percentage in head size reduction was below the ranges in the literature. However, the results obtained in experiments groups by comparing *gbx2* expression were promising. The signal with *gbx2* RNA probe obtained from *wdr81* morphant group was stonger than that of control groups. This might be indicating a compensation mechanism following knockdown of *wdr81*, still having obtained a change in expression suggests the method to continue with. Similar WMISH studies with other marker genes such as retinal homeobox gene 3 (rx3)[181] to observe development of eye, homeobox A2b (hoxa2b)[182] to observe development of hindbrain, orthodenticle homeobox 2 (otx2)[183–185] to observe anterior neural plate formation and midbrain might be used to confirm and improve this finding. The changes in the structures of brain and eye in the morphant group might be investigated comprehensively. Moreover, electron microscopy studies might be employed to detect some subtle changes such as differences in the number, size, type and composition of synapses in the morphant group compared to the control groups.

Another approach to continue morpholino experiments might be to knock down another CAMRQ associated gene, such as *vldlr*, in parallel with knock down of *wdr81* to observe whether similar phenotypes are obtained. As the function of *vldlr* in central nervous system is known as an integrative element in the reelin pathway and in guiding neuroblast migration in the developing cerebral cortex and cerebellum[26,27], the potential function of *wdr81* and the possibility of two genes taking place in the same pathway might be concluded by comparing the morphant phenotypes. Double knockdown of *wdr81* and *vldlr* might be also performed to detect whether a synergistic effect on the

morphants are obtained. A knockout model might be generated to perform functional experiments on zebrafish so that how the progress of a *wdr81* lacking zebrafish embryo to adulthood would be possible to monitor. This type of a model would be stable considering the longest effect of morpholino microinjection lasts for around five days[100]. Both WMISH with marker genes might be performed to detect the changes and relevance of *wdr81* with neuronal proliferation might be detected by using BrdU labeling, which was a method established during this study (Figure 33).

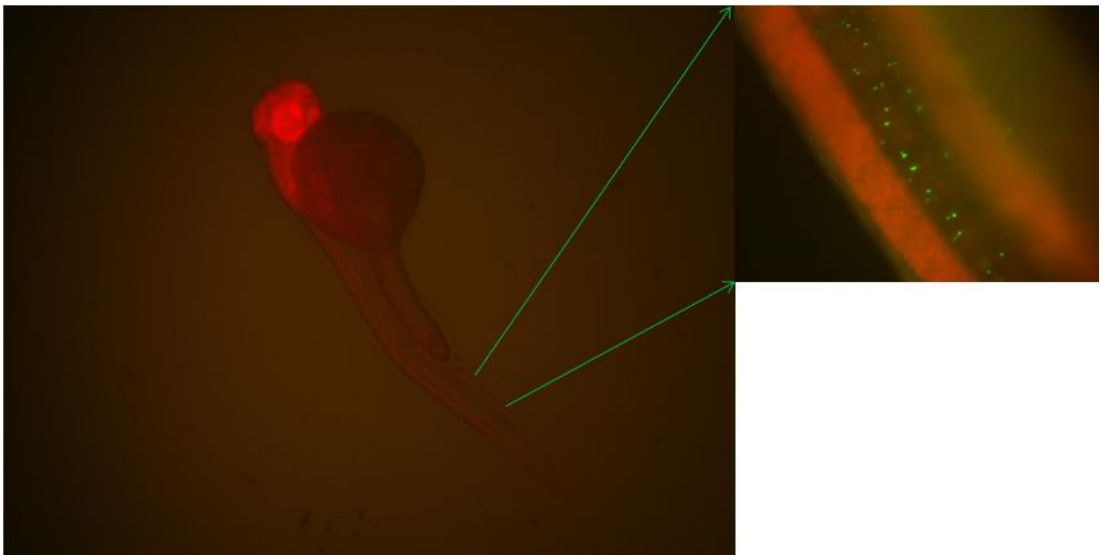

Figure 33. A twenty four hours post fertilization zebrafish embryo which was incubated with BrdU for 24 hours. BrdU label is in green and the nucleus is stained in red with 7-AAD. *Establishing the BrdU labelling method in our laboratory was important regarding our capability to employ this method in neuronal proliferation experiments.*

The cell culture system is an alternative method to devise a strategy for uncovering the function of *wdr81*. Primary neuron culture is an established method in the literature and neurons from zebrafish embryos might be cultivated[186]. Three experiment groups might be prepared as a primary neuron culture overexpressing *wdr81*, a primary neuron culture in which *wdr81* is knocked down and a wildtype culture. The migration capacity of these experiment groups might be compared so that the potential function of *wdr81* in neuronal migration would be possible to test.

References

1. Mitchell KJ. The genetics of neurodevelopmental disease. *Curr Opin Neurobiol*. 21(1):197-203. doi:10.1016/j.conb.2010.08.009.

2. Deutsch SI, Burket JA, Katz E. Does subtle disturbance of neuronal migration contribute to schizophrenia and other neurodevelopmental disorders ? Potential genetic mechanisms with possible treatment implications. *Eur Neuropsychopharmacol*.2010;20(5):281-287.

3. Hampson DR, Blatt GJ, Beversdorf DQ, Hampson DR. Autism spectrum disorders and neuropathology of the cerebellum. 2015;9(November):1-16. doi:10.3389/fnins.2015.00420.

4. Maurin T, Zongaro S, Bardoni B. Neuroscience and Biobehavioral Reviews Fragile X Syndrome : From molecular pathology to therapy. *Neurosci Biobehav Rev*. 2014;46:242-255. doi:10.1016/j.neubiorev.2014.01.006.

5. Banerjee A, Castro J, Sur M. Rett syndrome : genes , synapses , circuits , and therapeutics. 2012;3(May):1-13. doi:10.3389/fpsyt.2012.00034.

6. TAN U. a New Syndrome With Quadrupedal Gait, Primitive Speech, and Severe Mental Retardation As a Live Model for Human Evolution. *Int J Neurosci*. 2006;116(3):361-369. doi:10.1080/00207450500455330.

7. Türkmen S, Demirhan O, Hoffmann K, et al. Cerebellar hypoplasia and quadrupedal locomotion in humans as a recessive trait mapping to chromosome 17p. *J Med Genet*. 2006;43(October 2008):461-464. doi:10.1136/jmg.2005.040030.

8. Ozcelik T, Akarsu N, Uz E, et al. Mutations in the very low-density lipoprotein receptor VLDLR cause cerebellar hypoplasia and quadrupedal locomotion in humans. 2008.

9. Moheb LA, Tzschach A, Garshasbi M, et al. Identification of a nonsense mutation in the very low-density lipoprotein receptor gene (*VLDLR*) in an Iranian family with dysequilibrium syndrome. 2008:270-273.

10. Kolb LE, Arlier Z, Yalcinkaya C, Ozturk AK. Novel *VLDLR* microdeletion identified in two Turkish siblings with pachygyria and pontocerebellar atrophy. 2010:319-325. doi:10.1007/s10048-009-0232-y.

11. Türkmen S, Guo G, Garshasbi M, et al. CA8 mutations cause a novel syndrome characterized by ataxia and mild mental retardation with predisposition to quadrupedal gait. *PLoS Genet*. 2009;5(5):e1000487. doi:10.1371/journal.pgen.1000487.

12. Gulsuner S, Tekinay AB, Doerschner K, et al. Homozygosity mapping and targeted genomic sequencing reveal the gene responsible for cerebellar hypoplasia and quadrupedal locomotion in a consanguineous kindred. *Genome Res*. 2011;21(12):1995-2003. doi:10.1101/gr.126110.111.

13. Boycott KM, Flavelle S, Bureau A, et al. Homozygous Deletion of the Very Low Density Lipoprotein Receptor Gene Causes Autosomal Recessive Cerebellar Hypoplasia with Cerebral Gyral Simplification. 2005;164:477-483.

14. Emre Onat O, Gulsuner S, Bilguvar K, et al. Missense mutation in the ATPase, aminophospholipid transporter protein ATP8A2 is associated with cerebellar atrophy and quadrupedal locomotion. *Eur J Hum Genet*. 2012;21(3):281-285. doi:10.1038/ejhg.2012.170.

15. Tan U. Unertan Syndrome A New Theory on the Evolution of Human Mind. 2005;(4):250-255.

16. Uner P, Koroglu B. First Quadruped Man Was Found In Turkey A Hundred Years Ago First Quadruped Man Was Found In Turkey A Hundred Years Ago Abstract Case Report (s). 2010;1(10):1-6.

17. Boycott KM, Bonnemann C, Herz J, et al. Mutations in VLDLR as a cause for autosomal recessive cerebellar ataxia with mental retardation (dysequilibrium syndrome). *J Child Neurol*. 2009;24(10):1310-1315. doi:10.1177/0883073809332696.

18. Tan U. Evidence For " Unertan Syndrome " And The Evolution Of The Human Mind. 2006; (December 2005):763-774. doi:10.1080/00207450600588733.

19. Türkmen S, Hoffmann K, Demirhan O, Aruoba D, Humphrey N, Mundlos S. Cerebellar hypoplasia, with quadrupedal locomotion, caused by mutations in the very low-density lipoprotein receptor gene. *Eur J Hum Genet*. 2008;16(January):1070-1074. doi:10.1038/ejhg.2008.73.

20. Ali BR, Silhavy JL, Gleeson JG, Al-Gazali L. A missense founder mutation in VLDLR is associated with Dysequilibrium Syndrome without quadrupedal locomotion. *BMC Med Genet*. 2012;13(1):80. doi:10.1186/1471-2350-13-80.

21. Dixon-salazar TJ, Silhavy JL, Udpa N, et al. HHS Public Access. *Sci Transl Med*. 2012;4(138). doi:10.1126/scitranslmed.3003544.Exome.

22. Kaya N, Aldhalaan H, Al-Younes B, et al. Phenotypical spectrum of cerebellar ataxia associated with a novel mutation in the CA8 gene, encoding carbonic anhydrase (CA) VIII. *Am J Med Genet B Neuropsychiatr Genet*. 2011;156B(7):826-834. doi:10.1002/ajmg.b.31227.

23. Najmabadi H, Hu H, Garshasbi M, et al. Deep sequencing reveals 50 novel genes for recessive cognitive disorders. *Nature*. 2011;478(7367):57-63. doi:10.1038/nature10423.

24. Ensembl Genome Browser. http://www.ensembl.org/index.html. Accessed October 28, 2015.

25. VLDLR very low density lipoprotein receptor [Homo sapiens (human)] - Gene - NCBI. http://www.ncbi.nlm.nih.gov/gene/7436. Accessed January 18, 2016.

26. D'Arcangelo G, Miao GG, Chen SC, Soares HD, Morgan JI, Curran T. A protein related to extracellular matrix proteins deleted in the mouse mutant reeler. *Nature*. 1995;374(6524):719-723. doi:10.1038/374719a0.

27. D'Arcangelo G. Reelin in the Years: Controlling Neuronal Migration and Maturation in the Mammalian Brain. *Adv Neurosci*. 2014;2014:1-19.

28. Miyata T, Nakajima K, Mikoshiba K, Ogawa M. Regulation of Purkinje Cell Alignment by Reelin as Revealed with CR-50 Antibody. 1997;17(10):3599-3609.

29. Larouche M, Beffert U, Herz J, Hawkes R. The Reelin Receptors Apoer2 and Vldlr Coordinate the Patterning of Purkinje Cell Topography in the Developing Mouse Cerebellum. *PLoS One*. 2008;3(2):e1653. doi:10.1371/journal.pone.0001653.

30. Niu S, Renfro A, Quattrocchi CC, Sheldon M, D'Arcangelo G. Reelin Promotes Hippocampal Dendrite Development through the VLDLR/ApoER2-Dab1 Pathway. *Neuron*. 2004;41(1):71-84. doi:10.1016/S0896-6273(03)00819-5.

31. Niu S, Yabut O, D'Arcangelo G. The Reelin signaling pathway promotes dendritic spine development in hippocampal neurons. *J Neurosci*. 2008;28(41):10339-10348. doi:10.1523/JNEUROSCI.1917-08.2008.

32. DiBattista AM, Dumanis SB, Song JM, et al. Very low density lipoprotein receptor regulates dendritic spine formation in a RasGRF1/CaMKII dependent manner. *Biochim Biophys Acta*. 2015;1853(5):904-917. doi:10.1016/j.bbamcr.2015.01.015.

33. Tacken PJ, Teusink B, Jong MC, et al. LDL receptor deficiency unmasks altered VLDL triglyceride metabolism in VLDL receptor transgenic and knockout mice. *J Lipid Res*. 2000;41(12):2055-2062. http://www.ncbi.nlm.nih.gov/pubmed/11108739.

34. Tao H, Hajri T. Very low density lipoprotein receptor promotes adipocyte differentiation and mediates the proadipogenic effect of peroxisome proliferator-activated receptor gamma agonists. *Biochem Pharmacol*. 2011;82(12):1950-1962. doi:10.1016/j.bcp.2011.09.003.

35. Sarac O, Gulsuner S, Yildiz-Tasci Y, Ozcelik T, Kansu T. Neuro-ophthalmologic findings in humans with quadrupedal locomotion. *Ophthalmic Genet*. 2012;33(4):249-252. doi:10.3109/13816810.2012.689412.

36. Traka M, Millen KJ, Collins D, et al. WDR81 Is Necessary for Purkinje and Photoreceptor Cell Survival. *J Neurosci*. 2013;33(16):6834-6844. doi:10.1523/JNEUROSCI.2394-12.2013.

37. Donnard E, Asprino PF, Correa BR, et al. Mutational analysis of genes coding for cell surface proteins in colorectal cancer cell lines reveal novel altered pathways, druggable mutations and mutated epitopes for targeted therapy. *Oncotarget*. 2014;5(19):9199-9213.

38. Franceschini N, van Rooij FJA, Prins BP, et al. Discovery and fine mapping of serum protein loci through transethnic meta-analysis. *Am J Hum Genet*. 2012;91(4):744-753. doi:10.1016/j.ajhg.2012.08.021.

39. Goldwasser P, Feldman J. Association of serum albumin and mortality risk. *J Clin Epidemiol*. 1997;50(6):693-703. doi:S0895-4356(97)00015-2 [pii].

40. Nelson JJ, Liao D, Sharrett AR, et al. Serum albumin level as a predictor of incident coronary heart disease: the Atherosclerosis Risk in Communities (ARIC) study. *Am J Epidemiol*. 2000;151(5):468-477. http://www.ncbi.nlm.nih.gov/pubmed/10707915.

41. Cullinane AR, Schäffer A a., Huizing M. The BEACH Is Hot: A LYST of Emerging Roles for BEACH-Domain Containing Proteins in Human Disease. *Traffic*. 2013;14:749-766. doi:10.1111/tra.12069.

42. Xu C, Min J. Structure and function of WD40 domain proteins. *Protein {&} cell*. 2011;2(3):202-214. doi:10.1007/s13238-011-1018-1.

43. Pao SS, Paulsen IT, Saier MH. Major facilitator superfamily. *Microbiol Mol Biol Rev*. 1998;62(1):1-34.

44. Walczak-Sztulpa J, Eggenschwiler J, Osborn D, et al. Cranioectodermal Dysplasia, Sensenbrenner Syndrome, Is a Ciliopathy Caused by Mutations in the IFT122 Gene. *Am J Hum Genet*. 2010;86(6):949-956. doi:10.1016/j.ajhg.2010.04.012.

45. Kim HG, Ahn JW, Kurth I, et al. WDR11, a WD protein that interacts with transcription factor EMX1, is mutated in idiopathic hypogonadotropic hypogonadism and Kallmann syndrome. *Am J Hum Genet*. 2010;87(4):465-479. doi:10.1016/j.ajhg.2010.08.018.

46. Coussa RG, Otto EA, Gee HY, et al. WDR19: An ancient, retrograde, intraflagellar ciliary protein is mutated in autosomal recessive retinitis pigmentosa and in Senior-Loken syndrome. *Clin Genet*. 2013;84(2):150-159. doi:10.1111/cge.12196.

47. Halbritter J, Porath JD, Diaz KA, et al. Identification of 99 novel mutations in a worldwide cohort of 1,056 patients with a nephronophthisis-related ciliopathy. *Hum Genet*. 2013;132(8):865-884. doi:10.1007/s00439-013-1297-0.

48. Huber C, Wu S, Kim AS, et al. WDR34 mutations that cause short-rib polydactyly syndrome type 3/severe asphyxiating thoracic dysplasia reveal a role for the NF-kB pathway in cilia. *Am J Hum Genet*. 2013;93(5):926-931. doi:10.1016/j.ajhg.2013.10.007.

49. Schmidts M, Vodopiutz J, Christou-Savina S, et al. Mutations in the gene encoding IFT dynein complex component WDR34 cause jeune asphyxiating thoracic dystrophy. *Am J Hum Genet*. 2013;93(5):932-944. doi:10.1016/j.ajhg.2013.10.003.

50. Gilissen C, Arts HH, Hoischen A, et al. Exome sequencing identifies WDR35 variants involved in Sensenbrenner syndrome. *Am J Hum Genet*. 2010;87(3):418-423. doi:10.1016/j.ajhg.2010.08.004.

51. Mill P, Lockhart PJ, Fitzpatrick E, et al. Human and mouse mutations in WDR35 cause short-rib polydactyly syndromes due to abnormal ciliogenesis. *Am J Hum Genet*. 2011;88(4):508-515. doi:10.1016/j.ajhg.2011.03.015.

52. Pasutto F, Mardin CY, Michels-Rautenstrauss K, et al. Profiling of WDR36 missense variants in German patients with glaucoma. *Investig Ophthalmol Vis Sci*. 2008;49(1):270-274. doi:10.1167/iovs.07-0500.

53. Beales PL, Bland E, Tobin JL, et al. IFT80, which encodes a conserved intraflagellar transport protein, is mutated in Jeune asphyxiating thoracic dystrophy. *Nat Genet*. 2007;39(6):727-729. doi:10.1038/ng2038.

54. Cavalcanti DP, Huber C, Sang K-HLQ, et al. Mutation in IFT80 in a fetus with the phenotype of Verma-Naumoff provides molecular evidence for Jeune-Verma-Naumoff dysplasia spectrum. *J Med Genet*. 2011;48(2):88-92. doi:10.1136/jmg.2009.069468.

55. McInerney-Leo AM, Schmidts M, Cort??s CR, et al. Short-Rib polydactyly and jeune syndromes are caused by mutations in WDR60. *Am J Hum Genet*. 2013;93(3):515-523. doi:10.1016/j.ajhg.2013.06.022.

56. Bhat V, Girimaji S, Mohan G, et al. Mutations in WDR62, encoding a centrosomal and nuclear protein, in Indian primary microcephaly families with cortical malformations. *Clin Genet*. 2011;80(6):532-540. doi:10.1111/j.1399-0004.2011.01686.x.

57. Bilgüvar K, Oztürk AK, Louvi A, et al. Whole-exome sequencing identifies recessive WDR62 mutations in severe brain malformations. *Nature*. 2010;467(7312):207-210. doi:10.1038/nature09327.

58. Murdock DR, Clark GD, Bainbridge MN, et al. Whole-exome sequencing identifies compound heterozygous mutations in WDR62 in siblings with recurrent polymicrogyria. *Am J Med Genet A*. 2011;155A(9):2071-2077. doi:10.1002/ajmg.a.34165.

59. Yu TW, Mochida GH, Tischfield DJ, et al. Mutations in WDR62, encoding a centrosome-associated protein, cause microcephaly with simplified gyri and abnormal cortical architecture. *Nat Genet*. 2010;42(11):1015-1020. doi:10.1038/ng.683.

60. Nicholas AK, Khurshid M, Désir J, et al. WDR62 is associated with the spindle pole and is mutated in human microcephaly. *Nat Genet*. 2010;42(11):1010-1014. doi:10.1038/ng.682.

61. Hypogonadotropic hypogonadism 14 with or without anosmia in Human diseases.http://www.uniprot.org/diseases/?query=Hypogonadotropic+hypogonadism+14+with+or+without+anosmia&sort=score. Accessed May 2, 2016.

62. Di Sante G, Wang L, Wang C, et al. Sirt1-deficient mice have hypogonadotropic hypogonadism due to defective GnRH neuronal migration. *Mol Endocrinol*. 2015;29(2):200-212. doi:10.1210/me.2014-1228.

63. senior-loken syndrome 8 in Human diseases. http://www.uniprot.org/diseases/?query=senior-loken+syndrome+8&sort=score. Accessed May 2, 2016.

64. OMIM Entry - # 613091 - SHORT-RIB THORACIC DYSPLASIA 3 WITH OR WITHOUT POLYDACTYLY; SRTD3. http://www.omim.org/entry/613091. Accessed May 2, 2016.

65. Glaucoma 1, open angle, G in Human diseases. http://www.uniprot.org/diseases/?query=Glaucoma+1%2C+open+angle%2C+G+&sort=score. Accessed May 2, 2016.

66. Jiao Y. Carbonic Anhydrase-Related Protein VIII Deficiency Is Associated With a Distinctive Lifelong Gait Disorder in Waddles Mice. *Genetics*. 2005;171(3):1239-1246. doi:10.1534/genetics.105.044487.

67. CA8 carbonic anhydrase VIII [Homo sapiens (human)] - Gene - NCBI. http://www.ncbi.nlm.nih.gov/gene/767. Accessed January 19, 2016.

68. Hirota J, Ando H, Hamada K, Mikoshiba K. Carbonic anhydrase-related protein is a novel binding protein for inositol 1,4,5-trisphosphate receptor type 1. *Biochem J*. 2003;372:435-441. doi:10.1042/BJ20030110.

69. Taniuchi K, Nishimori I, Takeuchi T, Ohtsuki Y, Onishi S. cDNA cloning and developmental expression of murine carbonic anhydrase-related proteins VIII, X, and XI. *Mol Brain Res*. 2002;109(1-2):207-215. doi:10.1016/S0169-328X(02)00563-6.

70. Skaggs LA, Bergenhem NC, Venta PJ, Tashian RE. The deduced amino acid sequence of human carbonic anhydrase-related protein (CARP) is 98% identical to the mouse homologue. *Gene*. 1993;126(2):291-292. http://www.ncbi.nlm.nih.gov/pubmed/8482548. Accessed January 19, 2016.

71. Huang M-S, Wang T-K, Liu Y-W, et al. Roles of carbonic anhydrase 8 in neuronal cells and zebrafish. *Biochim Biophys Acta*. 2014;1840(9):2829-2842. doi:10.1016/j.bbagen.2014.04.017.

72. Aspatwar A, Tolvanen MEE, Jokitalo E, et al. Abnormal cerebellar development and ataxia in carp VIII morphant zebrafish. *Hum Mol Genet*. 2013;22(3):417-432. doi:10.1093/hmg/dds438.

73. Nishikata M, Nishimori I, Taniuchi K, et al. Carbonic anhydrase-related protein VIII promotes colon cancer cell growth. *Mol Carcinog*. 2007;46(3):208-214. doi:10.1002/mc.20264.

74. Ishihara T, Takeuchi T, Nishimori I, et al. Carbonic anhydrase-related protein VIII increases invasiveness of non-small cell lung adenocarcinoma. *Virchows Arch*. 2006;448(6):830-837. doi:10.1007/s00428-006-0199-0.

75. ATP8A2 ATPase, aminophospholipid transporter, class I, type 8A, member 2 [Homo sapiens (human)] - Gene - NCBI. http://www.ncbi.nlm.nih.gov/gene/51761. Accessed January 19, 2016.

76. Lopez-Marques RL, Theorin L, Palmgren MG, Pomorski TG. P4-ATPases: lipid flippases in cell membranes. *Pflügers Arch - Eur J Physiol*. 2014;466(7):1227-1240. doi:10.1007/s00424-013-1363-4.

77. Cacciagli P, Haddad M-R, Mignon-Ravix C, et al. Disruption of the ATP8A2 gene in a patient with a t(10;13) de novo balanced translocation and a severe neurological phenotype. *Eur J Hum Genet*. 2010;18(June):1360-1363. doi:10.1038/ejhg.2010.126.

78. Coleman J a., Kwok MCM, Molday RS. Localization, purification, and functional reconstitution of the P4-ATPase Atp8a2, a phosphatidylserine Flippase in photoreceptor disc membranes. *J Biol Chem*. 2009;284(47):32670-32679. doi:10.1074/jbc.M109.047415.

79. Zhu X, Libby RT, de Vries WN, et al. Mutations in a P-Type ATPase Gene Cause Axonal Degeneration. *PLoS Genet*. 2012;8(8):e1002853. doi:10.1371/journal.pgen.1002853.

80. Xu Q, Yang GY, Liu N, et al. P 4-ATPase ATP8A2 acts in synergy with CDC50A to enhance neurite outgrowth. *FEBS Lett*. 2012;586(13):1803-1812. doi:10.1016/j.febslet.2012.05.018.

81. Streisinger G, Walker C, Dower N, Knauber D, Singer F. Production of clones of homozygous diploid zebra fish (Brachydanio rerio). *Nature*. 1981;291(5813):293-296. doi:10.1038/291293a0.

82. Friedrich RW, Jacobson G a., Zhu P. Circuit Neuroscience in Zebrafish. *Curr Biol*. 2010;20(8):R371-R381. doi:10.1016/j.cub.2010.02.039.

83. Howe K, Clark MD, Torroja CF, et al. The zebrafish reference genome sequence and its relationship to the human genome. *Nature*. 2013;496(7446):498-503. doi:10.1038/nature12111.

84. Kabashi E, Brustein E, Champagne N, Drapeau P. Zebrafish models for the functional genomics of neurogenetic disorders. *Biochim Biophys Acta - Mol Basis Dis*. 2011;1812(3):335-345. doi:10.1016/j.bbadis.2010.09.011.

85. Nüsslein-Volhard C, Dahm R. *Zebrafish: A Practical Approach, Issue 975*. Oxford University Press; 2002. https://books.google.com/books?id=jfm0QgAACAAJ&pgis=1. Accessed October 28, 2015.

86. Schonthaler HB, Franz-Odendaal TA, Hodel C, et al. The zebrafish mutant bumper shows a hyperproliferation of lens epithelial cells and fibre cell degeneration leading to functional blindness. *Mech Dev*. 2010;127(3-4):203-219. doi:10.1016/j.mod.2010.01.005.

87. Higashijima S. Transgenic zebrafish expressing fluorescent proteins in central nervous system neurons. *Dev Growth Differ*. 2008;50(6):407-413. doi:10.1111/j.1440-169X.2008.01023.x.

88. Kimura Y. alx, a Zebrafish Homolog of Chx10, Marks Ipsilateral Descending Excitatory Interneurons That Participate in the Regulation of Spinal Locomotor Circuits. *J Neurosci*. 2006;26(21):5684-5697. doi:10.1523/JNEUROSCI.4993-05.2006.

89. *Patterning and Cell Type Specification in the Developing CNS and PNS: Comprehensive Developmental Neuroscience, Volume 1*. Academic Press; 2013. https://books.google.com/books?id=QvjurYuh-jMC&pgis=1. Accessed January 12, 2016.

90. Ivics Z, Hackett PB, Plasterk RH, Izsvák Z. Molecular Reconstruction of Sleeping Beauty, a Tc1-like Transposon from Fish, and Its Transposition in Human Cells. *Cell*. 1997;91(4):501-510. doi:10.1016/S0092-8674(00)80436-5.

91. Kawakami K, Shima A, Kawakami N. Identification of a functional transposase of the Tol2 element, an Ac-like element from the Japanese medaka fish, and its transposition in the zebrafish germ lineage. *Proc Natl Acad Sci U S A*. 2000;97(21):11403-11408. doi:10.1073/pnas.97.21.11403.

92. Shoji W, Yee CS, Kuwada JY. Zebrafish semaphorin Z1a collapses specific growth cones and alters their pathway in vivo. *Development*. 1998;125(7):1275-1283. http://www.ncbi.nlm.nih.gov/pubmed/9477326.

93. Placinta M, Shen M-C, Achermann M, Karlstrom RO. A laser pointer driven microheater for precise local heating and conditional gene regulation in vivo. Microheater driven gene regulation in zebrafish. *BMC Dev Biol*. 2009;9:73. doi:10.1186/1471-213X-9-73.

94. Asakawa K, Kawakami K. Targeted gene expression by the Gal4-UAS system in zebrafish. *Dev Growth Differ*. 2008;50(6):391-399. doi:10.1111/j.1440-169X.2008.01044.x.

95. Rodrigues FSLM, Doughton G, Yang B, Kelsh RN. A novel transgenic line using the Cre-lox system to allow permanent lineage-labeling of the zebrafish neural crest. *Genesis*. 2012;50(10):750-757. doi:10.1002/dvg.22033.

96. Doyon Y, McCammon JM, Miller JC, et al. Heritable targeted gene disruption in zebrafish using designed zinc-finger nucleases. *Nat Biotechnol*. 2008;26(6):702-708. doi:10.1038/nbt1409.

97. Huang P, Xiao A, Zhou M, Zhu Z, Lin S, Zhang B. Heritable gene targeting in zebrafish using customized TALENs. *Nat Biotechnol*. 2011;29(8):699-700.

98. Sander JD, Cade L, Khayter C, et al. Targeted gene disruption in somatic zebrafish cells using engineered TALENs. *Nat Biotechnol*. 2011;29(8):697-698. doi:10.1038/nbt.1934.

99. Varshney GK, Pei W, Lafave MC, et al. High-throughput gene targeting and phenotyping in zebrafish using CRISPR / Cas9. 2015:1030-1042. doi:10.1101/gr.186379.114.Freely.

100. Bill BR, Petzold AM, Clark KJ, Schimmenti LA, Ekker SC. A primer for morpholino use in zebrafish. *Zebrafish*. 2009;6(1):69-77. doi:10.1089/zeb.2008.0555.

101. de Bruijn E, Cuppen E, Feitsma H. Highly Efficient ENU Mutagenesis in Zebrafish. *Methods Mol Biol*. 2009;546:3-12. doi:10.1007/978-1-60327-977-2_1.

102. Moens CB, Donn TM, Wolf-Saxon ER, Ma TP. Reverse genetics in zebrafish by TILLING. *Briefings Funct Genomics Proteomics*. 2008;7(6):454-459. doi:10.1093/bfgp/eln046.

103. Yanicostas C, Barbieri E, Hibi M, Brice A, Stevanin G, Soussi-Yanicostas N. Requirement for Zebrafish Ataxin-7 in Differentiation of Photoreceptors and Cerebellar Neurons. *PLoS One*. 2012;7(11):1-13. doi:10.1371/journal.pone.0050705.

104. Wortmann SB, Ziętkiewicz S, Kousi M, et al. CLPB mutations cause 3-methylglutaconic aciduria, progressive brain atrophy, intellectual disability, congenital neutropenia, cataracts, movement disorder. *Am J Hum Genet*. 2015;96(2):245-257. doi:10.1016/j.ajhg.2014.12.013.

105. Akizu N, Cantagrel V, Zaki MS, et al. Biallelic mutations in SNX14 cause a syndromic form of cerebellar atrophy and lysosome-autophagosome dysfunction. *Nat Genet*. 2015;47(5):528-534. doi:10.1038/ng.3256.

106. Margolin DH, Kousi M, Chan Y-M, et al. Ataxia, dementia, and hypogonadotropism caused by disordered ubiquitination. *N Engl J Med*. 2013;368(21):1992-2003. doi:10.1056/NEJMoa1215993.

107. Zhang X, Ling J, Barcia G, et al. Mutations in QARS, encoding glutaminyl-trna synthetase, cause progressive microcephaly, cerebral-cerebellar atrophy, and intractable seizures. *Am J Hum Genet*. 2014;94(4):547-558. doi:10.1016/j.ajhg.2014.03.003.

108. Issa FA, Mazzochi C, Mock AF, Papazian DM. Spinocerebellar Ataxia Type 13 Mutant Potassium Channel Alters Neuronal Excitability and Causes Locomotor Deficits in Zebrafish. *J Neurosci*. 2011;31(18):6831-6841. doi:10.1523/JNEUROSCI.6572-10.2011.

109. Bae YK, Kani S, Shimizu T, et al. Anatomy of zebrafish cerebellum and screen for mutations affecting its development. *Dev Biol*. 2009;330(2):406-426. doi:10.1016/j.ydbio.2009.04.013.

110. Lewis KE, Eisen JS. From cells to circuits: development of the zebrafish spinal cord. *Prog Neurobiol*. 2003;69(6):419-449. doi:10.1016/S0301-0082(03)00052-2.

111. Schmidt R, Strähle U, Scholpp S. Neurogenesis in zebrafish - from embryo to adult. *Neural Dev*. 2013;8:3. doi:10.1186/1749-8104-8-3.

112. ZFIN: The Zebrafish Model Organism Database. http://zfin.org/. Accessed October 28, 2015.

113. Kimmel CB, Ballard WW, Kimmel SR, Ullmann B, Schilling TF. Stages of embryonic development of the zebrafish. *Dev Dyn*. 1995;203(3):253-310. doi:10.1002/aja.1002030302.

114. Neuroanatomy of the Zebrafish Brain - A Topological Atlas | Mario F. Wulliman | Springer. http://www.springer.com/us/book/9783034889797. Accessed December 31, 2015.

115. Lee JC, Mayer-Proschel M, Rao MS. Gliogenesis in the central nervous system. *Glia*. 2000;30(2):105-121. doi:10.1002/(SICI)1098-1136(200004)30:2<105::AID-GLIA1>3.0.CO;2-H.

116. Leung LC, Wang GX, Mourrain P. Imaging zebrafish neural circuitry from whole brain to synapse. *Front Neural Circuits*. 2013;7(April):1-8. doi:10.3389/fncir.2013.00076.

117. Appel B, Chitnis A. Neurogenesis and specification of neuronal identity. *Results Probl Cell Differ*. 2002;40:237-251.

118. Blader P, Strähle U. Zebrafish developmental genetics and central nervous system development. *Hum Mol Genet*. 2000;9(6):945-951. doi:10.1093/hmg/9.6.945.

119. *The Zebrafish: Cellular and Developmental Biology, Part 1*. Academic Press; 2010. https://books.google.com/books?id=rgD7ABqAt2MC&pgis=1. Accessed January 4, 2016.

120. Mueller T, Wullimann MF. Anatomy of neurogenesis in the early zebrafish brain. *Dev Brain Res*. 2003;140(1):137-155. doi:10.1016/S0165-3806(02)00583-7.

121. Cosacak MI, Papadimitriou C, Kizil C. Regeneration , Plasticity , and Induced Molecular Programs in Adult Zebrafish Brain. 2014;2015.

122. Kriegstein A, Alvarez-buylla A. The Glial Nature of Embryonic and Adult Neural Stem Cells. *Annu Rev Neurosci*. 2011:149-184. doi:10.1146/annurev.neuro.051508.135600.The.

123. Kelsh RN, Dutton K, Medlin J, Eisen JS. Expression of zebrafish fkd6 in neural crest-derived glia. *Mech Dev*. 2000;93(1-2):161-164. doi:S0925477300002501 [pii].

124. Hagström C, Olsson C. Glial cells revealed by GFAP immunoreactivity in fish gut. *Cell Tissue Res*. 2010;341(1):73-81. doi:10.1007/s00441-010-0979-3.

125. Wiley: Glial Physiology and Pathophysiology - Alexei Verkhratsky, Arthur Morgan Butt. http://eu.wiley.com/WileyCDA/WileyTitle/productCd-0470978538.html. Accessed January 13, 2016.

126. Lyons DA, Talbot WS. Glial cell development and function in zebrafish. *Cold Spring Harb Perspect Biol*. 2015;7(2):a020586. doi:10.1101/cshperspect.a020586.

127. Ransohoff RM, Cardona AE. The myeloid cells of the central nervous system parenchyma. *Nature*. 2010;468(7321):253-262. doi:10.1038/nature09615.

128. Kettenmann H, Verkhratsky A. Neuroglia: the 150 years after. *Trends Neurosci*. 2008;31(12):653-659. doi:10.1016/j.tins.2008.09.003.

129. Garner CC, Zhai RG, Gundelfinger ED, Ziv NE. Molecular mechanisms of CNS synaptogenesis. *Trends Neurosci*. 2002;25(5):243-250. doi:10.1016/S0166-2236(02)02152-5.

130. Waites CL, Craig AM, Garner CC. Mechanisms of Vertebrate Synaptogenesis. *Annu Rev Neurosci*. 2005;28(1):251-274. doi:10.1146/annurev.neuro.27.070203.144336.

131. Jontes JD, Emond MR. In Vivo Imaging of Synaptogenesis in Zebrafish. *Cold Spring Harb Protoc*. 2012;2012(5):pdb.top069237 - pdb.top069237. doi:10.1101/pdb.top069237.

132. Ono F, Higashijima S, Shcherbatko A, Fetcho JR, Brehm P. Paralytic zebrafish lacking acetylcholine receptors fail to localize rapsyn clusters to the synapse. *J Neurosci*. 2001;21(15):5439-5448. doi:21/15/5439 [pii].

133. Duval MG, Gilbert MJH, Watson DE, Zerulla TC, Tierney KB, Allison WT. Growth differentiation factor 6 as a putative risk factor in neuromuscular degeneration. *PLoS One*. 2014;9(2):e89183. doi:10.1371/journal.pone.0089183.

134. Sievers F, Wilm A, Dineen D, et al. Fast, scalable generation of high-quality protein multiple sequence alignments using Clustal Omega. *Mol Syst Biol*. 2014;7(1):539-539. doi:10.1038/msb.2011.75.

135. Robert X, Gouet P. Deciphering key features in protein structures with the new ENDscript server. *Nucleic Acids Res*. 2014;42(W1):W320-W324. doi:10.1093/nar/gku316.

136. SMART: Main page. http://smart.embl-heidelberg.de/. Accessed October 28, 2015.

137. TMpred Server. http://www.ch.embnet.org/software/TMPRED_form.html. Accessed October 28, 2015.

138. tblastn: search translated nucleotide databases using a protein query. http://blast.ncbi.nlm.nih.gov/Blast.cgi?PROGRAM=tblastn&PAGE_TYPE=BlastSearch&BLAST_SPEC=OGP__7955__9557&LINK_LOC=blasttab&LAST_PAGE=tblastn. Accessed May 1, 2016.

139. Doldur-Balli F, Ozel MN, Gulsuner S, et al. Characterization of a novel zebrafish (Danio rerio) gene, wdr81, associated with cerebellar ataxia, mental retardation and dysequilibrium syndrome (CAMRQ). *BMC Neurosci*. 2015;16(1):96. doi:10.1186/s12868-015-0229-4.

140. Yan J-J, Chou M-Y, Kaneko T, Hwang P-P. Gene expression of Na+/H+ exchanger in zebrafish H+ -ATPase-rich cells during acclimation to low-Na+ and acidic environments. *Am J Physiol Cell Physiol*. 2007;293(6):C1814-C1823. doi:10.1152/ajpcell.00358.2007.

141. ImageJ. http://imagej.nih.gov/ij/index.html. Accessed October 28, 2015.

142. Home - graphpad.com. http://graphpad.com/. Accessed October 28, 2015.

143. Thisse C, Thisse B. High-resolution in situ hybridization to whole-mount zebrafish embryos. *Nat Protoc*. 2008;3(1):59-69. doi:10.1038/nprot.2007.514.

144. Home | Gene Tools, LLC. http://www.gene-tools.com/. Accessed February 1, 2016.

145. Golzio C, Willer J, Talkowski ME, et al. KCTD13 is a major driver of mirrored neuroanatomical phenotypes of the 16p11.2 copy number variant. *Nature*. 2012;485(7398):363-367. doi:10.1038/nature11091.

146. Su Y, Meng A. The expression of gbx-2 during zebrafish embryogenesis. *Mech Dev*. 2002;113(1):107-110. doi:10.1016/S0925-4773(02)00011-4.

147. Kane DA, Kimmel CB. The zebrafish midblastula transition. *Development*. 1993;119(2):447-456. http://www.ncbi.nlm.nih.gov/pubmed/8287796.

148. Harvey S a, Sealy I, Kettleborough R, et al. Identification of the zebrafish maternal and paternal transcriptomes. *Development*. 2013;140(13):2703-2710. doi:10.1242/dev.095091.

149. Yao J, Zhou J, Liu Q, et al. Atoh8, a bHLH transcription factor, is required for the development of retina and skeletal muscle in zebrafish. *PLoS One*. 2010;5(6):1-13. doi:10.1371/journal.pone.0010945.

150. Nucleotide BLAST: Search nucleotide databases using a nucleotide query. http://blast.ncbi.nlm.nih.gov/Blast.cgi?PAGE_TYPE=BlastSearch&BLAST_SPEC=OGP__7955__9557. Accessed April 30, 2016.

151. Rossi CC, Kaji T, Artinger KB. Transcriptional control of Rohon-Beard sensory neuron development at the neural plate border. *Dev Dyn*. 2009;238(4):931-943. doi:10.1002/dvdy.21915.

152. Tuttle AM, Hoffman TL, Schilling TF. Rabconnectin-3a Regulates Vesicle Endocytosis and Canonical Wnt Signaling in Zebrafish Neural Crest Migration. *PLoS Biol*. 2014;12(5). doi:10.1371/journal.pbio.1001852.

153. Abbas L, Whitfield TT. Nkcc1 (Slc12a2) is required for the regulation of endolymph volume in the otic vesicle and swim bladder volume in the zebrafish larva. *Development*. 2009;136(16):2837-2848. doi:10.1242/dev.034215.

154. Mignone F, Gissi C, Liuni S, Pesole G. Untranslated regions of mRNAs. *Genome Biol*. 2002;3(3):REVIEWS0004. doi:10.1186/gb-2002-3-3-reviews0004.

155. White NL, Higgins CF, Trezise a E. Tissue-specific in vivo transcription start sites of the human and murine cystic fibrosis genes. *Hum Mol Genet*. 1998;7(3):363-369. http://www.ncbi.nlm.nih.gov/pubmed/9466991.

156. Liu RZ, Denovan-Wright EM, Wright JM. Structure, linkage mapping and expression of the heart-type fatty acid-binding protein gene (fabp3) from zebrafish (Danio rerio). *Eur J Biochem*. 2003;270(15):3223-3234. doi:10.1046/j.1432-1033.2003.03705.x.

157. Lianoglou S, Garg V, Yang JL, Leslie CS, Mayr C. Ubiquitously transcribed genes use alternative polyadenylation to achieve tissue-specific expression. *Genes Dev*. 2013;27(21):2380-2396. doi:10.1101/gad.229328.113.

158. Guo JH, Huang Q, Studholme DJ, Wu CQ, Zhao Z. Transcriptomic analyses support the similarity of gene expression between brain and testis in human as well as mouse. *Cytogenet Genome Res*. 2005;111(2):107-109. doi:10.1159/000086378.

159. Purves D. *Neuroscience Third Edition*. Vol 3.; 2004. doi:978-0878937257.

160. Leung YF, Ma P, Dowling JE. Gene expression profiling of zebrafish embryonic retinal pigment epithelium in vivo. *Invest Ophthalmol Vis Sci*. 2007;48(2):881-890. doi:10.1167/iovs.06-0723.

161. Arslan-Ergul A, Adams MM. Gene expression changes in aging zebrafish (Danio rerio) brains are sexually dimorphic. *BMC Neurosci*. 2014;15:29. doi:10.1186/1471-2202-15-29.

162. Purves D, Augustine GJ, Fitzpatrick D, et al. Neuroscience. 2001. http://www.ncbi.nlm.nih.gov/books/NBK10799/. Accessed February 17, 2016.

163. Nieuwenhuys R, Donkelaar HJ ten, Nicholson C. *The Central Nervous System of Vertebrates*. Vol 14. Springer; 2014. https://books.google.com/books?id=gsDqCAAAQBAJ&pgis=1. Accessed February 17, 2016.

164. Martin SC, Heinrich G, Sandell JH. Sequence and expression of glutamic acid decarboxylase isoforms in the developing zebrafish. *J Comp Neurol*. 1998;396(2):253-266.

165. Yazulla S, Studholme KM. Neurochemical anatomy of the zebrafish retina as determined by immunocytochemistry. *J Neurocytol*. 2001;30(7):551-592. doi:10.1023/A:1016512617484.

166. Jászai J, Reifers F, Picker A, Langenberg T, Brand M. Isthmus-to-midbrain transformation in the absence of midbrain-hindbrain organizer activity. *Development*. 2003;130(26):6611-6623. doi:10.1242/dev.00899.

167. Miyamura Y, Nakayasu H. Zonal distribution of Purkinje cells in the zebrafish cerebellum: Analysis by means of a specific monoclonal antibody. *Cell Tissue Res*. 2001;305(3):299-305. doi:10.1007/s004410100421.

168. Zhang L, Kendrick C, Jülich D, Holley SA. Cell cycle progression is required for zebrafish somite morphogenesis but not segmentation clock function. *Development*. 2008;135(12):2065-2070. doi:10.1242/dev.022673.

169. Wullimann MF, Knipp S. Proliferation pattern changes in the zebrafish brain from embryonic through early postembryonic stages. *Anat Embryol (Berl)*. 2000;202(5):385-400. doi:10.1007/s004290000115.

170. Huang S, Sato S. Progenitor cells in the adult zebrafish nervous system express a Brn-1-related POU gene, tai-ji. *Mech Dev*. 1998;71(1-2):23-35. doi:10.1016/S0925-4773(97)00199-8.

171. Mueller T, Wullimann MF. BrdU-, neuroD (nrd)- and Hu-studies reveal unusual non-ventricular neurogenesis in the postembryonic zebrafish forebrain. *Mech Dev*. 2002;117(1-2):123-135. doi:10.1016/S0925-4773(02)00194-6.

172. Kim CH, Ueshima E, Muraoka O, et al. Zebrafish elav/HuC homologue as a very early neuronal marker. *Neurosci Lett*. 1996;216(2):109-112. doi:10.1016/S0304-3940(96)13021-4.

173. Kyritsis N, Kizil C, Zocher S, et al. Acute inflammation initiates the regenerative response in the adult zebrafish brain. *Science*. 2012;338(6112):1353-1356. doi:10.1126/science.1228773.

174. Foudah D, Monfrini M, Donzelli E, et al. Expression of neural markers by undifferentiated mesenchymal-like stem cells from different sources. *J Immunol Res*. 2014;2014. doi:10.1155/2014/987678.

175. Goldshmit Y, Sztal TE, Jusuf PR, Hall TE, Nguyen-Chi M, Currie PD. Fgf-Dependent Glial Cell Bridges Facilitate Spinal Cord Regeneration in Zebrafish. *J Neurosci*. 2012;32(22):7477-7492. doi:10.1523/JNeurosci.0758-12.2012.

176. Zupanc GK, Hinsch K, Gage FH. Proliferation, migration, neuronal differentiation, and long-term survival of new cells in the adult zebrafish brain. *J Comp Neurol*. 2005;488(3):290-319. doi:10.1002/cne.20571.

177. Stenkamp DL. NIH Public Access. *Int Rev Cytol*. 2010;7696(06):1-42. doi:10.1016/S0074-7696(06)59005-9.Neurogenesis.

178. Cameron DA, Gentile KL, Middleton FA, Yurco P. Gene expression profiles of intact and regenerating zebrafish retina. *Mol Vis*. 2005;11(September):775-791. doi:v11/a93 [pii].

179. Gaudet P, Livstone MS, Lewis SE, Thomas PD. Phylogenetic-based propagation of functional annotations within the Gene Ontology consortium. *Brief Bioinform*. 2011;12(5):449-462. doi:10.1093/bib/bbr042.

180. Trede NS, Medenbach J, Damianov A, et al. Network of coregulated spliceosome components revealed by zebrafish mutant in recycling factor p110. *Proc Natl Acad Sci U S A*. 2007;104(16):6608-6613. doi:10.1073/pnas.0701919104.

181. Brown KE, Keller PJ, Ramialison M, et al. Nlcam modulates midline convergence during anterior neural plate morphogenesis. *Dev Biol*. 2010;339(1):14-25. doi:10.1016/j.ydbio.2009.12.003.

182. Prince VE, Moens CB, Kimmel CB, Ho RK. Zebrafish hox genes: expression in the hindbrain region of wild-type and mutants of the segmentation gene, valentino. *Development*. 1998;125(3):393-406.

183. Tian E, Kimura C, Takeda N, Aizawa S, Matsuo I. Otx2 is required to respond to signals from anterior neural ridge for forebrain specification. *Dev Biol*. 2002;242(2):204-223. doi:10.1006/dbio.2001.0531.

184. Chassaing N, Sorrentino S, Davis EE, et al. OTX2 mutations contribute to the otocephaly-dysgnathia complex. *J Med Genet*. 2012;49(6):373-379. doi:10.1136/jmedgenet-2012-100892.

185. Vernay B. Otx2 Regulates Subtype Specification and Neurogenesis in the Midbrain. *J Neurosci*. 2005;25(19):4856-4867. doi:10.1523/JNEUROSCI.5158-04.2005.

186. Ghosh C, Liu Y, Ma C, Collodi P. Cell cultures derived from early zebrafish embryos differentiate in vitro into neurons and astrocytes. *Cytotechnology*. 1997;23(1-3):221-230. doi:10.1023/A:1007915618413.

Appendix A

Buffer And Solutions

Boehringer Blocking Solution (50 ml)

- Blocking reagent……...……..0.5 g
- FBS…….....……2.5 ml
- TNT buffer is added to reach the final volume, the solution is heated at 60 °C, aliquoted after cooling and the aliquotes are stored at -20 °C.

Buffer B2 for ISH (1 liter)

- 1 M Tris pH:7.5……..100 ml
- 5 M NaCl……..…….30 ml
- 10% Tween 20……..……10 ml

Buffer B3 for ISH (1 liter)

- 1 M Tris pH:9.5…….…..100 ml
- 5 M NaCl…….……..20 ml
- 1 M $MgCl_2$.....50 ml

Buffer B4 for ISH (10 ml)

- BCIP (50 mg/ml)…….……37.5 µl
- NBT (100 mg/ml)……...…….37.5 µl
- Levamisole (24 mg/ml)……..…….2 drops
- Buffer B3……..……9.825 ml

Danieu's Solution (100 ml)

- 2 M NaCl…….….2.9 ml
- 3 M KCl……..….23.3 µl
- 100 mM $MgSO_4.7H_2O$…….....400 µl
- 100 mM $Ca(NO_3)_2.4H_2O$……...…...600 µl
- 1 M Hepes pH: 7.5……...…….500 µl
- pH should be between 7.1-7.3, the solution is filter sterilized and stored at 4 °C.

Denhardt's Solution (50x, 100 ml)

- Ficoll type 400……...……1 g
- Polyvinylpyrrolidone (PVP)……..1 g
- Bovine serum albumin (BSA) fraction V……...……1g
- The solution is mixed overnight at 4 °C, filter sterilized and aliquoted, the aliquotes are stored at -20 °C.

Ethidium Bromide Solution

- Stock solution: 10 mg/ml in water
- Working solution: 30 ng/ml

E3 Medium, Stock Solution (60x, 1 liter)

- NaCl……..17.2 g
- KCl……..……..0.76 g
- $CaCl_2.2H_20$…….…… 2.9 g
- $MgSO_4.7H_20$……..……..4.9 g
- The medium is autoclaved and the stock is stored in fridge.

E3 Medium, Working Solution (1x, 1 liter)

- 60x E3 medium……..…….16 ml
- 0.01% Methylene blue……..……3ml

Hybridization Buffer for ISH (50 ml)

- Formamide……...……..25 ml
- 20xSSC…….……..12.5 ml
- 50xDenhardt's solution……..……..……5 ml
- Yeast RNA (20 mg/ml)……625 µl
- Salmon sperm DNA (10 mg/ml)…….……..2.5 ml
- Heparin (5 mg/ml)……500 µl
- 0.5 M EDTA…….250 µl
- 10% Tween-20……..500 µl
- Chaps (1 mg/ml)……...……125 µl

Hybridization Buffer for WMISH (50 ml)

- Formamide…….25 ml
- 20xSSC……..…….12.5 ml
- Heparin (5 mg/ml)……..……..500 ul
- TorulaRNA……...……..…..25 mg
- 10% Tween 20…….……0.5 ml
- 1 M citric acid…….……0.46 ml
- Buffer is stored at -20 °C.

Luria Bertani (LB) Agar (500 ml)

- Tryptone…….5 g
- NaCl……5g
- Yeast Extract ……..……2.5 g
- Agar…….7.5 g
- The solution is autoclaved.

Luria Bertani (LB) Broth (500 ml)

- Tryptone…….5 g
- NaCl……5g
- Yeast Extract ……..……2.5 g
- The solution is autoclaved.

NTMT buffer (60 ml, needs to be prepared freshly)

- 5 M NaCl……...……...1.2 ml
- 1 M $MgCl_2$……..…….3 ml
- 1M Tris pH 9.5……....6 ml
- 10% Tween 20.....600 ul

PBS (10x, 1 liter)

- NaCl…….……80 g
- KCl…….……2 g
- $Na_2HPO_4.2H_2O$……...……..15.2 g
- KH_2PO_4…….……...…..2 g
- The stock solution is autoclaved, pH of 1xPBS solution should be between 7.2 and 7.4.

SOB Medium (250 ml)

- Tryptone……...……..5 g
- Yeast Extract……...……..1.25 g
- NaCl……0.146 g
- KCl……..0.047 g
- $MgCl_2.6H_2O$……...…….0.508 g
- $MgSO_4.7H_20$…….……..0.616 g

SSC Buffer (20x, 500 ml)

- NaCl…….…….87.7 g
- NaCitrate 5 ½ H_20……...……..63.5 g
- pH is adjusted to 7.0 and the buffer is filter sterilized.

TAE Buffer (50x, 500 ml)

- Trisma Base …….….121 g
- Acetic acid……...….28.55 ml
- EDTA……18.6 g

TNT buffer (500 ml)

- 1 M Tris-HCl pH: 8.0……...…..50 ml
- 5 M NaCl……...……15 ml
- 10% Tween 20……..……..……25ml

Transformation Buffer (400 ml)

- Pipes……..1.2096 g
- $CaCl_2.2H_20$……..0.882 g
- KCl……..……..7.4554 g
- All components except $MnCl_2.2H_20$ are added and the pH is adjusted to 6.7 with KOH.
- $MnCl_2.2H_20$……..….3.5612 g
- After adding $MnCl_2.2H_20$ to the buffer, it is filter sterilized and stored at 4 °C.

Appendix B

Molecular Size Markers

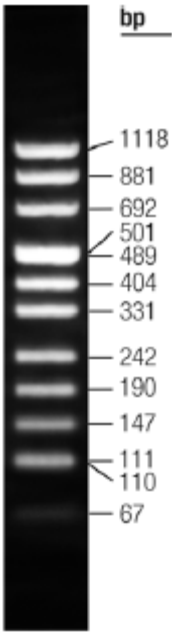

Figure B.1: pUC mix marker, 8, seperated on a 1.7% agarose gel (SM0303, Fermentas).

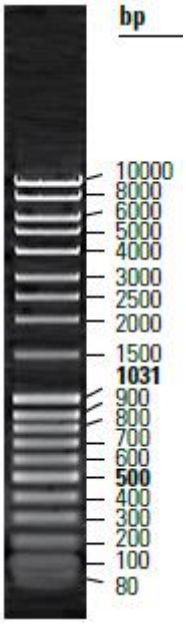

Figure B.2: MassRuler DNA ladder, seperated on a 1% agarose gel (SM0403, Thermo Scientific).

Appendix C

Cloning Vectors

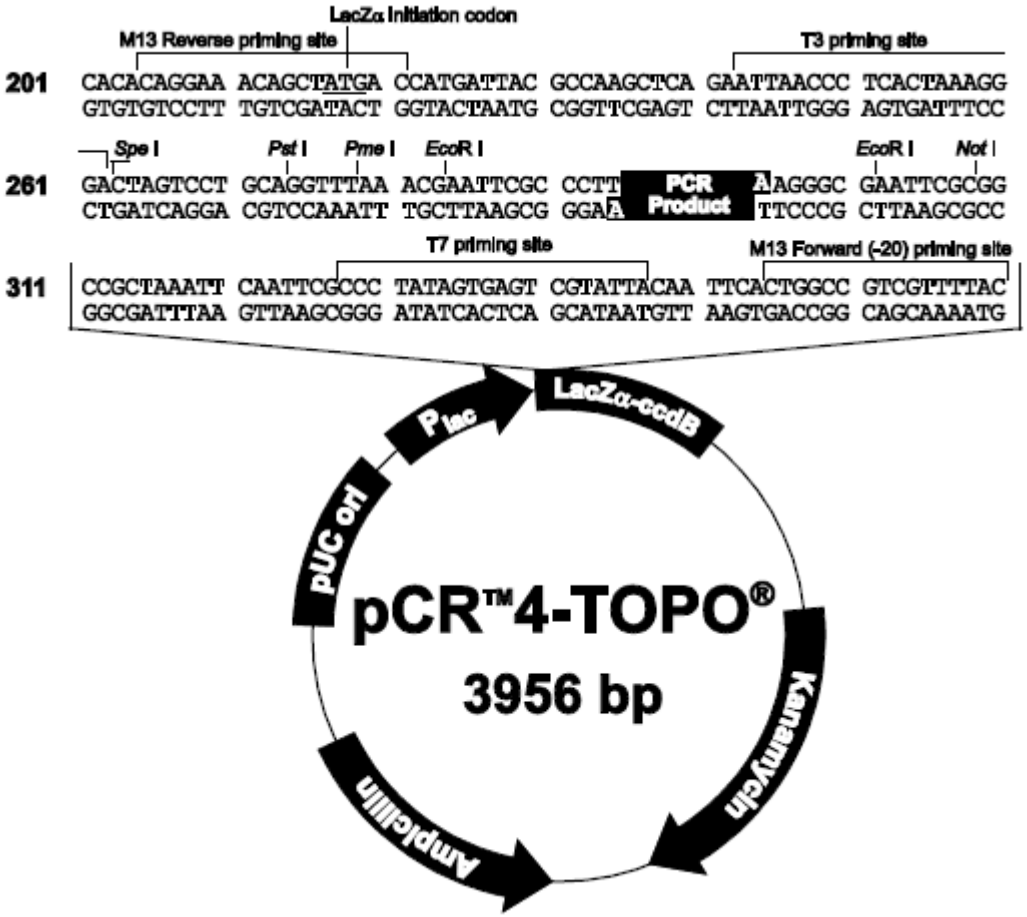

Figure C.1: pCR4-TOPO cloning vector (Invitrogen).

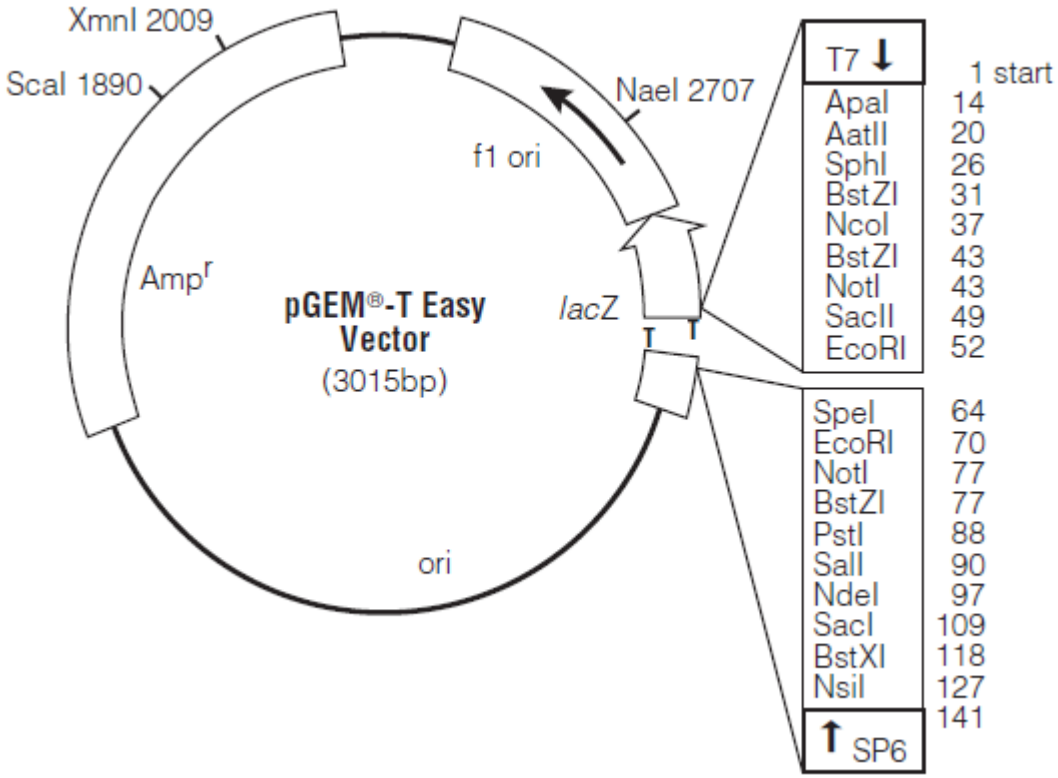

Figure C.2: pGEM-T Easy cloning vector (Promega).

Appendix D

```
gi_Danio            ---------------------------mewlapalerdlgidqrqtahsqrpnelvvlvpt
gi_Tetraodon        ------------------------------------------------------------
gi_Xenopus          --------------------------mewlleavkkelnidsrqlimaeegthvialvsq
gi_Gallus           ----------------maagplpgatmdallrsvekdlsinrwqlaaasdgthvtalvph
gi_Taeniopygia      --------------------------megflqsvekdlnidrrqla--perthvtafvpa
gi_Monodelphis      --------------------------megllqsverdlsidsrqlalapggthvvalvpv
gi_Mus              maqgsrrrkvvltagsegwspsspdmeellrsverdlnidarqlalapggthvvalvst
gi_Rattus           maqgsrrrkvvltagaegcssssgpdmeellrcaerdlnidarqlalapggthvvalvst
gi_Callithrix       maqgsggregtpstpaggwyplpgpdmrellrsverdlsidprqlapalrgthvvalvpa
gi_Pongo            maqgsggregalgtpaggwhsppspdmlellrsverdlsidprqlapapggthvvalvpa
gi_Homo             maqgsggregalrtpaggwhsppspdmqellrsverdlsidprqlapapggthvvalvpa
gi_Pan              maqgsggregalrtpaggwhsppspdmqellrsverdlsidprqlapapggthvvalvpa
gi_Oryctolagus      maqgrggrdvaltagaegwspppspdmeellrsverdlnidarqlapapggahvvalvpa
gi_Sus              malgnrgrevaltteaegwspalspdmeellrsverdlnidarqlapapggthvvalvpa
gi_Ailuropoda       malgskgrevalthgadgwslppspdmeellqsverdlnidarqlapapggthvvalvpa
gi_Equus            malgsrgrevalttgtegwspppspdmeellqsverdlnidarqlapalggthvvalvsa


gi_Danio            rwvmalrnkr--vtrcakyesfsegeictllqrsqmklpsgwtrvciqglrkrklgyrfa
gi_Tetraodon        ------------------------------------------------------------
gi_Xenopus          kwlasikerrtvssqcpkpegfssveiqtflqrsvhklpagwtrieihgvrkerlaypva
gi_Gallus           kwlanlrerralpalcprpeglsevevrtflqrsvqklpagwtrveihglckerltwplr
gi_Taeniopygia      kwlqslkerrvlpvacprpeglsevevrtflqhsvqklpagwtrveihglrkarlgyplr
gi_Monodelphis      rwlanlrerklppgpcprpeglgeaetktllqrsvqklpagwnrvevhglrkrklayplv
gi_Mus              rwlaslrerr--lgpcpraeglgeaevrtllqrsvqrlppgwtrvevhglrkrrlsypl-
gi_Rattus           rwlaslrerr--lgpcpraeglgeaevrtllqrsvqrlpqgwtrvevhglrkrrlsypl-
gi_Callithrix       rwlaslrdrrlppgpcpraeglaeaevrtllqrsvqrlppgwtrvevhglrkrrlsypl-
gi_Pongo            rwlaslrdrrlplgpcpraeglgeaevrtllqrsvqrlpagwtrvevhglrkrrlsypl-
gi_Homo             rwlaslrdrrlplgpcpraeglgeaevrtllqrsvqrlpagwtrvevhglrkrrlsypl-
gi_Pan              rwlaslrdrrlplgpcpraeglgeaevrtllqrsvqrlpagwtrvevhglrkrrlsypl-
gi_Oryctolagus      rwlaslrerr--lgpcpraeglseaevktllqrsvqrlppgwtrvevhglrkrrlsypl-
gi_Sus              rwlaslrerrlplgpcpraeglgeaevrtllqrsvqrlppgwtrvevhglrkrrlsypl-
gi_Ailuropoda       rwlgslrerrlpagpcpraeglseaevrtllqrsvqklppgwtrvevhglrkrrlsypl-
gi_Equus            rwlaslrerrlppgpcpraeglseaevrtllqrsvqrlppgwtrvevhglrkrrlsypl-


gi_Danio            retgc--hgeglsqdsfmtlmqgvsqsnfrnlwheaymthvqpyadsveqtpvlaldavr
gi_Tetraodon        ------------------------------------------------------------
gi_Xenopus          lndgfle-gknidseslirfmqciavqnynnmwnaarrtyvqpyesvhkvpsiqaldalk
gi_Gallus           v--ppvadprgggaetlhgfmqrvasqnyrnlwgrahclyvrpyrhahappavpvldalr
gi_Taeniopygia      a--qppeqrcggttdtlhgfmqsvathnyhnlwgrahglyarpyrrpdapptvpaldalr
gi_Monodelphis      lgsslpseehsglpetltrfmrdtaaqnyhnlwhgayhahgrpyshgnappegsaldsvr
gi_Mus              -gggvpfeegscspetltrfmqevaaqnyrnlwrhayhtygqpyshstapsalpaldsir
gi_Rattus           -srvlpfeegscspetltrfmqevaaqnyrnlwrhayhtygqpyshstapsaipaldsir
gi_Callithrix       -ggglasedgscspetlmrfmqdvaaqnyrnlwrhayqryaqpysrspapsaapalesvr
gi_Pongo            -ggglpfedgscgpetltrfmqevaaqnyrnlwrhayhtygqpyshspapsavpaldsvr
gi_Homo             -ggglpfedgscgpetltrfmqevaaqnyrnlwrhayhtygqpyshspapsavpaldsvr
gi_Pan              -ggglpfedgscgpetltrfmqevaaqnyrnlwrhayhtygqpyshspapsavpaldsvr
gi_Oryctolagus      -ggglpleegscgpetltrfmqdvaaqnyrnlwrrayhtyaqpysrspapsavpalesvr
gi_Sus              -g-glpfeegscspetltrfmqdvaaqnyrnlwrhayhtygqpyshipapsavpaldsvr
gi_Ailuropoda       -ggglpseegssspetltrfmqdvaaqnyrnlwrhayrtygqpyshnpapsavpaldlvr
gi_Equus            -ggglpfeegscspetltrfmrdvatqnyrnlwrhayhtygqpyshspapsavpaldsvr
```

Figure D.1: Multiple sequence alignment of *Danio rerio* (zebrafish) wdr81 amino acid sequence with WDR81 sequences from various species. *The symbol (*) stand for the conserved residues in all WDR81 proteins, (.) and (:) symbols represent substitutions of amino acid residues.*

```
gi_Danio            qalqklfcsnfistdrvspslspakekekdcpflstcsapkqsteslcpnvlpaeclles
gi_Tetraodon        ----------------mapkicg------vrlmantcsrmlgqsehlcpnvvpaegllet
gi_Xenopus          lslqrvygcpfvfinkavpslspskdsss-----------fvlgassssnivqaealles
gi_Gallus           aalqkaygcpilqvgrsvpsaspakg--------------issvpsscpnvlqaealles
gi_Taeniopygia      aalhraygcpvlqvgrnvagmspakes-------------vakavplcpnvlqaealles
gi_Monodelphis      qalqkvfgcpflqvgrgaqclspareaps-----------apragtvcpnllraealies
gi_Mus              qalqrvygctflpvgesipclsnvrdgpc-----------psrgspacpsllraealles
gi_Rattus           qalqrvygctflpvgesmqclsnvrdgp-------------srgssacpsllraealles
gi_Callithrix       qalqrvygcsflpvgeatqcpsharegpc-----------pprggpacpsllraealles
gi_Pongo            qalqrvygcsflpvgettqcpsyaregpc-----------pprgslacpsllraealles
gi_Homo             qalqrvygcsflpvgettqcpsyaregpc-----------pprgspacpsllraealles
gi_Pan              qalqrvygcsflpvgettqcpsyareapc-----------pprgspacpsllraealles
gi_Oryctolagus      qalqrvygcpflpvgeatqgpscardgpc-----------lprgsptcpsllraealles
gi_Sus              qalqrvygcpflpvgettqcpsyardgsc-----------pprgcpaspsllraealles
gi_Ailuropoda       qalqrvygcsfllvgeftqcpssardgpc-----------pprgslscpsllraealles
gi_Equus            qalqrvygcsflpvgeatqcpsyardgpc-----------pprgspacpsllraealles
                                          .                       . .:: ** *:*:

gi_Danio            eevlyvvfpytqytvhdivtyspaklansnakilfilyqlliamrechasgllcgelsll
gi_Tetraodon        aemlyvilpytqyslhdivsfspaklanshakvlfilyqllialqachsaglscgelsll
gi_Xenopus          vsilyiilpyiqyslydvvtfspaklanshakvlfilynvlqalkachqgglssgaltlr
gi_Gallus           aemlyiiypyvqyclhdivtfspakltnshakilfllfhvlqamrachqaglacgafslr
gi_Taeniopygia      admlyviypyvqyclhdvvtfspakltnshakilfllfhvlqamrachqaglacgdfslr
gi_Monodelphis      pemlyviyphvqyclhdvvtfspaklsnshakvlfilfhvlqamdachrqglacgalslc
gi_Mus              pemlyvvhpyvqfslhdvvtfspakltnsqakvlfllfrvlramdachrqglacgalslh
gi_Rattus           pemlyvvhpyvqfslhdvvtfspakltnsqakvlfilfrvlramdachrqglacgalslh
gi_Callithrix       pemlyvvhphlpfslhdvvtfspakltnsqakvlfilfrvlramdachrqglacgalslh
gi_Pongo            pemlyvvhpyvqfslhdvvtfspakltnsqakvlfilfrvlramdachrqglacgalslh
gi_Homo             pemlyvvhpyvqfslhdvvtfspakltnsqakvlfilfrvlramdachrqglacgalsly
gi_Pan              pemlyvvhpyvqfslhdvvtfspakltnsqakvlfilfrvlramdachrqglacgalsly
gi_Oryctolagus      pemlyvihpyvqfslhdvvtfspakltnsqakvlfllfrvlrameachrqglacgalslh
gi_Sus              pgmlyvvhpyvqfslhdvvtfspakltnsqakvlfilfrvlramdachrqglscgplslh
gi_Ailuropoda       pemlyvvhpdvqfslhdvvtfspakltnsqakvlfilfrvlramdachrqglacgaltlh
gi_Equus            pemlyvvhpyvqfslhdvvtfspakltnsqakvlfilfrvlramdachrqglacgalslh
                      :**:: *   : ::*:*::*****:**.**:**:*:.:* *:  **  ** .* ::*

gi_Danio            diavdeqlcsrlkislahyekfkeyrdavpyalqnkvpmsvstkdn-hnngvsgqlcrnc
gi_Tetraodon        dvavdeqlcarlklnlvhyeelgdegerdgnvtgiqmpkgvtqnevlcwsqedkrlcqdc
gi_Xenopus          svlvdeklcsqlrpnfidyereckstkvken--------------inteqlrtvglctsc
gi_Gallus           dvavdeklcsrlrvnfreyegprkeetn-aeadlervn-----eqsgagmrgdmarcytc
gi_Taeniopygia      dvavdeklcsrlrvnfrgyegpgeeeeenlkggldres-----eqs--cvqrqevtcsac
gi_Monodelphis      hvaideklcsqlqldlsayeaheeeeikpmsnileaes-----qcapesrkgeglmypic
gi_Mus              hiavdeklcselrldlsayempsedenqegseek-ngt-----giksekegegrtecptc
gi_Rattus           hiavdeklcselrldlsayempsedenqevseek-drt-----gvksekdgegrpgcptc
gi_Callithrix       hiavdeklcsqlrldlsayerpeedesqealvar-gea-----grkseeeragqpgpppc
gi_Pongo            hiavdeklcselrldlsayerpeedkneeapvar-dea-----gitsqeeqggrpgqptg
gi_Homo             hiavdeklcselrldlsayerpeedeneeapvar-dea-----givsqeeqggqpgqptg
gi_Pan              hiavdeklcselrldlsayerpeeneneeapvar-dea-----giasqeeqggqpgqptg
gi_Oryctolagus      hiavdeklcselrldlsayerpeddehqgspgvr-dga-----ggesgeegprgaacptr
gi_Sus              hiavdeklcselrldlrayerpkedeneespaar-ngv-----gaepgeeggrgpgcptc
gi_Ailuropoda       hiavdeklcselrldlsayerpqedeneeipvar-nga-----gigpgeeggrrpgcptc
gi_Equus            hiavdeklcselrldlsayerpkedekgetpvtr-dka-----gikpgeeggggprcptc
                     : :**:**:.*: .:  **   .

gi_Danio            qdelkslvldwvngqvsnfqylmelnrlagrregdpnyhpvlpwvvdftvpygrfrdlkk
gi_Tetraodon        fgelkslvldwvhgrvsnfcylmelnrlagrrqgdpnyhpvlpwvvdftvpfgkfrdlrr
gi_Xenopus          nnelkqilidwihgrisnydylmylnklagrregdpnyhpvlpwvvdfttkngkfrdlrk
gi_Gallus           qqelrdlvlqwvhgrvsnfdylmhlnslagrrmgdpnyhpvlpwvvdfttkngkfrdlrk
gi_Taeniopygia      qkdlrdlvlqwvhgqvsnfdylmrlnslagrrmgdpnyhpvlpwvvdfttkngkfrdlrk
gi_Monodelphis      qeelrslvldwvhgrvsnfhylmqlnwlagrrwgdpnyhpvlpwvvdfttengrfrdlrk
gi_Mus              qkelrglvldwvhgrisnfhylmqlnrlagrrqgdpnyhpvlpwvvdfttpygrfrdlrk
gi_Rattus           qkelrglvldwvhgrvsnfyylmqlnrlagrrqgdpnyhpvlpwvvdfttpygrfrdlrk
gi_Callithrix       qeelgglvldwvhgrisnfhylmqlnrlagrrpgdpnyhpvlpwvvdfttphgrfrdlrk
gi_Pongo            qeglrslvldwvhgrisnfhylmqlnrlagrrhgdpnyhpvlpwvvdfttphgrfrdlrk
gi_Homo             qeelrslvldwvhgrisnfhylmqlnrlagrrqgdpnyhpvlpwvvdfttphgrfrdlrk
gi_Pan              qeelrslvldwvhgrisnfhylmqlnrlagrrqgdpnyhpvlpwvvdfttphgrfrdlrk
gi_Oryctolagus      qeelrgfvldwvhgglsnfhylmqlnrlagrrqgdpnyhpvlpwvvdfstphgrfrdlrk
gi_Sus              qeelrglvldwvhgrisnfhylmqlnrlagrrqgdpnyhpvlpwvvdfttphgrfrdlrk
gi_Ailuropoda       qeelrglvldwvhgrisnfhylmqlnrlagrrqgdpnyhpvlpwvvdfttphgrfrdlrk
gi_Equus            qeelrglvldwvhgrisnfhylmqlnrlagrrqgdpnyhpvlpwvvdfttphgrfrdlrk
                       *  ::::*:.* :**: *** ** ***** ***************:.  *:****::
```

Figure D.1: continued

```
gi_Danio            skfrlnkgdkqldftyemtkealaavsgsg-gsnyppdlggpvvpggpgqsdhlhvphhi
gi_Tetraodon        skfrlnkgdkqldftyemtkealaaavgngvggsgvgdlsgsvgtgggggqpehlhvphhi
gi_Xenopus          skfrlnkgdkqldftyemtkqafvag-------------------gs--ssdhlhvphhi
gi_Gallus           skfrlnkgdkqldftyemtkqafvag-------------------gs--sgeqlhvphhi
gi_Taeniopygia      skfrlnkgdkqldftyemtkqafvag-------------------gs--sgeqlhvphhi
gi_Monodelphis      skfrlnkgdkqldftyemtrqafvas-------------------gggsggepphvphhi
gi_Mus              skfrlnkgdkqldftyemtrqafvag-------------------ga-gsgepphvphhi
gi_Rattus           skfrlnkgdkqldftyemtrqafvag-------------------ga-gsgeplhvphhi
gi_Callithrix       skfrlnkgdkqldftyemtrqafaag-------------------gt-gggepphvphhi
gi_Pongo            skfrlnkgdkqldftyemtrqafvag-------------------ga-gggepphvphhi
gi_Homo             skfrlnkgdkqldftyemtrqafvag-------------------ga-gggepphvphhi
gi_Pan              skfrlnkgdkqldftyemtrqafvag-------------------ga-gggepphvphhi
gi_Oryctolagus      skfrlnkgdkqldftyemtrqafvas-------------------ga-gggepphvphhi
gi_Sus              skfrlnkgdkqldftyemtrqafvag-------------------ga-gggepphvphhi
gi_Ailuropoda       skfrlnkgdkqldftyemtrqafvag-------------------gv-gggdpphvphhi
gi_Equus            skfrlnkgdkqldftyemtrqafvag-------------------gl-gggepphvphhi
                    ********************::*:.*                    *     :  ******

gi_Danio            sdvlsdityyvykarqtpksvlcshvrsqwepneypasmeriqswtpdecipefyrdpsi
gi_Tetraodon        sdvlsdityfvykarqtpksvlcshvrsqwepneypasmermqswtpdecipefytdpsi
gi_Xenopus          sdvlsdityyvykarrtpkivlcnhvrsqwepneypasmermqgwtpdecipefytdpti
gi_Gallus           sdvlsdityyvytarrtpksvlcchvrsqwepneypasmermqswtpdecipefytdpsi
gi_Taeniopygia      sdvlsdityyvytarrtpkavlcchvrsqwepneypasmermqswtpdecipefytdpsi
gi_Monodelphis      sdvlsdityyvytarrtpravlcghvraqwepheypasmermqswtpdecipefytdpti
gi_Mus              sdvlsdityyvykarrtprsvlcghvraqwepheypatmermqtwtpdecipefytdpsi
gi_Rattus           sdvlsdityyvykarrtprsvlcghvraqwepheypatmermqtwtpdecipefytdpsi
gi_Callithrix       sdvlsdityyvykarrtpravlcghvraqwepheypasmermqswtpdecipefysdpsi
gi_Pongo            sdvlsdityyvykarrtprsvlcghvraqwepheypasmermqnwtpdecipefytdpsi
gi_Homo             sdvlsdityyvykarrtprsvlcghvraqwepheypasmermqnwtpdecipefytdpsi
gi_Pan              sdvlsdityyvykarrtprsvlcghvraqwepheypasmermqnwtpdecipefytdpsi
gi_Oryctolagus      sdvlsdityyvykarrtprsvlcghvraqwepheypasmermqswtpdecipefytdpsi
gi_Sus              sdvlsdityyvykarrtprsvlcghvraqwepheypasmermqswtpdecipefytdpsi
gi_Ailuropoda       sdvlsdityyvykarrtprsvlcghvraqwepheypasmermqnwtpdecipefytdpsi
gi_Equus            sdvlsdityyvykarrtpravlcghvraqwepheypasmermqnwtpdecipefytdpsi
                    *********:**.**:**: *** ***:****.****:***:* *********** **:*

gi_Danio            frsihpdmpdldvppwcnsyeefiavhrqllesrevsqqlhhwidltfgyklsgkeaika
gi_Tetraodon        frsihpdmpdldvpswcksyedfievhrrllesrevsqhlhywidltfgyklsgkeaika
gi_Xenopus          fksihtdmpdleipswcssyedfihvhrallesrdvsqdlhhwidltfgykltgknalme
gi_Gallus           frsihpdmpdldvpswcssyeefievhrmllesrevsqdlhhwidltfgyklqgkdavke
gi_Taeniopygia      frsihpdmpdldvpswcssyeefievhrmllesrevsqdlhhwidltfgykllgkdavke
gi_Monodelphis      frsihpdmpdldvpawcssgedfvvahrallesrevsqdlhhwidltfgyklqgkeavke
gi_Mus              fcsihpdmpdldvpawcssnqefvaahralleswevsqdlhhwidltfgyklqgkeavke
gi_Rattus           fcsihpdmpdldvpawcssnqefvtahralleswevsqdlhhwidltfgyklqgkeavke
gi_Callithrix       fhsihpdmpdldvpswcgssqefvaahralleswevsqdlhhwidltfgyklqgkeavke
gi_Pongo            frsihpdmpdldvpawcsssqefvaahrallesrevsrdlhhwidltfgyklqgkeavke
gi_Homo             frsihpdmpdldvpawcsssqefvaahrallesrevsrdlhhwidltfgyklqgkeavke
gi_Pan              frsihpdmpdldvpawcsssqefvaahrallesrevsrdlhhwidltfgyklqgkeavke
gi_Oryctolagus      fcsihpdmpdldvpawcssseefvaahrallesqevsrdlhhwidltfgyklqgkeavke
gi_Sus              fcsihpdmpdldvpawcsssqefvaahrallesrevsqdlhhwidltfgyklqgkeavke
gi_Ailuropoda       fssihpdmpdldvpawcgssqefvsahrallesrevsqdlhhwidltfgyklqgkeavke
gi_Equus            fssihpdmpdldvpawcgssqefvaahwallespevsqdlhhwidltfgyklqgkeavke
                    * *** *****::* ** * ::*: .*  **** :**:.**:********** **:*:

gi_Danio            knvclhlvdnhthltsygvvqlfdhphpprlalyqyappepphfgrvn--vttw------
gi_Tetraodon        knvclhlvdnhtnlttygvvqlfdqphpprlspsqyapaepplglglasltvpsl------
gi_Xenopus          knvclhlvdnhtnltcfgvvqlfdqphpkrllgpscssfeppailst--qnisqmsawk-
gi_Gallus           knvclhlvdnhthlttygvvqlfdqphprrmvgpactpaeapaiarpllqniketviled
gi_Taeniopygia      knvclhlvdnhthlttygvvqlfdqphprrmvgpaytpaeapaiarpllqniretvvled
gi_Monodelphis      knvclhlvdnhthltsygvvqlfdqphpqrlvgppnlapeppviprpliqrvretsgred
gi_Mus              knvclhlvdahthltsygvvqlfdqphpqrlagspalapeppliprllvqpireatgqed
gi_Rattus           knvclhlvdahthltsygvvqlfdqphpqrlagapalapeppliprllvqpiqeatgqed
gi_Callithrix       knvclhlvdahthlasygvvqlfdqphpqrlagtlallpeppliprlliqtiqetegre-
gi_Pongo            knvclhlvdahthlasygvvqlfdqphpqrlagapalapeppliprllvqtiqettgred
gi_Homo             knvclhlvdahthlasygvvqlfdqphpqrlagapalapeppliprllvqtiqettgred
gi_Pan              knvclhlvdahthlasygvvqlfdqphpqrlagapalapeppliprllvqtiqettgred
gi_Oryctolagus      knvclhlvdahthltsygvvqlfdqphpqrlagtpalapeppplprllvqtiqettgqed
gi_Sus              knvclhlvdahthltnygvvqlfdqphpqrlagapalapeppliprllfqtiqestgred
gi_Ailuropoda       knvclhlvdghthltsygvvqlfdqphpqrlagapalapeppliprvlfqtiqesigred
gi_Equus            knvclhlvdghthltsygvvqlfdqphpqrlagapvlapeppfiprllfqtiqestgqed
                    ********* **.*: :*******:*** *:        * * :
```

Figure D.1: continued

```
gi_Danio            qipplettmdgvdglvpeatgcess--gwsvvgrdeeleqaiealdlsgsssstsasvsi
gi_Tetraodon        yippfdrvadsldglvpestgcets--sfm-vdkddeleqgmealdslgtspaa---cpv
gi_Xenopus          ----dehtgngvngpvveatvceavwntdkvcagdeeleqgtealdslsivgkgndqvci
gi_Gallus           i---pcpvtdavnglvleatptettwsgekpitgeddleqgtealdsisvssrapdqpcs
gi_Taeniopygia      i---qgqvtdavnglvleatpsettwsgekpiageddleqgtealdsisapgrapdqpca
gi_Monodelphis      i---pcqladgtnglvleatpceapwggdrplggddeleqatealdsislagkaadqacp
gi_Mus              i---sgqlingagrlvveatpcetgwtrdrpgtgeddleqatealdsislpgkagdqpgs
gi_Rattus           i---sgqlingagrhvvevtpcesgwtrerptageddleqatealdsisipgkagdqpgs
gi_Callithrix       ---dpgqlpngvgqpvleaipceatwardrpvageedleqatealdsisvagksgdqlat
gi_Pongo            ftenlgqlpngvgrpvleatpceaswtrdrpvageddleqatealdsislagkagdqlgs
gi_Homo             ftenpgqlpngvgrpvleatpceaswtrdrpvageddleqatealdsislagkagdqlgs
gi_Pan              ltenpgqlpngvgrpvleatpceaswtrdrpvageddleqatealdsislagkagdqlgs
gi_Oryctolagus      f---qgqlangmgrvvleaapceagwtrdrpvageddleqatealdsislagkagdqlga
gi_Sus              l---pgqlangmgrpvleatpceagwardrpavgeddleqatealdsialagkagdqlgp
gi_Ailuropoda       l---pgqltngvgrlvleataceggwardrpvageddleqatealdsislvgkageqlgs
gi_Equus            f---pgqltngvgrlvleatpceagwardrsvvgeddleqatealdsislvgkagdqlgs
                              :.    * *    *           :::***. ****  .

gi_Danio            pvvgsaagktsgetiglvvspshgsfpgeatgnvtntlgsgirtamlhraasvskk---p
gi_Tetraodon        pipg-----kmgehatlivsqspssfpgdfts--------gsrsallprsgatnkkhreg
gi_Xenopus          ps-----------------vqv-ts----anifqgenrppgskpnrisrat---------
gi_Gallus           s-------------------sa-q--pstlpayptegkasgvrplrrskag-------aa
gi_Taeniopygia      tv------------------ppa-q--pstlpayvtdskssgvrplrrskag-------av
gi_Monodelphis      ss-----------------sl--------pasghpfsststtrlgrrnkag-------gv
gi_Mus              ss-----------------s-------qaspgllsfsapsgsrpgrrskaa-------gl
gi_Rattus           ss-----------------s-------qaspgllpfsapsgsrpgrrskat-------gl
gi_Callithrix       ss-----------------g-------qaapsllsfsvasasrpgrrnkaa-------ga
gi_Pongo            s------------------s-------qaspgllsfsvssasrpgrrnkaa-------ga
gi_Homo             s------------------s-------qaspgllsfsvasasrpgrrnkaa-------ga
gi_Pan              s------------------s-------qaspgllsfsvasasrpgrrnkaa-------ga
gi_Oryctolagus      ss-----------------s-------papagllsfsvastsrpsrrhraa-------ga
gi_Sus              ss-----------------sps-ssssqapagllsfsgasasrpgrrnkaa-------ga
gi_Ailuropoda       ss-----------------s----assqappgllsfsvasasrpgrrskpa-------ga
gi_Equus            ss-----------------------snqvppgllsfsvasasrpgrrnkaa-------ga
                                                          :     :

gi_Danio            easnledfkislpdgfkplqpleeleklntflvkglhseiehtmdlginkkdlrsvpkvp
gi_Tetraodon        svtngedvkitlpegfnplqpleeleklnnflvkslhadvcdtpgsgekme------esl
gi_Xenopus          tnaeesqrkllldsfnpvqaleelekldnfllrglhstllpveks---------skifp
gi_Gallus           dqadrddmkitlpegfnplqaleelekldnflvkglssdmqlmeqp---------geepl
gi_Taeniopygia      dq---ldmkitlpegfnplqaleelekldnflvkglssemqlmeql---------weepp
gi_Monodelphis      dagdgdegkivlpegfnplqaleelekfgnfmarglcgkmeapeqc---------pakpa
gi_Mus              dpgegeegkivlpegfspiqaleelekvgnflakglgsqleepekp---------haqpp
gi_Rattus           dsgegdegkivlpegfspiqaleelekvgnflarglgsqleepekp---------qaqpp
gi_Callithrix       dpgegeegrillpegfhpmqaleelertgnflakglgglwevpeqp---------qgrpa
gi_Pongo            dpgegeegrillpegfnpvqaleelektgnflakglggllevpeqp---------rvqpa
gi_Homo             dpgegeegrillpegfnpmqaleelektgnflakglggllevpeqp---------rvqpa
gi_Pan              dpgegeegrillpegfnpvqaleelektgnflakglggllevpeqp---------rvqpa
gi_Oryctolagus      dpgegeegkillpegfnpvqaleelekmgnflakglggqlqvperp---------rgqpp
gi_Sus              dpgegeegrvflpegfnpvqaleeleklgnfltkglggrlevpeqp---------qvrpt
gi_Ailuropoda       dpgegeegkillpegfnpvqalegleklgnfltkglgsqlevleqp---------qvqpp
gi_Equus            dlgegeegkillpeafnpvqaleeleklgnfltkglggrlevpeqp---------qvqlp
                          : :: **:.* *:* ** **:  .*: :.* .

gi_Danio            lsftdlfqrdmqalgvliaeifyssklrglrpethlrdrfqavlklcstnlrdvplplhh
gi_Tetraodon        pslsqlhqrdmqalgvliaeifyssklrglkpdsplkkrfqavmklccaslrdvplslhh
gi_Xenopus          lsllglfqrdmqalgvmiaeivfagkihttppktslleryilvrnlsrhhpkeiplpllq
gi_Gallus           lglsdlfqrdmqalgiliaeiifaprirpskpdasllerflmvrnlcryhpkeipaplqh
gi_Taeniopygia      lslsdlfqrdmqalgilvaeiifaprlrpskpdaslserflmvrnlcryhpkeipaplqh
gi_Monodelphis      lkltdlfqrdmqalgvlvaeivfaarvrmlrphaplwerflivrgfcsrypkeipiplqp
gi_Mus              vhlqslfhrdmqvlgvllaemvfatrvrilqpdaplwvrfeavrglcirhskdipvslqp
gi_Rattus           vylqslfhrdmqvlgvllaemvfatrvrilqpdaplwvrfeavrglctrhskdipvslqp
gi_Callithrix       mplqhlfhrdmqalgvllaemvfasrvrtlqpdaplwvrfqavrglctrhprevpvslqp
gi_Pongo            vplqcllhrdmqalgvllaemvfatrvrtlqpdaplwvrfqavrglctrhpkevpvslqp
gi_Homo             vplqcllhrdmqalgvllaemvfatrvrtlqpdaplwvrfqavrglctrhpkevpvslqp
gi_Pan              vplqcllhrdmqalgvllaemvfatrvrtlqpdaplwvrfqavrglctrhpkevpvslqp
gi_Oryctolagus      vqlrdlfhrdmqalgvllaemvfatrvrtlpphaplwvrfeairglclrhpkevpvslqp
gi_Sus              aqlrdlfhrdmqalgvllaemvfatrvrtlqpdaplwvrfkavrglcrrylkevpvslqp
gi_Ailuropoda       vqlqelfhrdmqalgvllaemvfatrvrtlqpdaplwvrfevvrglclrhpkevpvslqp
gi_Equus            vqlrdlfhrdmqalgvllaemvfatrvrtlqpdaplwlrfetvrglctrhpkevpvslqp
                      :  * :****.**:::**:.:: :::   *.: *  *:  :  :.    :::*  *
```

Figure D.1: continued

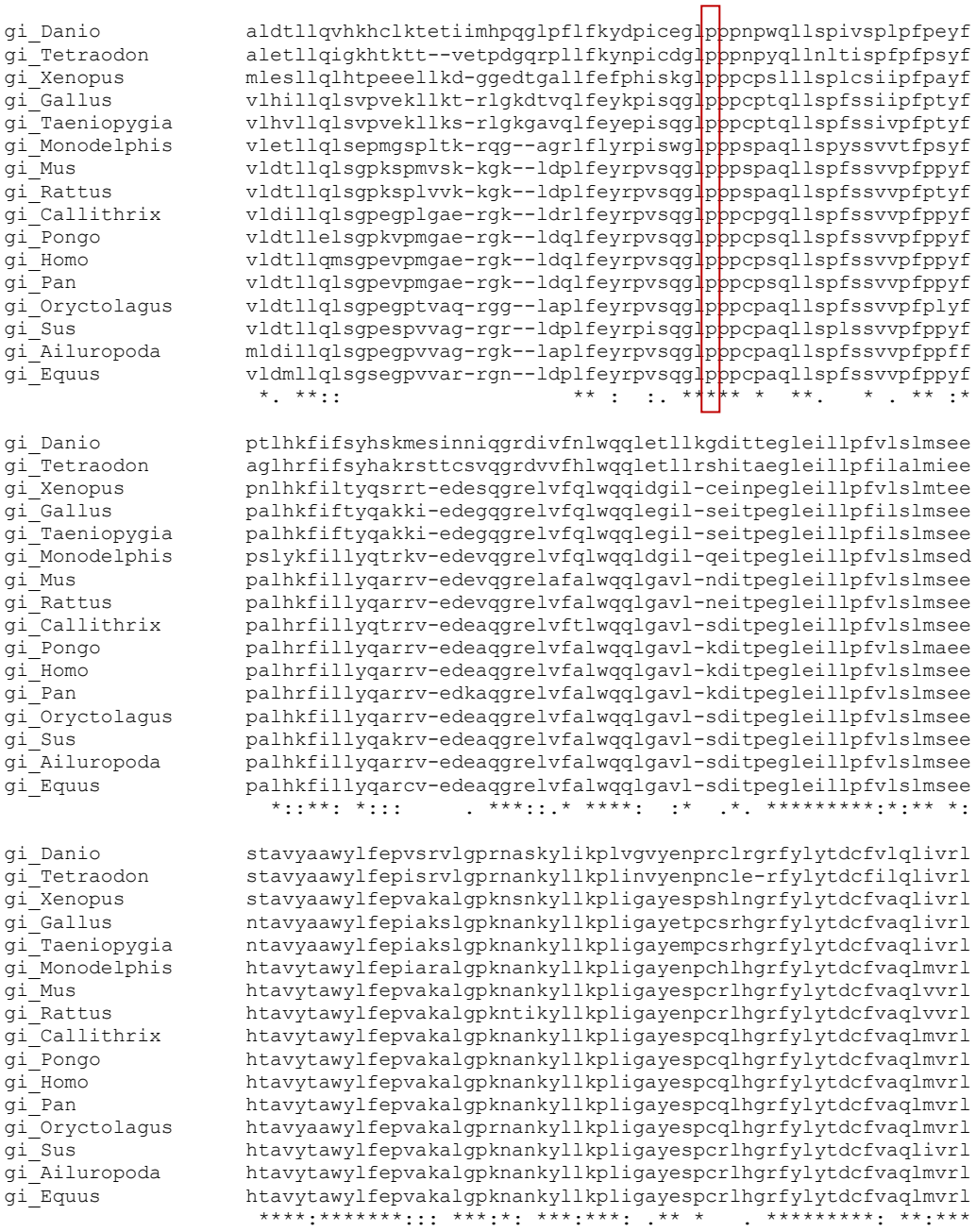

Figure D.1: continued. The mutation site in human patients, proline at residue 856, is conserved among all of the species of vertebrates, which were included to this alignment.

```
gi_Danio            glqvflssllphvlqvmtgfescntaagtewegmkvlrgaagaldeeeeeyecddrrssn
gi_Tetraodon        glqaflssllphvlqvitgfescipglsget--ckgltdg-tmhleeeedfrcdesrhss
gi_Xenopus          glqaflsnllnhvlqiligletsgee-------rkllsggae---deesg--g-d-----
gi_Gallus           glqsfilnllphilqilvgiessree-------sksllgaae---ddesg--g-g-----
gi_Taeniopygia      glqpfllnllphilqilvgiessree-------sksflgtae---ddesg--g-e-----
gi_Monodelphis      glqpflshllphvlqvlagvetsqek-------tkclggtte---deeigegd-e-----
gi_Mus              glqafllthllphvlqvlagveasqee-------gkglvgtte---deeselpv-s-----
gi_Rattus           glqaflihllphvlqvlagveasqee-------gkglvgtte---deenelpv-p-----
gi_Callithrix       glqafllthllphvlqvlagteasqee-------tkdlvaaae---deesglpg-a-----
gi_Pongo            glqafllthllphvlqvlagaeasqee-------skdlagaae---eeesglpg-a-----
gi_Homo             glqafllthllphvlqvlagaeasqee-------skdlagaae---eeesglpg-a-----
gi_Pan              glqafllthllphvlqvlagaeasqee-------skdlagaae---eeesglpr-a-----
gi_Oryctolagus      glqaflvhllphvlqvlagveasqee-------skglagaae---deevalpg-p-----
gi_Sus              glqaflvhllphilqvlagveasqee-------skglvgaae---deesglpg-a-----
gi_Ailuropoda       glqaflshllphvlqvlagveasqee-------skglvgaae---dedgelag-a-----
gi_Equus            glqaflvhllphvlqvlagveasqee-------skglagaae---deesglpg-a-----
                    *** *:  ** *:**:: * *:.          * :        :::

gi_Danio            atssgkvgggsgggsggvgvvgdqglvdyssgislndqvflnegedfqngfyvnnsasga
gi_Tetraodon        gsvsgtmg-gsggaaggvagvgdtglsnypsgislndqvflsdaedfqnefyvnsgaagk
gi_Xenopus          spvscnfg-earqtsidqs-asshelldytsgvtfhdqgylaenedfqgtlyvsdpl---
gi_Gallus           spmscmfg-eeikmdvehs-staldlldytsgvsfhdqaylpesedfqsglyvgesl---
gi_Taeniopygia      spvscvfg-eeikmdvehs-saaldlldytsgvsfhdqaylpegedfqsglyvgesl---
gi_Monodelphis      gqgpcafg-eaiqmegdpg-ssglelldytsgvsfhdqtdlpesedfqaglyvsgsp---
gi_Mus              gpgscafg-eeiqmdgqpaassglglpdyrsgvsfhdqadlpdtedfqaglyvaesp---
gi_Rattus           gpgscafg-eeiqmggqpaassglglpdyrsgvsfhdqadlpdtedfqaglyvaesp---
gi_Callithrix       gpgscafg-eeipmdgepsassglglpdytsgvsfhdqadlpetedfqaglyvtesp---
gi_Pongo            gpgscafg-eeipmdgeppassglglpdytsgvsfhdqadlpetedfqaglyvtesp---
gi_Homo             gpgscafg-eeipmdgeppassglglpdytsgvsfhdqadlpetedfqaglyvtesp---
gi_Pan              gpgscafg-eeipmdgeppassglglpdytsgvsfhdqadlpetedfqaglyvtesp---
gi_Oryctolagus      gpgscafg-eeiqmdeepatsaglglpdytsgvsfhdqadlpetedfqggglyvagsp---
gi_Sus              gpsscafg-eemqmdgeptassglglpdytsgvsfhdqadlpetedfqaglyvaesp---
gi_Ailuropoda       rpsscafr-eeipmdgepaassglglpdytsgvsfhdqaylpetedfqaglyvaesp---
gi_Equus            rasscafg-eeiqmdgepaassglglpdytsgvsfhdqadlpetedfqaglyvaesp---
                          .                 * :* **:::.**  * : ****  :**

gi_Danio            ttvgtkqqnqstankdqdqeslsvgklsdkssasevsigd------------raslksad
gi_Tetraodon        ------epnqnsackdqdqesvsvgklsdksstselslgd------gdsmrdraslksad
gi_Xenopus          --------------qpqepeslslgrlsdkssasevslgdekvtd-sdslkekgslksgd
gi_Gallus           --------------qpqeqeslslgrlsdkssasevslgedrpvd-gdsqkdksslksvd
gi_Taeniopygia      --------------qpqeqeslslgrlsdkssasevslgedrpad-gdsqkdksslksmd
gi_Monodelphis      --------------qpqepeslslgrlsdksstsdaslgedrpgdeigltr-------dk
gi_Mus              --------------qpqeaeavslgqlsdksstseasqgeergqddggapadknsvksgd
gi_Rattus           --------------qpqeaeavslgqlsdksstseasqgeergqddggapvdknsvksgd
gi_Callithrix       --------------qpqeaeavslgrlsdksstsetslgeerapddgaapmdkssslrsgd
gi_Pongo            --------------qpqeaeavslgrlsdksstsetslgeerapdeggapvdkssslqsgd
gi_Homo             --------------qpqeaeavslgrlsdksstsetslgeerapdeggapvdkssslrsgd
gi_Pan              --------------qpqeaeavslgrlsdksstsetslgeerapdeggapvdkssslrsgd
gi_Oryctolagus      ----------------qeaealslgrlsdksstsdtslgeeragdegcapvdkssslrsgd
gi_Sus              --------------qpqeaeavslgrlsdksstsetslgeervadeggapvdkssslrsgd
gi_Ailuropoda       --------------qpqeaeavslgrlsdksstsetslgeeraaeeggapvdkssslrsgd
gi_Equus            --------------qpqeaeavslgrlsdksstseaslgeera-degsapvdkssslksgd
                                  *: *::*:*:******:*: * *:                  .

gi_Danio            ssqdlkqasdgedggeledeeetvedr-------ei--tv-qrvpslemtlsvcteesea
gi_Tetraodon        ssqdlkqasegeeggeldeeevpetse-----geeg--tdgtvascleltlsg---vtqt
gi_Xenopus          ssqdlkqseeseeeedr-----------------------epspglseltlsvntdvsv-
gi_Gallus           ssqdlkqsedseeeee-ereeeerddta----------vdaelvgavdvgvsvdagtsv-
gi_Taeniopygia      ssqdlkhllgeeeeeeeeheedehedav----------vdpeltvv-----vdaagasv-
gi_Monodelphis      ssqdlkqsegseeeeeeedeevvgqggdvgeeeeeeedeqdstpavseftls-dpgvst-
gi_Mus              ssqdlkqsegseee---eeee-----gcvvleed----qedevtgtseltls-dtmlsm-
gi_Rattus           ssqdlkqsegseeee--eeee-----gcvvleee----eqdevtgtseltls-dtilsm-
gi_Callithrix       ssqdlkqsegseee---eeed-----gcvlleeeeg--eqeevtgaseltls-dtvlsm-
gi_Pongo            ssqdlkqsegseeee--eeed-----scmvleeeeg--eqeevtgaseltls-dtvlsm-
gi_Homo             ssqdlkqsegseeee--eeed-----scvvleeeeg--eqeevtgaseltls-dtvlsm-
gi_Pan              ssqdlkqsegseeee--eeed-----scvvleeeeg--eqeevtgapeltls-dtvlsm-
gi_Oryctolagus      ssqdlkqsegsedee--eeee-----gcvvleeeegv-eqdevtgaseltls-dtvlsm-
gi_Sus              ssqdlkqsegseeee--eeed-----gcvvlee--geeeqdevpeaseltls-dtvlsm-
gi_Ailuropoda       ssqdlkqsegseeeeeegeee-----gcvvleeeegdgeqdeitraselalp-dtvlsm-
gi_Equus            ssqdlkqsegseeee--eeee-----gcvvleeeegegeqdevtgaseltlp-dpvlsm-
                    ******:    *:                                          :
```

Figure D.1: continued

```
gi_Danio            tvatlegdvmngivqedgeknmeeeetehdpledseekehkilldtvcktvrwlsaklgp
gi_Tetraodon        svttlegeftnnltmnetekgdvgaqeehdpsgdseekehrilqdtvcktvrwlsatlgp
gi_Xenopus          -----------dtvlasesr--edeeeeqdlnnqteekeqkilidttckmvrwlsaklgp
gi_Gallus           -----------dvtladd-gsepedgegeelpdhsddkeqtilldtackmvrwlsaklgp
gi_Taeniopygia      -----------dvtladd-ssepedgegeelpdhsddkeqtilldtackmvrwlsaklgp
gi_Monodelphis      -----------dtvlpndggn---geeeedisdqsevkeqkilldtacktvrwlsaklgp
gi_Mus              -----------etvvapgdgr-dreeeeeplteqtegkeqkilldtackmvrwlsaklgp
gi_Rattus           -----------etvvapgdgr-dreeeeeplpeqtegkeqkilldtackmvrwlsaklgp
gi_Callithrix       -----------eavvagssgg-dgegqeeplpeqsegkeqkilldtackmvrwlsaklgp
gi_Pongo            -----------etvvaggsgg-dgeeeeeplpeqsegkeqki------------------
gi_Homo             -----------etvvaggsgg-dgeeeeealpeqsegkeqkilldtackmvrwlsaklgp
gi_Pan              -----------etvvasgsgg-dgeeeeealpeqsegkeqkilldtackmvrwlsaklgp
gi_Oryctolagus      -----------etvvagdgqg-dgeeeeepltgqsegkehrilldtackmvrwlsaklgp
gi_Sus              -----------dtvvaggggaddgeeeeeplteqsegkeqkilldtackmvrwlsaklgp
gi_Ailuropoda       -----------dtvvargget-ggeedteplteqsegkeqkilldtackmvrwlsaklgp
gi_Equus            -----------dtvvagggga-dgeeaeeplteqsegkeqqilldtackmvrwlaaklgp
                                      .              .    .:: **: *

gi_Danio            tltsrfiarnllrlltscyigldkhqfmlsvneens-lecvgsvyekkpvvgdqtarpvl
gi_Tetraodon        tvtsryvarnllrlltncyigpanhqlvtpvseeklesagmsnvyekktvvgdqtarpvl
gi_Xenopus          tvtsryiarnllrlltscyvgpqrqqfvanmeens--pls-----vkkpvcgdqvskpvl
gi_Gallus           tvtsrfiarnllrlltscyigptrqqfvpsndeng--plstgniyqkrpvlgdqvskpvl
gi_Taeniopygia      tvtsrfiarnllrlltscyigltrqqfvpssdens--plstgniyqkrpvlgdqvskpvl
gi_Monodelphis      tvtsryvarnllrlltscyvgatrqqfmgsssdts--plssgniyqkrpvlgdvasvpvl
gi_Mus              tvasrhvarnllrlltscyvgptrqqftvssddtp--plnagniyqkrpvlgdivsgpvl
gi_Rattus           tvasrhvarnllrlltscyvgptrqqftvscddsp--plnagniyqkrpvlgdivsgpvl
gi_Callithrix       tvasrhvarnllrlltscyvgptrqqftassgdsp--slsagniyqkrpvlgdvasgpvl
gi_Pongo            ------------------------------------------------------------
gi_Homo             tvasrhvarnllrlltscyvgptrqqftvssgesp--plsagniyqkrpvlgdivsgpvl
gi_Pan              tvasrhvarnllrlltscyvgptrqqftvssgesp--plsagniyqkrpvlgdivsgpvl
gi_Oryctolagus      tvasrhvarnllrlltscyvgptrqqftvssgesp--plsagniyqrrpvlgdvvsapvl
gi_Sus              tvasrhvarnllrlltscyvgptrqqftasngesp--plsagniyqkrpvlgdivsgpvl
gi_Ailuropoda       tvasryvarnllrlltscyvgptrqqftvssgesp--plsagsiyqkrpvlgdivsgpvl
gi_Equus            tvasrhvarnllrlltscyvgptrqqftmssgesp--plsagniyqkrpvlgdivsgpvl


gi_Danio            ecliyiahlygepvltyqylpyigylvsppss---crlntrkeagllgavvltqkiivfl
gi_Tetraodon        dcliyvaqlygepvltyqylpyigylvsppss---qrlntrkeasllgaialtrkivvfl
gi_Xenopus          dclmylahlygepfltyqylpyinylvaptsg---crlnsrkeasllaavtltqkiivyl
gi_Gallus           acllhvaylygepvltyqylpyisylvapgsgsgggrlnsrkeagllaavtltqkivvcl
gi_Taeniopygia      aclvhvaylygepvltyqylpyisylvapgagsggvrlnsrkeagllaavtltqkivvcl
gi_Monodelphis      gclmhiaclygepvltyqylpyisylvapgggggpsrlnsrkeagllaavtltqkiivyl
gi_Mus              scllhiaylygepvltyqylpyisylvapgsnsnpsrlnsrkeagllaavtltqkiivyl
gi_Rattus           scllhiahlygepvltyqylpyisylvapgsnsspsrlnsrkeagllaavtltqkiivyl
gi_Callithrix       scllhlahlygepvltyqylpyisylvapgsasgpsrlnsrkeagllaavtltqkiivyl
gi_Pongo            ------------------------------------------------------------
gi_Homo             scllhiarlygepvltyqylpyisylvapgsasgpsrlnsrkeagllaavtltqkiivyl
gi_Pan              scllhiarlygepvltyqylpyisylvapgsasgpsrlnsrkeagllaavtltqkiivyl
gi_Oryctolagus      scllhiahlygepvltyqylpyisylvapgsasgpsrlnsrkeagllaavtlaqkitvyl
gi_Sus              scllhvahlygepvltyqylpyisylvapgstsgpsrlnsrkeagllaavtltqriivyl
gi_Ailuropoda       scllhiahlygepvltyqylpyisylvapgstsgpsrlnsrkeagllaavtltqkiivyl
gi_Equus            scllhiaylygepvltyqylpyisylvapgstsgpsrlnsrkeagllaavtltqkiivyl


gi_Danio            sdttlmdmlmkinqevllplldlltstkmgfpsgvqtrsavclktlslmaliclrigrem
gi_Tetraodon        sdttlmdmlmkinqdvllplldllttpcmgfpsgvhtrtvvclktlslialiclrigrem
gi_Xenopus          sdttlmdilpkinqdvllpvlsiltsatvgfpsgaqarialcvkcssllsliclrigrem
gi_Gallus           sdttlmdilpkisqevllpvlgfltslsvgfpsgaqarvvlciktislialiclrigqem
gi_Taeniopygia      sdttlmdilpkisqevllpvlgfltspavgfpsgaqarvvlcvktislialiclrigqem
gi_Monodelphis      sdttlmdilprishevllpvlssltslvtgfpggaqartvlcvktislialiclrigqem
gi_Mus              sdttlmdilprishevllpvlgfltsfvtgfpsgaqartvlcvktislialiclrigqem
gi_Rattus           sdttlmdilprishevllpvlsfltsfvtgfpsgaqartvlcvktislialiclrigqem
gi_Callithrix       sdttlmdilprishevllpvlsfltslvtgfpsgaqartilcvktislialiclrigqem
gi_Pongo            ------------------------------------------------------------
gi_Homo             sdttlmdilprishevllpvlsfltslvtgfpsgaqartilcvktislialiclrigqem
gi_Pan              sdttlmdilprishevllpvlsfltslvtgfpsgaqartilcvktislialiclrigqem
gi_Oryctolagus      sdttlmdilprlshevllpvlsfltslvtgfpsgaqartvlcvktislialiclrigqem
gi_Sus              sdttlmdilprishevllpvlsfltslvtgfpsgaqartvlcvktislialiclrigqem
gi_Ailuropoda       sdttlmdilprishevllpvlsfltslvtgfpsgaqartvlcvktisligliclrigqem
gi_Equus            sdttlmdilprishevllpvlsfltslvtgfpsgaqartvlcmktislialiclrigqem
```

Figure D.1: continued

```
gi_Danio            vqqhmaetlsrffqvfsllqflqnqigsapr----revaectyldlripdgaeltielgv
gi_Tetraodon        vqqhmadtlrqffavfsllnslqpqvlhahvthadlivadvtvvdvctsdnsfvtyelgv
gi_Xenopus          vqqhlgdtlriffsnftlmqelheqglvmen----pdslepvvqhvqckdgstlpvdlsl
gi_Gallus           vqqhlsdtvrnffgafsllqelqdqgltaes----lsgcevpvmevplregkllaldpav
gi_Taeniopygia      vqqhlsdtvrnffgafsllqelqdqgltaes----lsscempvmevplsdgkllaldpsv
gi_Monodelphis      vqqhlsetvatffqvfslvhelqcqalrpdt----pspneghvlevpfsdgqqravdpal
gi_Mus              vqqhlsepvatffqvfshlhelrqqdlpldp----kgctegqlpeatfsdgqrrpvdptl
gi_Rattus           vqqhlsepvatffqvfshlhelrqqdlqldl----kgctegqlpeatfsdgqrrpvdptl
gi_Callithrix       vqqhlsepvaaffqvfsqlhelrqqdlkldp----tgrsegqlpevvfsdgqqrpvdptl
gi_Pongo            ------------------------------------------------------------
gi_Homo             vqqhlsepvatffqvfsqlhelrqqdlkldp----agrgegqlpqvvfsdgqqrpvdpal
gi_Pan              vqqhlsepvatffqvfsqlhelrqqdlkldp----agrgegqlpqvvfsdgqqrsvdpal
gi_Oryctolagus      vqqhlsepvatffqvfsqlhelrhqdlkwds----agrsegqlpeaafsdgqqrpvdpal
gi_Sus              vqqhlsepvatffqvfsrlhdlqhqdwkles----mgrsegqlpevafsdgqlrlvdptv
gi_Ailuropoda       vqqhlsepvatffqvfsqlhelrhqdlkldp----tgrsegqlpevafsdgqqrpvdptl
gi_Equus            vqqhlsepvatffqvfsqlhelqhldlklds----vsrsegqlpevafsdgqqrpvdptl


gi_Danio            leelqavfnpemayasyipfycligdsgirklvtnhelvwslaqsyheraspgspesnpv
gi_Tetraodon        leelrcvfnpemayasyvpfccligdmairklvpnheliwqltqsylqsvsqrgpecnpa
gi_Xenopus          ldelekvynaemayatyvpfscligdg-ighvipnhdliwkltmvyqeavipkdiespaa
gi_Gallus           llelqkvfnpemayityipfscllgdv-irtvvpnhslveklaslylenvnpknlqv-vg
gi_Taeniopygia      lvelqkvfnpemayityipfscllgdv-irtvvpnhslveklaslhlenvnpqnxqg-vg
gi_Monodelphis      ldelqkvftlemaymtyvpfscllgdv-iqkivpnhglvgqlagqylesaspvg-qdpmn
gi_Mus              leelqkvftlemaytiyvpfscllgdi-irkiipnhelvgelaglylesmspss-rnpas
gi_Rattus           leelqkvftlemaytiyvpfscllgdi-irkiipnhelvgelaglylesmspsslrnpas
gi_Callithrix       ldelekvftlqmaytiyvpfscllgdi-iwkiipnhelvgelaglylesispss-hspas
gi_Pongo            ------------------------------------------------------------
gi_Homo             ldelqkvftlemaytiyvpfscllgdi-irkiipnhelvgelaalylesispss-rnpas
gi_Pan              ldelqkvftlemaytiyvpfscllgdi-irkiipnhelvgelaalylesispss-rnpas
gi_Oryctolagus      ldelqkvftlemaytiyvpfscllgdi-irkiipnhelvgelaglylesislss-qnpas
gi_Sus              ldelqkvftlemaytiyvpfscllgdi-irkiipnhelvgqlaglylesispss-rspas
gi_Ailuropoda       ldelqkvftlemaytiyvpfscllgdi-irkiipnhelvgelaglylesvspss-rspas
gi_Equus            ldelqkvftlemaytiyvpfscllgdi-irkiipnhelvgelaglylksispns-rspas


gi_Danio            ggqrasav----glspsmgrqmsrspfpapssts tplggdilpesgtfgshlvgnriqvt
gi_Tetraodon        stsrvevsapsaavssgfprrvgcsafpaptfs---stgnlipesgtfgshlvgnriqvs
gi_Xenopus          plssgsr---------------igssf---------yiaeddgqsgtfgsvmvgnriqvp
gi_Gallus           leqapsma------gsdqdm-rgteaf---------sspqedshsgtfgsvlvgnriqvp
gi_Taeniopygia      leqtpsvv------gsdqdp-rgaepf---------sspqedthsgtfgsvlvgnriqvp
gi_Monodelphis      l-apmpsa------speqdp-qg---r---------gvnhddgnsgtfgsvlvgnriqip
gi_Mus              meptmasa------gpewdp-qs---g---------sclqddghsgtfgsvlvgnriqip
gi_Rattus           mepvtpsa------gpewnp-qs---g---------sclqddghsgtfgsvlvgnriqip
gi_Callithrix       veptvpsm------gpewdp-qg---g---------rcpqddghsgtfgsvlvgnriqip
gi_Pongo            ------------------------------------------------------------
gi_Homo             veptmpgt------gpewdp-hg---g---------gcpqddghsgtfgsvlvgnriqip
gi_Pan              veptvpst------gpewdp-qg---g---------gcpqddghsgtfgsvlvgnriqip
gi_Oryctolagus      veptvpss------saerdp-qg---g---------gcpqddshsgtfgsvlvgnriqip
gi_Sus              leptapst------spewdp-qg---g---------scpqddghsgtfgsvlvgnriqip
gi_Ailuropoda       veptvpst------gpewdp-qs---g---------gcprddghsgtfgsvlvgnriqip
gi_Equus            veptvpst------gpgwds-qg---g---------gcpqddghsgtfgsvlvgnriqip


gi_Danio            rdteacgspnlssletwthgrpygsnappmslattalssagps--fshssyswvmgptpe
gi_Tetraodon        pgadydsnpnlslssswgrsah------ttpiittassftgpsagtaslssswvtgftte
gi_Xenopus          kdiqypmsrs-----------------------------------t-cctpvmetfqsd
gi_Gallus           vdtqreglgllrl-------------------------------sagtd----gfipsssse
gi_Taeniopygia      vdtqreglgllrl---------------------------------sagad----gfapsssse
gi_Monodelphis      vdtqpespsplgp-------------------------------ssgvc-gsvgglcemgge
gi_Mus              d-sqpqspgplgs-------------------------------lsgvg-s-sggl-snrne
gi_Rattus           d-sqpqssgplgs-------------------------------isgvg-s--ggl-ssrne
gi_Callithrix       adsqpespgplgp-------------------------------isga---------gsgse
gi_Pongo            ------------------------------------------------------------
gi_Homo             ndsrpenpgplgp-------------------------------isgvg-g--ggl-gsgsd
gi_Pan              ndsrpenpgplgp-------------------------------isgvg-g--ggl-gsgsd
gi_Oryctolagus      sdpqpespgplgp-------------------------------isgvg-s--ggl-gagae
gi_Sus              gdsqpespgplgp-------------------------------isgvg-g--ggv-gslse
gi_Ailuropoda       ddsqpespgllgp-------------------------------ipgvg-s--ggl-sse-e
gi_Equus            ddshpdspgplgp-------------------------------isgvg-s--ggl-gsene
```

Figure D.1: continued

```
gi_Danio            dsalkqdlprssrslqgnwlaywqyeiglnqqdshfhfhqirlqsfighsgtakclapla
gi_Tetraodon        dsalkqelprsgrslqgnwlaywqyeiglnqqdphfhfhqirlqsfighsgttkclaplt
gi_Xenopus          ensfkqdlqknaqglcgnwlaywqyeigvsqqephfcfhqiklqsfvghsgaikcvkpls
gi_Gallus           entlkhdlprsthvlcgnwlaywqyeigvsqhdprfhfhqiklqsfsghsgaikcvapls
gi_Taeniopygia      esalkhdlprsthmlcgnwlaywqyeigvsqhdprfhfhqiklqsfsghsgaikcvaplg
gi_Monodelphis      enslkrdlprcahglsgnwlaywqyeigvsqhdahfhfhqirlqsflghsgavkcvaplg
gi_Mus              dnalkrelprsahglsgnwlaywqyeigvsqqdahfhfhqirlqsfpghtgavkcvaals
gi_Rattus           dnalkrelprsahglsgnwlaywqyeigvsqqdahfhfhqirlqsfpghtgavkcvaals
gi_Callithrix       dnalkqelprsahglsgnwlaywqyeigvsqqdahfhfhqirlqsfpghsgavkcvapls
gi_Pongo            ------------------------------------------------------------
gi_Homo             dnalkqelprsvhglsgnwlaywqyeigvsqqdahfhfhqirlqsfpghsgavkcvapls
gi_Pan              dnalkqelprsvhglsgnwlaywqyeigvsqqdahfhfhqirlqsfpghsgavkcvapls
gi_Oryctolagus      dnalkrelprsahglsgnwlaywqyeigvsqqdahfhfhqirlqsfpghsgavkcvaals
gi_Sus              dnalkrelprsahglsgnwlaywqyeigvsqqdahfrfhqirlqsfpghsgaikcvvpls
gi_Ailuropoda       dnalkrelprsahglsgnwlaywqyeigvsqqdahfhfhqirlqsfpghsgavkcvapls
gi_Equus            dnalkrelprsahglsgnwlaywqyeigvsqqdahfhfhqirlqsfpghsgavkcvapls


gi_Danio            gedyflsgskdktvrlwplynhgdgtreveprltytehrksifyvgqlealqevvscdgt
gi_Tetraodon        gedyflsgskdktvklwplhnhgdgtkevepkltysdhrksvfyvgqleasqevvscdgt
gi_Xenopus          gedffmsgskdktvrlwplynygdgtrdiearhiyaehkrsvfyvgqlesvqqlvscdga
gi_Gallus           sedfflsgskdktvrlwplynygdgtsevpprftysehkksvfyvsqleasqhvvscdgt
gi_Taeniopygia      sedfflsgskdktvrlwplynygdgtsevpprftyaehkksvfyvsqleapqhvvscdgt
gi_Monodelphis      nedfflsgskdrtvrlwplyncgdgtsetvprlvysqhrksifyvsqleasqqvvscdgt
gi_Mus              sedfflsgskdrtvrlwplynygdgtnetasrliyaqhrksvfyvgqleapqyvvscdga
gi_Rattus           sedfflsgskdrtvrlwplynygdgtsetaprliyaqhrksvfyvgqleapqyvvscdga
gi_Callithrix       gedfflsgskdrtvrlwplynygdgtcetaprlvytqhrksvffvdqlealqhvvscdga
gi_Pongo            ------------------------------------------------------------
gi_Homo             sedfflsgskdrtvrlwplynygdgtsetaprlvytqhrksvffvgqleapqhvvscdga
gi_Pan              gedfflsgskdrtvrlwplynygdgtsetaprlvytqhrksvffvgqleapqhvvscdga
gi_Oryctolagus      sedfflsgskdrtvrlwplynygdgtsetaprlvytqhrksvfyvgqleapqyvvscdga
gi_Sus              sedfflsgskdrtvrlwplynsgdgtretaprlvytqhrksvffvgqleapqcvvscdga
gi_Ailuropoda       sedfflsgskdrtvrlwplynsgdgtgetaprlvyaqhrksvffvgqleapqyvvscdga
gi_Equus            sedfflsgskdrtvrlwplynsgdgtsetaprliyaqhrksvffvgqleapqcvvscdga


gi_Danio            vhlwdqftgknircnepldgknpitavttmpaphcsvvfasadsvlrfidprkpglqhef
gi_Tetraodon        vhlwdqytgkqirsyeavdgkspitavstmpgphcsvvfgsadsvlrfidprkpglqhef
gi_Xenopus          vhiwdqytgksirtyeaadsklpitavatmpppycsvtvgsadsilrfidlrkpglqhef
gi_Gallus           vhiwdqftgklirtfdeldskapitavttmpppyhsisvasadsvlrfidhrkpglqhef
gi_Taeniopygia      vhiwdqftgkllrtfdeldskvpitavttmpppyhsisvasadsvlrfidhrkpglqhef
gi_Monodelphis      vhvwdpftgktvrtveawdsrvpltavavmsaphtsitlasadstlrfvdcrkpglqhef
gi_Mus              vhvwdpftgktlrtvdpsdsrvpltavavmpaphtsitmassdstlrfvdcrkpglqhef
gi_Rattus           vhvwdpftgktlrtvdpsdsrvpltavavmpaphtsitmassdstlrfvdcrkpglqhef
gi_Callithrix       vhvwdpftgktlravelldsrvpltavavmpaphtsitmassdstlrfvdcrkpglqhef
gi_Pongo            ------------------------------------------------------------
gi_Homo             vhvwdpftgktlrtvepldsrvpltavavmpaphtsitmassdstlrfvdcrkpglqhef
gi_Pan              vhvwdpftgktlrtvepldsrvpltavavmpaphtsitmassdstlrfvdcrkpglqhef
gi_Oryctolagus      vhvwdpftgktlrtvepsdsrvpltavavmpaphasitmassdstlrfvdcrkpglqhef
gi_Sus              vhiwdpftgktlrtvepsdsrvpltavavmpapytsitmassdstlrfvdcrkpglqhef
gi_Ailuropoda       vhvwdpftgktlrvmepwdsrvpltavavmpaphtsitmassdstlrfvdcrkpglqhef
gi_Equus            vhvwdpftgktlrtvepadsrvpltavavmpaphtsitmassdstlrfvdcrkpglqhef


gi_Danio            rlaysnlsaglirclavspggrtiaagfstgfivlldartglvlrgwpghegdilqmkaa
gi_Tetraodon        rlaynnvgaglirylavspsgrtvaagfssgfivlldartglilrgwpahegdilqmkaa
gi_Xenopus          kla-snvnaglirclavspngrsvvagyssgfiilldtrtglvlrgwpahegdilqmkaa
gi_Gallus           rla-ggvnaglirclavspngrsvmagfssgfivlldtrtglimrgwpahegdilqikaa
gi_Taeniopygia      rla-sgvsaglirclavspsgrsvvagfssgfivlldtrtglimrgwpahegdilqikaa
gi_Monodelphis      rlg-gglnaglvrslavspsgrsvvagfssgfmvlldtrtglilrgwpahegdilqikav
gi_Mus              rlg-gglnpglvrslavspsgrsvvagfssgfmvlldtrtglvlrgwpahegdilqikav
gi_Rattus           rlg-gglnpglvrslavspsgrsvvagfssgfmvlldtrtglvlrgwpahegdilqikav
gi_Callithrix       rlg-sglntglvrslavspsgrsivagfssgfmvlldtrtglvlrgwpahegdilqikav
gi_Pongo            ------------------------------------------------------------
gi_Homo             rlg-gglnpglvralaispsgrsvvagfssgfmvlldtrtglvlrgwpahegdilqikav
gi_Pan              rlg-gglnpglvralavspsgrsvvagfssgfmvlldtrtglvlrgwpahegdilqikav
gi_Oryctolagus      rlg-gglnpglvrslavspsgrsvvagfssgfmvlldtrtglilrgwpahegdilqikav
gi_Sus              rls-gglnpglvrslavspsgrsvvagfssgfmvlldtrtglvlrgwpahegdilqikav
gi_Ailuropoda       rlg-gglnpglvrslavspsgrsvvagfssgfmvlldtrtglvlrgwpahegdilqikav
gi_Equus            rlg-gglnpglvrslavspsgrsvvagfssgfmvlldtrtglvlrgwpahegdilqikav
```

Figure D.1: continued

```
gi_Danio            egnllvsssdhtltvwkdvehkplhqyrtpsdpihafdlygaeivagtvankigvysil
gi_Tetraodon        egnlvissssdytltvwkeleqkplrqyksqsdpihafdlygselvtgtvankigvysma
gi_Xenopus          dgnivvssstdhsltvwkeleqkplhqfksnsdpihvfdlygneivtgtvankigiysml
gi_Gallus           egnvlissssdhsmtvwkeleqkplhhyksasepihafdlygnevvtgtvankigvysml
gi_Taeniopygia      egnvlissssdhsltvwkeleqkplhhyksasepihafdlygnevvtgtvankigvysml
gi_Monodelphis      egsilissssdhsltiwkeldqkpthhykspsdpihtfdlygsevvtgtvankigvcsmm
gi_Mus              egsvlissssdhsltvwkeleqkpthhyksasdpihtfdlygsevvtgtvankigvcsll
gi_Rattus           egsvivssssdhsltvwkeleqkpthhyksasdpihtfdlygsevvtgtvankigvcsll
gi_Callithrix       egsvlvssssdhsltvwkeleqkpthhyksasdpihtfdlygsevvtgtvsnkigvcsll
gi_Pongo            ------------------------------------------------------------
gi_Homo             egsvlvssssdhsltvwkeleqkpthhyksasdpihtfdlygsevvtgtvsnkigvcsll
gi_Pan              egsvlvssssdhsltvwkeleqkpthhyksasdpihtfdlygsevvtgtvsnkigvcsll
gi_Oryctolagus      egsvlvssssdhsltvwkeleqkpthhyksasdpihtfdlygsevvtgtvankigvcsll
gi_Sus              egsllvssssdhsltvwkelepkpthhyksasdpihtfdlygsevvtgtvankigvcsll
gi_Ailuropoda       egsvlvssssdhsltvwkeleqkpthhyksasdpihtfdlygsevvtgtvankigvcsll
gi_Equus            egsvlvssssdhsltvwkeleqkpthhyksasdpihtfdlygsevvtgtvankigvcsll


gi_Danio            dstaslagstklstenfrgtltslsvlptkrllllgsdngairlla
gi_Tetraodon        disvspvsctklssenfrgtltslavlptkrllllgsdngairlla
gi_Xenopus          dslalpnsttklssenfrgtltnlavlptkrllllgsdngvvrlla
gi_Gallus           essalpvsttklssenfrgtltslavlpmkchlllgsdngvirlla
gi_Taeniopygia      essalptsttklssenfrgtltslavlptkchlllgsdngiirlla
gi_Monodelphis      epps--qattklssenfrgtltslavlptkrhlllgsdngairlla
gi_Mus              epps--qattklssenfrgtltslallptkrhlllgsdngiirlla
gi_Rattus           epps--qattklssenfrgtltslallptkrhlllgsdngiirlla
gi_Callithrix       epps--qattklssenfrgtltslallptkrhlllgsdngvirlla
gi_Pongo            ---------------------------------------------
gi_Homo             epps--qattklssenfrgtltslallptkrhlllgsdngvirlla
gi_Pan              epps--qattklssenfrgtltslallptkrhlllgsdngvirlla
gi_Oryctolagus      epps--qattklssenfrgtltslallptkrhlllgsdnglirlla
gi_Sus              epps--qattklssenfrgtltslallptkrhlllgsdngvirlla
gi_Ailuropoda       epps--qattklssenfrgtltslallptkrhlllgsdngvvrlla
gi_Equus            epps--qattklssenfrgtltslallptkrhlllgsdngvirlla
```

Figure D.1: continued.

Appendix E

Tblastn Search for wdr81

Table E.1: Tblastn Scores of Zebrafish *wdr81*

Sequences producing significant alignments:		(Bits)	Value
ref|NC_007126.6|	Danio rerio strain Tuebingen chromosome 15,	2262	0.0
ref|NC_007112.6|	Danio rerio strain Tuebingen chromosome 1,	49.3	0.001
ref|NC_007121.6|	Danio rerio strain Tuebingen chromosome 10,	49.3	0.002
ref|NC_007117.6|	Danio rerio strain Tuebingen chromosome 6,	42.4	0.18
ref|NC_007116.6|	Danio rerio strain Tuebingen chromosome 5,	48.1	0.004
ref|NC_007118.6|	Danio rerio strain Tuebingen chromosome 7,	49.3	0.001
ref|NC_007124.6|	Danio rerio strain Tuebingen chromosome 13,	60.8	4e-07
ref|NC_007127.6|	Danio rerio strain Tuebingen chromosome 16,	47.8	0.004
ref|NC_007134.6|	Danio rerio strain Tuebingen chromosome 23,	37.4	5.3

Table E.2: List of the Hits Obtained As A Result of Tblastn Search of Zebrafish *wdr81*

Features

ref|NC_007126.6| WD-repeat containing protein 81, neurobeachin isoform X2 and neurobeachin isoform X6

ref|NC_007112.6| lipopolysaccharide-responsive and beige-like anchor protein isoform and transcription initiation factor TFIID subunit 5

ref|NC_007121.6| neurobeachin a isoform X1 and neurobeachin a isoform X4

ref|NC_007117.6| neurobeachin-like protein 1

ref|NC_007116.6| WD repeat and FYVE domain-containing protein 3 isoform X3 and WD repeat and FYVE domain-containing protein 3 isoform X7

ref|NC_007118.6| Protein FAN

ref|NC_007124.6| lysosomal-trafficking regulator isoform X1, lysosomal-trafficking regulator isoform X2, WD repeat- and FYVE domain-containing protein 4 isoform X1, WD repeat- and FYVE domain-containing protein 4 isoform X2

ref|NC_007127.6| neurobeachin-like protein 2 isoform X5 and neurobeachin-like protein 2 isoform X3

ref|NC_007134.6| 57258 bp at 5' side: keratin and 515440 bp at 3' side: keratin, type II cytoskeletal 8